DEVELOPMENT OF AN IMPROVED EXTRAVEHICULAR SPACE SUIT THERMAL INSULATION

report to

NATIONAL AERONAUTICS AND SPACE ADMINISTRATION
MANNED SPACECRAFT CENTER
HOUSTON, TEXAS

CONTRACT NAS 9-7519

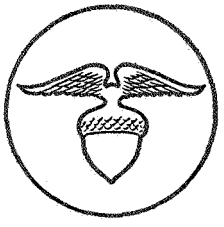

Arthur D. Little, Inc.

FINAL REPORT

DEVELOPMENT OF AN IMPROVED EXTRAVEHICULAR SPACE SUIT THERMAL INSULATION

by

David L. Richardson

prepared for

NATIONAL AERONAUTICS AND SPACE ADMINISTRATION
MANNED SPACECRAFT CENTER
HOUSTON, TEXAS

Contract NAS9-7519

C-69743

Arthur D. Little, Inc.
Cambridge, Massachusetts

FOREWORD

Improved extravehicular space suit thermal insulations were developed by Arthur D. Little, Inc., Cambridge, Massachusetts, for the National Aeronautics and Space Administration, Manned Spacecraft Center, under Contract NAS9-7519. The author acknowledges the assistance and cooperation of Burrell French, the project monitor, Dr. Frederick S. Dawn, and Dr. Matthew I. Radnofsky of the Crew Systems Division, NASA Manned Spacecraft Center. The principal Arthur D. Little, Inc., personnel contributing to the program included: Dr. Alfred E. Wechsler, technical review of the project; Dr. John L. Miles, development of germanium overcoating for aluminized polyimide film; John L. Burke, measurement of space suit insulation conductance; Leon M. Bablouzian, measurement of surface emittance; and Frank E. Ruccia, design and space simulation tests of a section of thermal micrometeoroid garment.

TABLE OF CONTENTS

LIST OF TABLES

LIST OF FIGURES

LIST OF FIGURES (Cont'd)

I. SUMMARY

A. PURPOSE

The purpose of this program by Arthur D. Little, Inc., (ADL) for the National Aeronautics and Space Administration (NASA) was to develop an improved thermal micrometeoroid garment whose insulation and mechanical properties and non-flammability are substantially better than Gemini-type thermal micrometeoroid garments.

B. SCOPE

The program included selection, screening, and experimental evaluation of insulation radiation shields and spacer materials; measurement of thermal conductance of 17 thermal micrometeoroid garment insulations in a guarded cold-plate calorimeter; analysis of thermal micrometeoroid garment fabrication techniques and the types of failure which have occurred, and development of improved fabrication techniques which adapt spacecraft multilayer insulation techniques to space suits; and flexure-wear and space simulation testing with a flexible elbow calorimeter of a thermal micrometeoroid garment section which incorporated the best insulation and fabrication techniques developed in the program. Preliminary specifications were established for the thermal insulation material and fabrication of improved micrometeoroid garments.

C. RESULTS

1. Materials Development

- The abrasive wear resistance of low-emittance aluminized surfaces of radiation shields was substantially improved by overcoating the surfaces with 500 Å of vapor-deposited germanium. With less than 1000 cycles of abrasive wear against fiberglass marquisette spacers at a compression of 0.2 psi, the surface of aluminized 0.5-mil polyimide (DuPont Kapton)--a radiation shield even more advanced technically than the Gemini-type

radiation shield--was visibly degraded and the measured emittance of the surface increased from 0.025 to 0.20. Samples of germanium-overcoated aluminized 0.5-mil polyimide film were subjected progressively to 500 cycles of wear against the same material at 9 incremental loads from 0.2 to 1.8 psi and the surface did not show appreciable degradation. The emittance increased from 0.026 before wear to values in the range from 0.027-0.029 after wear.

- The low-emittance surfaces of radiation shields are not significantly degraded by vapor-deposited germanium overcoatings. An overcoating of 500 Å of germanium increases the emittance of vapor-deposited aluminum surfaces from 0.025 to 0.027 and the emittance of vapor-deposited gold surfaces from 0.016 to 0.017.

- Effective radiation shields can also be achieved by applying gold to polyimide film by a commercial liquid bright gold process. These radiation shields have an emittance of 0.018. The surface has good abrasion resistance; after 500 cycles of abrasive wear against fiberglass marquisette spacers at 9 successively increasing loads from 0.2 to 1.8 psi, the measured surface emittance increased to 0.025.

- All polymeric film materials available for use as radiation shields are flammable in 16.2-psia oxygen. Germanium-overcoated 0.5-mil aluminized polyimide and liquid bright gold-coated 0.5-mil polyimide radiation shields range from self-extinguishing to flammable in air while aluminized polyester (baseline Gemini-type radiation shields) are highly flammable in air.

2. Evaluation of Radiation Shield and Spacer Combinations

a. Thermal Conductance at No-load

- All of the thermal micrometeoroid garment samples with double-aluminized or double gold-coated radiation shields and loose spacers of flexible polyurethane foam, Beta marquisette fiberglass, or multiple plain-weave fiberglass have conductances in the range of 0.0012-0.003 Btu/sq ft hr°F for the boundary temperatures 70 to -250°F and thermal conductances in the range of 0.0044-0.0082 Btu/sq ft hr°F for the boundary temperatures 300 to 70°F.
- One sample with a composite radiation shield and spacer and other samples with radiation shields laminated to Beta marquisette spacers have thermal conductances in the range of 0.0024-0.0045 Btu/sq ft hr°F for the boundary temperatures 70 to -250°F and thermal conductances in the range of 0.008-0.018 Btu/sq ft hr°F for the boundary temperatures 300 to 70°F.

b. Thermal Conductance at 1.0 psi Compression

- Conductance at compressive loads of 1.0 psi depends primarily upon the type and amount of spacers and the boundary temperatures. Samples with 0.030-inch-thick flexible open-cell polyurethane foam spacers or samples with a Beta marquisette spacer laminated to the radiation shield and one additional loose Beta marquisette spacer have conductances in the range of 0.06-0.08 Btu/sq ft hr°F for the boundary temperatures 70 to -250°F and the thermal conductance in the range of 0.16-0.21 for the boundary temperatures 300 to 70°F.
- Samples with single loose Beta marquisette spacers, three loose plain weave fiberglass spacers, or single Beta marquisette spacers laminated to the radiation shield have conductances in the range of 0.08-0.10

Btu/sq ft hr°F for the boundary temperatures 70 to -250°F and conductances in the range of 0.20-0.30 Btu/sq ft hr°F for the boundary temperatures 300 to 70°F.

3. Thermal Micrometeoroid Garment Analysis

- The Gemini space suit insulation fabrication technique, which consists of alternate radiation shields and spacers applied separately, is a good construction technique. However, the technique of taping each spacer and shield layer in the seam allowed thermal short circuits to develop when adjacent layers adhered to each other. The insulation layers became load-bearing and high stress concentrations were developed where the radiation shields and spacers were firmly stitched together at the seams and penetrations.
- The greatest improvement in integrity and thermal performance of the thermal micrometeoroid garment is achieved when the insulation layers are not load bearing and are designed to hang loosely on the pressure-retaining layers of the space suit.
- The radiation shields should stop just short of the edge seam and the shield spacers should be anchored in the edge seam by firm, tight stitches. The external layers should be carried around the end of the insulation for flame protection in the event of fire. The seam stitches should be made with double threads, one of Nomex and one of Beta fiberglass.

4. System Tests

Space chamber tests with a flexible elbow calorimeter and a section of a garment incorporating the materials (germanium-overcoated aluminized polyimide radiation shields and Beta marquisette spacers) and improved garment fabrication techniques developed in the program showed that:

- The heat flow through the garment can be accurately determined both before and after wear by flexing. The measured heat loss from the garment during simulated lunar nighttime conditions (space chamber walls at -320°F and calorimeter temperature at 70°F) was 0.54 Btu/sq ft hr before wear and 0.76 Btu/sq ft hr after 10,000 cycles of flexing. The heat flow into the garment during simulated lunar daytime conditions (space chamber walls at 250°F and calorimeter temperature at 70°F) was 1.47 Btu/sq ft hr before wear and 1.92 Btu/sq ft hr after 10,000 cycles of wear.

- The measured heat flux per unit area in the garment section before wear was 23 percent higher than was predicted from conductance measurements in the guarded cold-plate calorimeter for boundary temperatures of 250 to 70°F and 18 percent lower than predicted for boundary temperatures of 70 to -320°F. After 10,000 cycles of wear, the measured heat flux per unit area was 50 percent higher than was predicted from conductance measurements for boundary temperatures of 250 to 70°F and equal to that predicted for boundary temperatures of 70 to -320°F.

- The durability of the space suit insulation and the integrity of the fabrication techniques were demonstrated for the thermal micrometeoroid garment section. The germanium-overcoated radiation shields withstood the abrasion of the fiberglass spacers. However, the 0.5-mil polyimide film shield substrate had some small cracks after 10,000 flexures in a vacuum environment under lunar nighttime conditions.

D. RECOMMENDATIONS

1. On the basis of our investigation of materials, we recommend that multilayer insulations be used which have:

   (a) Radiation shields of 0.5-mil polyimide film with 500 to 800 Å of vapor-deposited aluminum and an overcoating of 500 Å of vapor-deposited germanium on both sides, or

   (b) Radiation shields of 0.5-mil polyimide film with 1000 Å of gold applied to both sides by a liquid bright gold process.

   (c) Shield spacers made from single layers of Beta fiberglass yarn in an open leno-weave similar to the marquisette materials--J. P. Stevens Style 2530 with 9362 finish, or

   (d) Shield spacers made from three layers of commercial fiberglass yarns in plain weave (similar to Style 104) with 5-8% of non-flammable yarn stabilization (3M Fluorel) to prevent unraveling.

2. On the basis of our conductance measurements of thermal micrometeoroid garment insulations, we recommend that seven radiation shields and eight spacers be used in combinations with internal and external garment layers as required for normal wear and micrometeoroid protection. A spacer must be between each radiation shield and the inner and outer garment layers to minimize contact conduction.

3. From our investigation of the Gemini thermal micrometeoroid cover layer, we find that the garment should be designed and fabricated so that:

   (a) The insulation hangs loosely on the garment.

   (b) The inner layer of the garment is load-bearing.

(c) The spacer layers are firmly anchored in the seams and penetrations, and the radiation shields terminate no closer than 0.5 inch to seams or penetrations.

(d) Tight stitches are never made through the radiation shield layers.

4. From our system tests, we recommend that all developmental thermal micrometeoroid garments have a section tested for flexure endurance and heat loss (or gain) in simulated space thermal environment in order to prove their durability and thermal protection capability. Such garment sections and insulation layups should incorporate exactly the same construction techniques as the full garment.

II. INTRODUCTION

A. BACKGROUND

As our astronauts gain more experience in manned space exploration and perform longer missions outside of their spacecraft, space suits for extravehicular activity will assume an increasingly important role. A vital component of the extravehicular space suit is the thermal micrometeoroid overgarment or layer required to protect the astronaut from his external environment. Thermal protection of an astronaut on lunar or planetary surfaces or while in orbit outside his spacecraft requires that he be thermally decoupled from the external space environment.

To achieve this thermal protection the Gemini and Apollo extravehicular space suits have been designed with external thermal micrometeoroid protection layers which are either integral with the basic space suit or are incorporated as an overgarment. The thermal micrometeoroid garment has an outer protective cover, an insulation comprised of alternate thermal radiation shields and spacers, an inner protective layer, and one or more additional micrometeoroid buffer layers. Each component of this garment has multiple functions: the multilayers of the insulation contribute to the garment's effectiveness as a micrometeoroid shield, and the solar absorptance and radiative emittance of the outer surface enhance the garment's thermal protection capacity. The properties of the thermal micrometeoroid garment also affect the astronaut's mission. The insulation should provide sufficient thermal protection so that the portable life support system is not taxed and the total garment should be sufficiently compact so the astronaut's mobility is not impaired.

Multilayer insulation is necessary for thermally isolating an astronaut from his external environment. Roth[1] estimates that the maximum permissible heat loss from a space suit should not exceed 10 Btu/sq ft hr. On the lunar surface at night, this corresponds to a maximum space suit conductance of 0.03 Btu/sq ft hr°F. Multilayer insulation evacuated by exposure to the space environment is the only type which can

provide this low conductance in lightweight thin construction. Other insulations like evacuated fibers or powders can achieve this low conductance; however, they require up to 10 times more insulation thickness for the same thermal protection as multilayer insulation.

Multilayer insulations consist of layers of alternate heat-reflecting radiation shields separated by low-conductivity spacers. Each layer contains a thin, low-emittance radiation shield that permits the layer to reflect a large percentage of the radiation it receives from a warmer surface. The radiation shields are separated from each other by spacers to reduce the heat transferred from shield to shield by contact conduction. The space between the shields is evacuated to less than 10^{-4} torr to decrease gas conductance.

In space garments, exposure to the vacuum of space effectively reduces the gas conduction to a negligible value in a matter of a few seconds. The primary insulation requirement for radiation shields is that both surfaces have a low hemispherical total emittance. Gold and aluminum are typical low-emittance materials that can be used either as coatings on thin polymeric sheets or as thin foils. Aluminum foils and vapor-deposited aluminum on plastic films are most frequently selected for radiation shields.

Spacers are required to separate the radiation shields and to minimize solid conduction between adjacent radiation shields, particularly when compressive loads are applied. A fibrous mat arranged with the fibers in a random array is an effective multiple-resistance spacer. Netting has crossover points (knots) which are effective point-contact spacers between radiation shields.

B. BASELINE INSULATION FOR THE STUDY

The baseline insulation used in the Gemini-type thermal micrometeoroid garments was made from alternate radiation shields of 0.25-mil thick polyester film (DuPont Mylar) aluminized on one side with approximately 300 Å of vapor-deposited aluminum (NRC-2, National Research Corp.) and spacers of non-woven Dacron batt (15 grams/sq yd $\pm$ 2 grams/sq yd

National Research Corp.). The minimum thermal conductance[2] of the garment (including insulation, inner and outer protective layers, and the micrometeoroid protection layers) was 0.004 Btu/sq ft hr°F for a sample thickness 0.25 inch and temperature boundary conditions of 76 to -310°F. The minimum conductance was 0.018 Btu/sq ft hr°F for a sample thickness of 0.22 inch and temperature boundary conditions of 301 to 70°F.

All components of the garment, including the insulation, are flammable in 16.5-psia oxygen. It appears that the garment was assembled in such a way that the insulation layers became load bearing during normal usage and caused the insulation layers to rip along some of the seams. In all seams and penetrations, the radiation shields and spacers were firmly anchored by the seam stitches, thereby allowing high conductance in these areas. The low-emittance surface on the radiation shields appeared to be abraded during normal astronaut activity.

C. APPROACH

The program was divided into five major phases: (1) materials development, (2) evaluation of radiation shield and spacer combinations, (3) thermal micrometeoroid garment analysis, (4) system test in simulated lunar environment, and (5) preparation of preliminary specifications for thermal insulation and garment fabrication.

In the materials development phase of the program, we discussed the identification, screening, and experimental evaluation of components which might be used in insulations for extravehicular space garments. The procedure was to first list all candidate insulation materials which might possibly be used for both radiation shields and spacers. Initially, little consideration was given to whether the materials were technically feasible, available, or practical in terms of fabrication or cost. The materials were then screened, in accordance with criteria set forth in the contract, and ranked. We then selected for further laboratory evaluation those materials which we believed to have a better chance of improving astronaut space suit insulations. These evaluations included flammability in 100% oxygen, abrasion resistance for radiation shields,

total hemispherical emittance for radiation shield surfaces, tensile strength, tear strength, fold endurance, and stability in vacuum.

A consideration which entered our material development and fabrication study was that, in many instances, we could identify materials which might be non-flammable or abrasion resistant. Some of these materials we eliminated because they were not readily available or were too expensive to be included in this program. For them we substituted less-desirable materials of the same basic insulation properties so that we might evaluate the feasibility of the basic material as insulation components.

In the evaluation of radiation shield and spacer combinations, we measured the basic thermal conductance of both ADL-developed and NASA-MSC-supplied samples of space suit insulation layups. Conductance was measured under compressive loads in the range from "no load" to 15 psi, in the temperature ranges from 70 to -250° and from 300 to 70°F, and at a vacuum of 10^{-5} torr.

Four combinations of ADL-developed insulations were subjected to non-destructive simulated wear tests prior to being tested for thermal conductance. On the basis of the initial thermal conductance tests, we chose the two most desirable material combinations for further testing in the unworn condition. We also measured the thermal conductance of an insulation similar to the layup used in the Gemini space suits and two additional samples: one, a laminate; the other, a composite shield and spacer layup. In addition to these nine samples tested under our portion of the program, NASA-MSC provided eight supplemental samples that were tested for thermal conductance.

In the analysis of thermal micrometeoroid garments, we learned from discussions with personnel from NASA-MSC of the failures which had occurred in space suit insulation layups. Post-flight photographs of these failures were studied to determine their causes. An experimental Gemini-type of overgarment was dismembered to determine construction and seaming techniques. Additional failures reported to us verbally by NASA-MSC involved the degradation of vapor-deposited surfaces under simulated wear conditions. The construction details in Gemini-type space

suit insulations were analyzed and assembly techniques were recommended for space garments which reflect the techniques used in cryogenic multilayer insulation systems. Both preferred and alternative assembly techniques for space suits were recommended.

In the system test, measurements were made of heat flow in a test section of an experimental thermal micrometeoroid garment which incorporates the insulation and fabrication techniques developed during this program. Heat flow through the garment section was measured with a guarded calorimeter which is integrated into the pressurized elbow section from an astronaut's space suit. A unique feature of this elbow calorimeter is that it can operate in a laboratory-sized space-simulation chamber. Heat flow into the thermal micrometeoroid garment can be measured for simulated lunar daytime conditions and heat flux out of the garment can be measured for simulated nighttime conditions. In addition, the garment section can be subjected to cyclical flexing during simulated lunar nighttime conditions to simulate the actual wear encountered during normal space suit operation.

As a result of this program, we established preliminary specifications for thermal insulation and garment fabrication. The specifications are valid only for laboratory investigation; they are not space-qualified and the space capability of the insulations and garment fabrication have not been demonstrated.

III. MATERIALS DEVELOPMENT

The insulation materials in Gemini-type space suits have a low probability of survival both in insulating ability and in physical integrity under the repeated usage required in long-duration space exploration missions. An important part of this program was to develop improved insulation radiation shields and spacers. Candidate materials were surveyed under this program and those which were identified as having a good chance of improving astronauts' space suit insulations were procured and tested for flammability, physical properties, abrasion resistance, and surface emittance.

Eighty materials and six low-emittance coatings and overcoatings were considered for radiation shields. Two substrate and coating combinations showed marked improvement over Gemini-type radiation shields: one was polyimide film with 500 Å vapor-deposited aluminum and 500 Å vapor-deposited germanium overcoating on both surfaces, and the other was polyimide film with 1,000 Å gold applied by a liquid bright gold process. Sixteen materials were considered for spacers. Two types of fiberglass spacers proved successful: one was a Beta marquisette and the other was three layers of lightweight plain weave fabric. An open-cell polyurethane foam, although flammable in 100% oxygen, was considered for applications where extreme compressive loads are anticipated.

A. CANDIDATE RADIATION SHIELDS AND SPACERS

1. Identification of Materials

a. Radiation Shield Substrates

The candidate substrate materials for radiation shields are listed in Table 1. The polymers are listed as: commercially available as films, in bulk, and under development. Their flammability in air is compared to polyester. In addition, metal foil radiation shields and composite radiation shields and spacers are included.

TABLE 1. RADIATION SHIELD MATERIALS

A. POLYMERS

1. Commercially Available as Films

Less Flammable Than Polyester in Air (these materials warrant further study)

- Polyimide (Kapton)
- Polytetrafluoroethylene (TFE)
- Polychlorotrifluoroethylene (CTFE)
- Fluorinated ethylene propylene (FEP)

Flammability Similar to That of Polyester in Air

- Polycarbonate
- Vinylidene fluoride (Kynar)
- Rubber hydrochloride
- Vinylidene chloride

More Flammable Than Polyester Film in Air

- Polyvinyl fluoride (Tedlar)
- Polypropylene
- Linear co-polyester
- Ethyl cellulose
- Cellulose propionate
- Polyamide (Nylon)
- Polymethylmethacrylate
- Polyethylene
- Ionomer
- Vinylnitrile rubber
- Expanded polystyrene foam
- Polyvinyl alcohol
- Polyuranylchloride
- Vinylchloride acetate co-polymers
- Regenerated cellulose
- Cellulose acetate
- Cellulose triacetate
- Cellulose acetate butyrate
- Polyurethane

2. Commercially Available in Bulk

Flammability Similar to Polyester in Air

- Polyphenylene oxide (PPO)
- Polysulfone

TABLE 1 (cont'd)

Commercially Available in Bulk (Cont'd)

More Flammable Than Polyester in Air

Polyallomers
Acrylics
Acrylonitrile butadiene styrene
Styrene acrylonitrile
Phenoxy
Poly-p-xylyene (Parylene)
Acetals

3. Materials Under Development

Possibly Less Flammable Than Polyester (these materials warrant further study)

Polyperfluorotriazine
Carboxynitroso rubber
Polycarboranesiloxane
Silicone phthalocyanin derivatives
Polybenzothiazole
Metal polyphosphinates
Phenylsilsesquioxane polymer
Triazine polymer
Pyrolyzed polyacrylonitrile
Chlorinated polyether (Penton)
Fluorinated polyurethane

Flammability Similar to Polyester

Polyamide-imide
Polybenzimidazole
Polyimidazopyrrolone
Polyhydrazide
Polyamibines
Polysulfanyldibenzamide
Polytetrephthal amides
Polyoxadizole
Polytriazole
Polybenzoxazole
Polyquinoxaline
Silicone metallic polymers

More Flammable Than Polyester

Polythiazole
Polyphenylene sulfide
Methylsilicone rubber
Polypyrazole

TABLE 1 (cont'd)

Polymers Under Development (cont'd)

More Flammable Than Polyester (cont'd)

Polyesterimide
Polysiloxane
Polyphenylene
Phenolphthalein polymers
Polyaryloxysilane
Polyisocyanurate
Titanium polymers
Phosphorus polymers
Tin polymers
Polyvinylisocyanate ladder polymer
PNP polymers

Possibly Less Flammable Than Polyester But Hydrolytically Unstable

Polyphosphonamide
Diazadiphosphetidine
Phosphonitrilic polymer

B. METAL FOILS

Aluminum - best available
Silver - lowest emittance, oxidizes easily
Copper - low emittance, oxidizes rapidly
Gold - low emittance, very expensive

C. COMPOSITES

Integrated spacer and radiation shield - good load-bearing insulation and easy fabrication
Spacers attached to radiation shield - easy fabrication
Metal foils laminated on flexible substrate - low flammability in oxygen
Heavy deposition of metal on thin polymeric film substrate - low flammability in oxygen

b. Low-Emittance Surfaces and Overcoatings

Total hemispherical emittance (at room temperature) of less than 0.05 for both surfaces of radiation shields is necessary in space suit insulations to minimize the heat transfer through the astronaut's garment. In addition, the low-emittance surfaces should not degrade during the normal life of the space suit. Table 2 identifies candidate coatings which might be applied to radiation shield substrates, the techniques by which the coatings may be applied to the substrate, and overcoating materials and techniques for protecting the coatings. A good overcoating material should not degrade the emittance characteristics of the radiation shield. Since emittance at room temperature is dominated by radiation in the 5 to 45 micron waveband, overcoating materials should exhibit good radiation transmission in this waveband.

c. Spacers

Radiation shield spacers separate adjacent layers of multilayer insulation radiation shields without transmitting significant amounts of thermal energy from one layer to the next. They should provide high thermal contact resistance, be of low conductivity, be capable of carrying compressive loads without transmitting heat, be durable, be compatible with the radiation shield, and be easy to fabricate. For a space suit insulation application, spacer materials should also be non-flammable in 100% oxygen.

Table 3 lists spacer materials which have been used successfully for high-temperature thermal protection systems and for protecting reentry vehicles. Except for plastics, the materials are believed to be non-flammable in 100% oxygen at 16.5-psia. Wherever possible, the fabricated form of the material as it might be used as a spacer has been indicated. However, some of the materials shown in Table 3 have not been fabricated in forms which can be used successfully in space suit insulations.

2. Initial Screening of Materials

Many of the candidate materials summarized in Tables 2 and 3 had to

TABLE 2. LOW-EMITTANCE COATINGS AND OVERCOATINGS

Material	Coating Technique	Remarks
Low-Emittance Coatings		
Aluminum	Vapor deposition	Low emittance, commercially available, durable
Gold	Vapor deposition	Emittance lower than aluminum, commercially available, not durable
	or	
	Liquid-bright-gold process	Commercially available, very durable
Silver	Vapor deposition or liquid-silver process	Emittance lower than gold, tarnishes easily
Copper	Vapor deposition	Emittance lower than gold, tarnishes easily
Protective Overcoatings		
Aluminum Oxide	Annodization	Good infrared transmission, commercial process
Germanium	Vapor deposition	Good infrared transmission
Silicon Monoxide	Vapor deposition	

TABLE 3. SPACER MATERIALS

	Remarks
Fiberglass and silica - fabrics, nonwoven batts	Good candidates - abrasive to radiation shields
Glass and silica hollow and solid spheres	Good candidates
Boron nitride - felts and fabrics	Non-abrasive
Boron fibers	
Chromium fibers	
Alumina fibers (sapphire whiskers)	Highly abrasive to radiation shields
Zirconia fibers	
Silicon carbide fibers	
Ceramic flakes	
Mica sheets (synthetic)	Inflexible
Glass and silica - foams	
Plastic - foams, hollow or solid spheres	Flammable in oxygen

be eliminated in the initial screening process as being unsuitable for application to space suit insulation. Slightly different criteria were used for the radiation shields and for the spacers.

a. Radiation Shields

The criteria which were used for screening candidate radiation shields and coatings include (in order of importance) flammability in oxygen, useful temperature range, degradation temperature, flexibility, density, adhesion of low-emittance coatings, emittance of coatings, dimensional stability, tear strength, tensile strength, weight, availability, fabricability, and cost. Our initial screening of radiation shields according to these criteria is summarized in Table 4.

All of the materials considered were flammable in oxygen. The metal foils were undesirable because they were not flexible enough, particularly if used in multiple layers.

Neglecting flammability, the most promising radiation shields were thin polymeric films with low-emittance coatings and composite radiation shields with the spacers attached to the polymeric film shields. The problem was then reduced to determining which thin polymeric shields might be least flammable in oxygen. The flammability of polymeric materials was compared to the flammability in air of polyester, since the baseline insulation uses polyester radiation shields. Four of the film materials seemed to be less flammable than polyester in air, thus warranting further study. Among the materials commercially available in bulk form, but which, to our knowledge, have not been fabricated as films, we found none better than polyester. Among the polymers under development, ten seem to be less flammable than polyester, thus warranting further study. Several other materials identified as being less flammable than polyester were hydrolytically unstable.

b. Spacer Materials

The criteria which were used in the screening of candidate radiation spacer materials included (in order of importance) flammability in oxygen, useful temperature range, degradation temperature, flexibility, density,

TABLE 4 INITIAL SCREENING OF RADIATION SHIELDS

Criteria	Thin Polymeric Films with Low-Emittance Coatings	Metal Foils	Composite Radiation Shields: Integrated Spacer and Radiation Shield	Composite Radiation Shields: Spacers Attached to Film Shields	Composite Radiation Shields: Foils on Flexible Substrates
Flammability in oxygen	Flammable	Flammable	Flammable	Flammable	Flammable
Useful temperature range	Good	Excellent	Good	Good	Good
Degradation temperature	Average	High	Average	Average	Average
Flexibility	Good	Poor	Fair	Good	Poor
Density	Low	High	Low	Low	Average
Adhesion of low-emittance coatings	Good	n.a.	Good	Good	Excellent
Emittance of coatings	Excellent	Excellent	Excellent	Excellent	Excellent
Dimensional stability	Good	Fair	Good	Good	Good
Tear strength	Low	Low	High	High	Average
Tensile strength	Average	High	High	High	Average
Weight of lay-up	Low	High	Low	Low	Low
Availability	Available	Available	Development	Available	Development
Fabricability	Good	Poor	Excellent	Excellent	Fair
Cost	Low	Low	Reasonable	Reasonable	Reasonable

contribution to heat transfer, dimensional stability, tear strength, tensile strength, weight of the layup, availability, fabricability, and cost. Our initial screening of spacer materials is summarized in Table 5. Of the original candidate materials, only fiberglass and silica fabrics and non-woven mats warranted further study.

B. MATERIALS DEVELOPMENT AND OPTIMIZATION

The emphasis in the development and optimization phase of the program was on the modification or adaptation of available materials, wherever possible, to the space suit to improve its insulation, wear, fabricability. (NASA-MSC had several concurrent programs to develop non-flammable materials for the crew areas in the Apollo lunar command modules; some of these materials were used in the late phases of this program.) During the early phases of our program, we often substituted a less desirable (usually more flammable) but available material in order to determine if the insulation layup could be improved. If such a material were demonstrated to produce an improvement, then a less flammable substitute material of the same type could be developed.

1. Sources of Materials

We prepared laboratory samples (up to three-inch diameter) of aluminum and gold surfaces, and overcoatings of germanium and silicon monoxide by vapor-deposition on polyimide film. Samples of aluminum oxide overcoating on vapor-deposited aluminum were prepared by an anodizing process. Larger laboratory samples of radiation shields (up to 13-inch diameter) were also prepared by vapor-depositing both sides with aluminum and germanium overcoatings. A pilot production quantity of germanium-overcoated aluminized half-mil polyimide film was obtained from National Metallizing Division of Standard Packaging, Cranberry, New Jersey. Half-mil and one-mil polyimide films with gold coatings applied by the liquid bright gold process were prepared by AGC Corporation of Meriden, Connecticut.

Fiberglass fabrics suitable for spacers were obtained from J. P. Stevens and Company and Hess, Goldsmith and Company, a division of

TABLE 5. INITIAL SCREENING OF SPACER MATERIALS

Criteria	Fiberglass and Silica		Glass and Silica		Plastic	
	Fabrics (Plain weave, leno weave)	Nonwoven Mats	Foams	Hollow or Solid Spheres	Foams	Hollow or Solid Spheres
Flammability in oxygen	Nonflammable	Nonflammable	Nonflammable	Nonflammable	Flammable	Flammable
Useful temperature range	Excellent	Excellent	Excellent	Excellent	Good	Good
Degradation temperature	High	High	High	High	Average	Average
Flexibility	Excellent	Fair	Poor	Fair	Fair to good	Fair
Density	Medium	Medium	High	Medium	Low	Low
Contribution to heat transfer	Average	Average	Above average	Low	Below average	Low
Dimensional stability	Excellent	Excellent	Excellent	Poor	Fair	Poor
Tear strength	High	Low	n.a.	None	Fair	None
Tensile strength	High	Low	High	None	Fair	None
Weight	Average	Low	High	Above average	Low	Low
Availability	Good	Good	Good	Good	Good	Good
Fabricability	Excellent	Good	Poor	Poor	Good	Poor
Cost	Low	Low	Low	Low	Low	Low

Burlington Industries, both of New York. We were unable to find a manufacturer who had made or could make a fiberglass bridal veil (tulle) as a replacement for the silk bridal veil which is used successfully as spacers in cryogenic insulations.

Thin samples (0.030 inch) of open-cell, flexible polyurethane foam were obtained from the Scott Paper Company, Chester, Pennsylvania. We attempted to prepare extremely thin samples of this foam (approximately 0.005 inch) by first impregnating a large block of foam with fine-crystalline wax, and then skiving thin sheets from it. The results were not satisfactory, primarily because the wax-impregnated foam did not skive uniformly, but deformed ahead of the skiving knife to produce a non-uniform thickness.

2. Experimental Evaluation of Shields and Spacers

Information was not available on the flammability of many of the candidate materials in oxygen or their abrasion resistance, surface emittance, and mechanical properties. Therefore, we obtained such data either by testing in our laboratory or by testing in the NASA-MSC laboratory (flammability in oxygen). At the same time, we also developed and tested some new materials, particularly low-emittance coatings and protective overcoatings for thin polymeric films. The net results of these developments and evaluations were: (1) two superior radiation shields--both half-mil polyimide film; one with vapor-deposited aluminum and an abrasion-resistant germanium overcoating; the other with a gold surface applied by a commercial liquid bright gold process, and (2) two radiation shield spacers non-flammable in oxygen--one, a Beta marquisette fiberglass; the other, a plain-weave sheer fiberglass scrim.

a. Flammability in Oxygen

All candidate radiation shield materials were submitted to NASA-MSC for flammability evaluation in 100% oxygen. In many instances, these materials, particularly the basic raw materials still under development, were not in a form which might be used in a space suit insulation.

The results of these flammability tests at NASA-MSC are summarized

in Table 6. Of the materials tested, two development materials appeared to be less flammable in oxygen than polyimide film: polyperfluorotriazine* (Sample Nos. 9-11--Air Force Materials Laboratory, Wright-Patterson Air Force Base), particularly when cured for long periods at 500°F; and a polycarboranesiloxane (Sample No. 13--Dexsil from Olin Chemicals). Both of these warrant further study and development as possible non-flammable materials for space applications and particularly as radiation shields in space suit insulations.

The fiberglass materials considered for radiation shield spacers were tested by NASA-MSC under other programs and found to be non-flammable in 16.5-psia oxygen. Several modifications of the basic spacer material tested by NASA-MSC (NASA Style 4697) were tested. The results of the test of one particular sample (Style 104) which had been stabilized with a fluorel compound indicate that the stabilization is self-extinguishing when bottom-ignited in 16.5-psia oxygen.

One of the prime candidate materials for inclusion in the space suit insulation study was 0.5-mil double-aluminized polyimide (Sample No. 22, Table 6) overcoated with approximately 500 Å of vapor-deposited germanium. Unfortunately, this material was found to be highly flammable in 16.5-psia oxygen. Until some of the more promising polymeric materials become available (polyperfluorotriazine and polycarboranesiloxane), the best available material from a flammability point of view is polyimide (Kapton), principally on the basis that it is less flammable than polyester (Mylar) in air.

b. Abrasion Test for Radiation Shields

Space suit insulations are subjected to combined abrasion and flexing during normal use. During the evaluation of low-emittance shields and overcoatings, we screened them initially on the basis of their resistance to abrasion. Later in the program, samples were subjected to

*The samples were small and a non-standard flammability test was used.

TABLE 6. SUMMARY OF FLAMMABILITY TESTS

Sample No.	Manufacturer	Sample Specifications	Flammability Test Results			Remarks
			16.5 psia Oxygen	6.2 psia Oxygen	Ambient	
1	General Electric	Polyphenylsilsesquioxane unplasticized film, 0.002"	Flash	5 in/sec	Burns	
2	General Electric	Polyphenylsilsesquioxane plasticized (Arochlor plasticizer) film 0.0015 in.	Flash	5 in/sec	Burns	
3	Hercules, Inc.	Chlorinated polyether (Penton)	Flash	10 in/sec	--	
4	Raybestos Manhattan	Fluorosilicone (filled)L-3236-1	No Ignition	no ignition	--	Very highly filled; not suitable for a radiation shield
5	3M	Fluorel (filled) L-2231	self-extinguishing	--	--	
6	Raybestos Manhattan, Inc.	Fluorel (filled) L3251-3 0.016 in.	No Ignition	No Ignition	--	Highly filled; 0.009 in. sample ignited at 16.5 psia
7	Raybestos Manhattan, Inc.	Fluorel (filled) L3203-6 0.028 in.	0.041 in/sec	No Ignition	--	Highly filled; 0.065 in. sample no ignition at 16.5 psia
8	Abex Corp.	Polybenzothiazole laminate	No Ignition	No Ignition	--	Not suitable for a radiation shield
9	WPAFB/AFML	Polyperfluorotriazine cured at 200°F for 15 hrs	1.0 in/sec	--	--	Samples were small and a non-standard flammability test was used
10	WPAFB/AFML	Polyperfluorotriazine cured at 500°F for 24 hrs	0.5 in/sec	--	--	
11	WPAFB/AFML	Polyperfluorotriazine cured at 500°F for 11 days	0.17 in/sec	--	--	One of the best materials tested
12	Dow Corning	Aerospace sealant 93-079, 0.065 in.	0.5 in/sec	0.19 in/sec	--	
13	Olin	Polycarboranesiloxane Dexsil 202 - Lot 5	0.17 in/sec	--	--	One of the best materials tested
14	Arthur D. Little, Inc.	Composite of fiberglass and Kapton - Pyre ML-RC 5057 cured at 316°C for 1 hour	Flash	2.0 in/sec	--	
15	Pennsalt Chemical Corp.	Metal polyphosphinate $[C_r(H_2O)(OH)(OPPh_2O)_2]$ x 40% TCP #3098-63 0.002 in.	-	Flash	--	Film had no strength
16	Abex Corp.	Polybenzothiazole - fiberglass laminate (one-ply)	self-ext. top and bottom ignition	--	--	Not suitable for a radiation shield
17	Raybestos Manhattan, Inc.	RL-3520 - Stevens Style 2530 fiberglass cloth impregnated with Fluorel	0.33 in/sec	--	--	Not suitable for a radiation shield
18	du Pont	Surlyn A Ionomer, 0.004 inch	--	Flash	--	Burned in less than 1 sec.
19	du Pont	Teflon FEP Type A, 0.005 inch	--	0.5 in/sec	--	
20	du Pont	Tedlar-Polyvinyl Fluoride, 0.002 inch	--	Flash	--	

TABLE 6 (Cont)

Sample No.	Manufacturer	Sample Specifications	Flammability Test Results			Remarks
			16.5 psia Oxygen	6.2 psia Oxygen	Ambient	
21	du Pont	Kapton-Polyimide, 0.0005 inch	Flash	4.2 in/sec	burns	Yellow-white flame in O_2
22	Arthur D. Little, Inc.	Kapton-Polyimide, 0.0005 inch both sides with 300 Å Aluminum and 500 Å Germanium overcoat	Flash	Flash	burns	
23	du Pont	Laminate of 0.5-mil FEP Teflon, 1 mil Kapton and 0.5-mil FEP Teflon	--	0.83 in/sec	--	
24	Arthur D. Little, Inc.	Composite of Stevens Style 1659 dipped in Kapton, film cured at 200°C and coated both sides with 500 Å vapor-deposited aluminum	2.9 in/sec	--	--	
25	Polyflex Products Corp	400A Tissuglas 0.004 inch	Flash	Flash	--	
26	Polyflex Products Corp	T-10G-6N Fiberfilm 0.001 inch	Flash	Flash	--	
27	Polyflex Products Corp	T-20A-60 Fiberfilm 0.002 inch	Flash	Flash	--	
28	Polyflex Products Corp	TX-10-40 Emfab 0.001 inch	Flash	Flash	--	
29	Scott Paper Company	Polyurethane foam 0.13 inch	Flash	Flash	--	
30	Arthur D. Little, Inc.	Kapton-polyimide, 0.005 inch both sides coated with 1100 Å of liquid bright gold	--	2.0 in/sec	burns	Yellow sparking flame in O_2
31	NASA/MSC	Style 104 fiberglass fabric with Kel F Edgelock KV 19139 (Gaco FR 86J)	Self-extinguishing	Self-extinguishing	--	
32	NASA/MSC	Glass fabric coated with Fluorel R/M-L3203-6	Self-extinguishing	Self-extinguishing	--	Two pairs of samples--each behaved the same
33	Arthur D. Little, Inc.	Style 104 fiberglass fabric with Kel F Edgelock KV 19139 (Gaco FR 86J)	Self-extinguishing	--	--	Three pairs of samples with 3, 5, and 10% stabilization by weight; each behaved the same
34	Arthur D. Little, Inc.	Style 104 fiberglass fabric stabilized with Fluorel R/M-L3203-6	Self-extinguishing	Self-extinguishing	No ignition	

a simulated wear test which combined both flexure and abrasion.

The initial investigation involved determining a standard against which to abrade the radiation shield. Samples of double-aluminized Kapton were rubbed against various spacer materials and configurations under a constant 0.5-pound load for 1,000 cycles, then examined visually and microscopically. Of the spacer materials tested, the loose-weave Beta marquisette fiberglass spacers (Stevens Style 2530) were by far the most abrasive. Deep jagged "windows" appeared in the aluminum coatings on the radiation shields when they were abraded by this spacer. The "windows" were caused by the extremely abrasive particles of glass which result from the breakdown of the glass yarns in the material. These glass particles appeared to extrude from the yarns by the abrading motion and readily cut through the aluminum film.

Other spacer materials considered for standards for abrasion were (in order of abrasiveness) tight weave Beta cloth (Stevens Style 15035), silk bridal veil, Nomex cloth (3 ounce), nonwoven Dacron batt, and boron nitride nonwoven felt. The boron nitride felt was markedly nonabrasive when compared with the loose-weave Beta marquisette fiberglass. Because the loose-weave Beta marquisette was the most abrasive of the materials, we chose it as a standard against which to compare all our samples of low-emittance surfaces.

The procedure in evaluating the abrasion resistance of radiation shields was to mount the samples on a 2.5-inch-diameter aluminum disc (also used in the emissometer). The disc was then placed in the Stoll abrasion tester and a fresh sample of Stevens Style 2530 Beta marquisette was attached to the top platen. With a one-pound weight added to the top platen, the sample was subjected to 500 cycles of wear and the surface was examined visually. If little degradation was noted, an additional one-pound weight was added to the top platen and the sample was subjected to another 500 cycles of wear. This procedure was repeated until the sample either showed noticeable degradation of the low-emittance surface or until the load-limit of the abrasion tested was reached. The loading in the abrasion tester was varied from a minimum of 0.20 psi to a

maximum 1.83 psi in nine incremental steps (corresponding to addition of successive one-pound loads to the upper platen).

In conjunction with the abrasion test, emittance tests were made on the radiation shields. Because the results of the abrasion tests are closely related to the emittance measurements and the development of abrasion resistance shields, the results of both the abrasion and the emittance tests on all samples are discussed in the section on development of abrasion-resistant radiation shields.

c. Emittance Measurements for Radiation Shield Surfaces

The total hemispherical emittance (hereafter referred to as emittance) of the radiation shield surface is the most important parameter in understanding the behavior and predicting the performance of multilayer insulations. During this program, many emittance measurements were made of the surfaces of candidate shields to evaluate their potential for incorporation in space suit insulation layups. The emissometer was designed and constructed by ADL in earlier NASA programs for the development of high-performance multilayer insulations for cryogenic storage vessels. (A description of the theory and operation of the emissometer is included in Reference 3.)

Table 7 summarizes the results of all the emittance tests on samples developed or used throughout the whole program. These samples include NASA-MSC-supplied materials for use in the early phases of the program, the samples developed by us--particularly those with various overcoating materials--and materials specially procured for this program. Each sample is identified, its surface condition noted, and the wear tests (if any) are noted. In several cases, the surface of the radiation shield sample was so badly worn that measurement of the emittance would have been useless. In these instances, the condition of the surface was simply noted and no emittance measurements were made. Other sample emittances were measured both before and after being subjected to successive stages of wear. In the case of those materials which withstood wear, particularly the germanium-overcoated surfaces, a full cycle of wear tests was completed, including nine incremental increases in the platen weight on the Stoll

TABLE 7. SUMMARY OF EMITTANCE AND ABRASION TESTS

Emittance Test No.	Substrate	Coating	Abrasion or Wear Test Description	Measured Emittance	Remarks
756	0.5-mil Kapton	NASA double-aluminized (300 Å)	1175 cycles at 0.204 psi	0.22	
757	0.5-mil Kapton	NASA double-aluminized (300 Å)		0.039	Not Worn
758	0.5-mil Kapton	NASA double-aluminized (300 Å)	500 cycles at 0.204 psi	0.12	
759	0.5-mil Kapton	NASA double-aluminized (300 Å)	700 cycles at 0.204 psi	0.15	
760	0.25-mil Mylar	double-aluminized	13,000 cycles in the small wear simulator	0.036	
761	0.5-mil Kapton	NASA double-aluminized (300 Å)	100 cycles at 0.204 psi	0.056	
762	0.5-mil Kapton	NASA double-aluminized (300 Å)	1000 cycles at 0.102 psi	0.083	
763	0.5-mil Kapton	NASA double-aluminized (300 Å)	500 cycles at 0.102 psi	0.054	
764	0.5-mil Kapton	NASA double-aluminized (300 Å)	100 cycles at 0.102 psi	0.050	
765	0.5-mil Kapton	NASA double-aluminized (300 Å)	700 cycles at 0.102 psi	0.070	
	1-mil Kapton	800 Å aluminum, 1000 Å anodized alum. 1800 Å aluminum	500 cycles wear at 0.204 psi	Not Measured	Adhesion of base aluminum is poor in spots, top coat of aluminum wore through in places exposing the anodized layer

TABLE 7 (Cont)

Emittance Test No.	Substrate	Coating	Abrasion or Wear Test Description	Measured Emittance	Remarks
	1-mil Kapton	200-500 Å chromium sublayer 1800 Å aluminum	500 cycles wear at 0.204 psi	Not Measured	Aluminum wore through over large area of sample
	0.5-mil Kapton	NASA double-aluminized (300 Å)	Beta Marquisette spacer was coated with heavy layer of indium metal; sample subjected to 100 cycles at 0.204 psi	Not Measured	Aluminum surface badly worn away; indium metal probably masked the silicone lubrication in the Beta Marquisette spacer
	0.5-mil Kapton	NASA double-aluminized (300 Å); lightly coated with dimethyl polysiloxane	500 cyles wear at 0.204 psi	Not Measured	Slight signs of wear
	1-mil Kapton	5000 Å of germanium vapor-deposited	500 cycles at 0.204 psi 500 additional cycles at 0.306 psi	Not Measured	No sign of wear Slight sign of wear
777 } 781	0.5-mil Kapton	NASA double-aluminized (300 Å) and 1100 Å vapor-deposited germanium	As coated 600 cycles at 0.204 psi 400 cycles at 0.306 psi	0.025 0.026	
778	0.5-mil Kapton	NASA double-aluminized (300 Å)	-	0.025	Material tested as received
782 } 786	0.5-mil Kapton	NASA double-aluminized (300 Å) and 500 Å vapor-deposited germanium	As coated 600 cycles at 0.204 psi and 400 cycles at 0.306 psi	0.026 0.026	
783 787	0.5-mil Kapton	NASA double-aluminized (300 Å) and 2000 Å vapor-deposited germanium	As Coated 600 cycles at 0.204 psi and 400 cycles at 0.306 psi	0.065 0.066	

TABLE 7 (Cont)

Emittance Test No.	Substrate	Coating	Abrasion or Wear Test Description	Measured Emittance	Remarks
784	Style 1659 dipped in Kapton	500 Å vapor-deposited aluminum	-	0.047	ADL developed composite shield-and-spacer
788	0.25-mil Mylar	NRC single-aluminized (NRC stock)	-	0.029	
789	0.25-mil Mylar	NRC single-aluminized (ADL stock)	-	0.023	
790	0.5-mil Kapton	NASA double-aluminized (300 Å) 1% Dow-Corning 704 silicone oil	500 cycles at 0.20 psi 500 cycles at 0.31 psi	0.067	
	0.5-mil Kapton	0.1% Dow-Corning 704 silicone oil	Same above		
	0.5-mil Kapton	0.01% Dow-Corning 704 silicone oil	Same above	Badly worn; not tested	
	0.5-mil Kapton	0.001% Dow-Corning 704 silicone oil	Same above		
	0.5-mil Kapton	0.0001% Dow-Corning 704 silicone oil	Same above		
791	0.5-mil Kapton	NASA double-aluminized (300 Å) 1% D.C. 704 applied to abrasion fabric	Same above	0.097	
792	0.25-mil Mylar	Gold-standard sample No. 352A		0.017	
793	0.25-mil Mylar	NRC single-aluminum (ADL Stock)		0.33	Uncoated side
794	0.5-mil Kapton	NASA double-aluminized (300 Å) bonded to Stevens Style 2530		0.032	Aluminized side

TABLE 7 (Cont)

Emittance Test No.	Substrate	Coating	Abrasion or Wear Test Description	Measured Emittance	Remarks
795	0.5-mil Kapton	NASA double aluminized (300 Å);bonded to Stevens Style 2530		0.037	Aluminized side
796	0.5-mil Kapton	NASA double aluminized (300 Å); bonded to Stevens Style 2530		0.029	Aluminized side
797	Beta Marquisette	NASA double aluminized (300 Å); bonded to Stevens Style 2530		0.56	Spacer side
798	Beta Marquisette	NASA double aluminized (300 Å); bonded to Stevens Style 2530		0.51	Spacer side
799	Beta Marquisette	NASA double aluminized (300 Å); bonded to Stevens Style 2530		0.53	Spacer side
800	Beta Marquisette	NASA double aluminized (300 Å); bonded to Stevens Style 2530		0.56	Spacer side
802	0.5-mil Kapton	NASA double aluminized (300 Å); 1% Dow-Corning 700 silicone oil	500 cycles at 0.20 psi 500 cycles at 0.31 psi	0.052	
804	0.5-mil Kapton	NASA double aluminized (300 Å); 1% Dow-Corning 704 silicone oil	Same	0.041	
805	0.5-mil Kapton	NASA double aluminized (300 Å); 1% Dow-Corning 550 silicone oil	Same	0.027	
809	0.5-mil Kapton	NASA double aluminized (300 Å); 1% Dow-Corning silicone oil applied to abrasion fabric	Same	0.034	

TABLE 7 (Cont)

Emittance Test No.	Substrate	Coating	Abrasion or Wear Test Description	Measured Emittance	Remarks
808	0.5-mil Kapton	NASA double aluminized (300 Å); 1% Dow-Corning 550 silicone oil on aluminized surface	As coated	0.047	
807	0.5-mil Kapton	1% Dow-Corning 200 silicone oil	As coated	0.027	
806	0.5-mil Kapton	1% Dow-Corning 704 silicone oil	As coated	0.028	
803	0.5-mil Kapton	NASA double aluminized (300 Å); 600 Å germanium and 1% Dow-Corning 200 silicone oil (1000Å)	500 cycles at 0.20 psi 500 cycles at 0.31 psi 500 cycles at 0.41 psi 500 cycles at 0.61 psi 500 cycles at 0.82 psi 500 cycles at 1.02 psi 500 cycles at 1.22 psi 500 cycles at 1.43 psi 500 cycles at 1.63 psi 500 cycles at 1.83 psi	0.029	Emittance was not measured before wear
810	Beta Marquisette	Schjeldahal Style 993		0.53	Spacer side
811	0.5-mil Kapton			0.029	Shield side
813	0.5-mil Kapton	NASA double aluminized (300 Å); 600 Å germanium	500 cycles at 0.20 psi 500 cycles at 0.31 psi 500 cycles at 0.41 psi 500 cycles at 0.61 psi 500 cycles at 0.82 psi 500 cycles at 1.02 psi 500 cycles at 1.22 psi 500 cycles at 1.43 psi 500 cycles at 1.63 psi 500 cycles at 1.83 psi	0.027	
812	0.5-mil Kapton	NASA double aluminized (300 Å); 600 Å germanium; 1% Dow-Corning 550 silicone oil		0.028	

TABLE 7 (Cont)

Emittance Test No.	Substrate	Coating	Abrasion or Wear Test Description	Measured Emittance	Remarks
815	ADL Kapton on Stevens Style 2530	500 Å aluminum, vapor-deposited	-	0.021	
816	1-mil Kapton	1000 Å gold, vapor-deposited	-	0.016	
817	1-mil Kapton	1000 Å gold, vapor-deposited; 600 Å germanium	-	0.017	
817-A	1-mil Kapton	1000 Å gold, vapor-deposited; 600 Å germanium	1500 cycles at 0.20 psi 500 cycles at 0.82 psi 1500 cycles at 2.0 psi	0.027	
818	0.5-mil Kapton	NASA double-aluminized (300 Å); 1000 Å silicon monoxide		0.047	
819	0.5-mil Kapton	NASA double-aluminized (300 Å); 1000 Å silicon monoxide	500 cycles at 0.20 psi 300 cycles at 0.82 psi 1000 cycles at 2.0 psi	0.047	
-	1-mil Kapton	1000 Å aluminum, vapor-deposited	500 cycles at 0.20 psi 500 cycles at 0.41 psi	-	Badly worn, not tested
820	1-mil Kapton	1000 Å gold, vapor-deposited	750 cycles at 0.20 psi 500 cycles at 0.41 psi 640 cycles at 0.61 psi 800 cycles at 0.82 psi 750 cycles at 1.22 psi 500 cycles at 2.0 psi	0.025	
-	1-mil Kapton	1000 Å aluminum, vapor-deposited; half of sample anodized to oxide thickness of 200 Å	500 cycles at 1.83 psi	-	Nonanodized surface was badly worn; anodized surface not significantly worn

TABLE 7 (Cont)

Emittance Test No.	Substrate	Coating	Abrasion or Wear Test Description	Measured Emittance	Remarks
821	1-mil Kapton	1000 Å gold, vapor-deposited	500 cycles at 0.20 psi 500 cycles at 1.02 psi 500 cycles at 1.83 psi	0.025	
822	1-mil Kapton	1000 Å gold, vapor-deposited; 600 Å germanium	500 cycles at 0.20 psi 500 cycles at 1.02 psi 500 cycles at 1.83 psi	0.018	
823	1-mil Kapton	Hanovia 8342 liquid bright gold fired at 600°F	-	0.0185	
827				0.0186	
824	1-mil Kapton	Hanovia 8342 fired at 600°F	500 cycles at 0.20 psi 500 cycles at 1.02 psi 500 cycles at 1.83 psi	0.022	
825	1-mil Kapton	Hanovia 9342 fired at 600°F; 1% Dow-Corning 550		0.020	
826	1-mil Kapton	Hanovia 8342 fired at 600°F; 600 Å germanium		0.020	
828	ADL Kapton on Stevens Style 1659	500 Å aluminum vapor-deposited		0.060	
830	0.5-mil Kapton	NASA double-aluminized (300 Å)		0.027	As received
831	0.5-mil Kapton	NASA double-aluminized (300 Å)	1000 cycles in the pilot wear tester, 0.81 psi load	0.027	
832	0.5-mil Kapton	NASA double-aluminized (300 Å)	1500 cycles in the pilot wear tester, 0.81 psi load	0.023	

TABLE 7 (Cont)

Emittance Test No.	Substrate	Coating	Abrasion or Wear Test Description	Measured Emittance	Remarks
833	0.5-mil Kapton	NASA double-aluminized (300 Å)	2000 cycles in the pilot wear tester, 0.81 psi load	0.024	
834	0.5-mil Kapton	NASA double-aluminized (300 Å)	10,000 cycles in the pilot wear tester, 0.81 psi load	0.031	
835	0.5-mil Kapton	NASA double-aluminized (300 Å) with 500 Å germanium both sides	-	0.022	A side
837			-	0.030	B side
836	0.25-mil Mylar	Vapor-deposited gold	-	0.016	ADL calibration sample No. 352A
838	0.5-mil Kapton	NASA double-aluminized (300 Å)		0.026	B side
840	0.5-mil Kapton	NASA double-aluminized (300 Å) with 500 Å germanium both sides	1000 cycles in the pilot wear tester, 0.81 psi	0.027	A side
841				0.031	B side
843	0.5-mil Kapton	NASA double-aluminized (300 Å) with 500 Å germanium both sides	10,000 cycles in the pilot wear tester, 0.81 psi	0.031	B side
844	0.5-mil Kapton	NASA double-aluminized (300 Å) with 500 Å germanium both sides	100,000 cycles in the pilot wear tester	0.029	A side
845				0.032	B side
846	0.5-mil Kapton	500 Å aluminum, 500 Å germanium	-	0.024	ADL prepared sample
865	1.0-mil Kapton	Liquid bright gold	-	0.014	AGC sample No. 64-58-1

TABLE 7 (Cont)

Emittance Test No.	Substrate	Coating	Abrasion or Wear Test Description	Measured Emittance	Remarks
872	1.0-mil Kapton	1100 Å liquid bright gold, both sides	As received	0.018	
874	1.0-mil Kapton	1100 Å liquid bright gold, both sides	500 cycles at 0.20 psi 500 cycles at 0.41 psi 500 cycles at 0.61 psi 500 cycles at 0.82 psi 500 cycles at 1.02 psi 500 cycles at 1.22 psi 500 cycles at 1.43 psi 500 cycles at 1.63 psi 500 cycles at 1.83 psi	0.025	Lot acceptance tests for materials from AGC, Inc. in Meriden, Conn.
873	0.5-mil Kapton	900 Å aluminum and 500 Å germanium overcoating both sides	As Received	0.026	
875	0.5-mil Kapton	900 Å aluminum and 500 Å germanium overcoating both sides	500 cycles at 0.20 psi 500 cycles at 0.41 psi 500 cycles at 0.61 psi 500 cycles at 0.82 psi 500 cycles at 1.02 psi 500 cycles at 1.22 psi 500 cycles at 1.43 psi 500 cycles at 1.63 psi 500 cycles at 1.83 psi	0.025	Lot acceptance tests for materials from National Metallizing Div., Cranbury, N.J.
876	0.5-mil Kapton	900 Å aluminum both sides	As received	0.021	
948	0.25-mil Mylar	vapor-deposited gold	-	0.016	ADL calibration sample No. 352A

TABLE 7 (Cont)

Emittance Test No.	Substrate	Coating	Abrasion or Wear Test Description	Measured Emittance	Remarks
949 950	0.5-mil Kapton	900 Å and 500 Å germanium overcoating both sides	As received	0.021 0.023	Inside of Roll Outside of Roll Materials from National Metallizing Div., Cranbury N.J.
951 952	0.5-mil Kapton	900 Å aluminum, both sides	As received	0.020 0.020	Inside of roll Outside of roll Materials from National Metallizing Div., Cranbury N.J.
953 954	0.5-mil Kapton	900 Å aluminum and 500 Å germanium overcoating, both sides	10,000 cycles of wear in a space suit section	0.038 0.045	A side B side Space suit section tested on the elbow calorimeter is simulated lunar environments

abrasion tester until the load limit of the tester was reached (9-pound load--a compressive loading of 1.83 psi).

d. Physical Properties

(1) Tensile Strength. The ultimate tensile strength of radiation shields, spacers, and composite radiation shield and spacers was measured by the grab method [Federal Specification-interim method 5100.1 (DOD) CCC-T-191b]. The specimens were four inches wide and six inches long with the long dimension parallel to the direction being tested. In the case of woven fabrics, the long dimension was parallel to the warp when determining warp breaking strength, and parallel to the fill when determining fill strength. In each determination, a minimum of three specimens for each direction was tested from each sample unit. The pulling clamp had a uniform speed of 12 $\pm$ 0.5 inches per minute. The results of the tensile strength tests, as well as results of tests of other physical properties, are summarized in Table 8.

(2) Tear Strength. The tear strength of woven fabrics used as spacer materials and in composite radiation shields was measured by the tongue (single-rip) method in a tensile-testing machine with a constant rate of extension. The tear resistance of plastic film and thin sheeting was tested in the same manner. A rectangular specimen, cut in the center of the shorter edge to form two tongues (or tails), is gripped in the clamps of a recording tensile-testing machine and pulled to simulate a rip. The force to continue the tear is determined from the average of the five highest peaks. If the tear in the material was not substantially lengthwise, the sample was described as untearable in that direction by this test method. The results of tear strength (propagating) tests are summarized in Table 8.

(3) Fold Endurance. The flexure endurance of radiation shields, spacers, and composites was measured in an MIT-type folding apparatus according to ASTM standard D2176-63T. A sample strip, 15 millimeters wide, is held on one end in a spring-loaded clamping jaw and a load from 0.5 to 1.5 kilograms is applied to the sample strip. The strip is held on the other end by an oscillating folding head which has

TABLE 8. SUMMARY OF MEASURED RADIATION SHIELD AND SPACER PROPERTIES

Description of Material	Flammability: 100% Oxygen 16.5 psia	Flammability: 100% Oxygen 6.2 psia	Flammability: Air 14.7 psia	Ultimate Tensile Strength (lbs/in)	Tear Strength (Propagating) (grams)	Flexure Endurance Under Load[2] (cycles)	Flexure Endurance Under Load[2] (kg)	Useful Temperature Range[3] (°F)	Stability in Vacuum[4] (% weight change)	Adhesion of Coatings	Surface Emittance	Abrasion Resistance
RADIATION SHIELDS												
Polyimide film, 0.5-mil Kapton with 300 Å vapor-deposited aluminum on both sides	F	F	F	35	2.7	11,000	1.5	-450 to 750	1.1	G	0.025	F
Polyimide film, 0.5-mil Kapton with 300 Å vapor-deposited aluminum and 500 Å vapor-deposited germanium overcoating on both sides	F	F	F	35	2.7	26,000	1.5	-450 to 750	0.9	G	0.026	E
Polyimide film, 1-mil Kapton with 1000 Å liquid bright gold on both sides	F	F	F	76	8	<16,000	1.5	-450 to 750	0.5	G	0.019	G
Polyimide film, 1-mil Kapton with 1000 Å liquid bright gold and 600 Å vapor-deposited germanium overcoating on both sides	F	F	F	76			-	-450 to 750	0.8	G	0.020	E
Polyester film, 0.25-mil Mylar with vapor-deposited aluminum on both sides	F	F	F	15	1.3	<27,000	0.5	-75 to 300		G	0.023	P
Laminated film, 0.5-mil polyimide (Kapton) and 0.5-mil fluorinated ethylene propylene (FEP Teflon)	F	F	F	60	36	17,000	1.5	-100 to 400				
COMPOSITE RADIATION SHIELD AND SPACER												
Integrated spacer and radiation shield, Stevens Style 1659 dipped in Kapton and with 500 Å vapor-deposited aluminum on both sides	F	F		120w 140f	NT	80w 60f	1.0 1.0	-450 to 750	1.0	G	0.047-0.060	-
Laminate of radiation shield and spacer, Schjeldahl Style X993, 0.5-mil Kapton with vapor-deposited aluminum on both sides bonded to Beta Marquisette with self-extinguishing Schjeldahl adhesive A61 which was applied to the radiation shield	F	F		55w 53w	NT	<30,000w <13,000f	1.5 1.5	-300 to 500		G	0.021-0.037al 0.51-0.56sp	
Laminate of radiation shield and spacer, 0.5-mil Kapton with vapor-deposited aluminum on both sides bonded to Stevens Style 2530 Beta Marquisette with RTV silicone rubber (GE 102) which was applied to the spacer	F	F		100w 80f	NT	4,000w <18,000f	1.5 1.5	-300 to 500	1.1	G	0.029al 0.53sp	

TABLE 8 (Cont)

Description of Material	Flammability: 100% Oxygen 16.5 psia	Flammability: 100% Oxygen 6.2 psia	Flammability: Air 14.7 psia	Ultimate Tensile Strength (lbs/in)	Tear Strength (Propagation) (grams)	Flexure Endurance Under Load(2) (cycles)	(kg)	Useful Temperature Range (°F)	Stability in Vacuum(4) (% weight change)	Adhesion of Coatings	Surface Emittance	Abrasion Resistance
SPACERS												
Beta fiberglass Marquisette, Stevens Style 2530 unstabilized	NF	NF		36w 54f	NT	20,000w <40,000f	0.5 0.5	-450 to 1000	0.9			
Beta fiberglass Marquisette, Stevens Style 2530 stabilized with approximately 5% of epoxy (Shell Type 828 and 10% TETA curing agent)	F(1)	F(1)		71w 71f	NT	280w 480f	0.5 0.5	-70 to 300	1.4			
Fiberglass plain weaver, Stevens Style 104 unstabilized	NF Q	NF		2.7w 2.5f	NT	<40,000w <10,000f	0.5 0.25	-450 to 1000				
Fiberglass plain weave, Stevens Style 104 stabilized with approximately 5% of epoxy (Shell Type 828 and 10% TETA curing agent)	F(1)	F(1)		40w 20f	NT	3,500w 3,500f	0.5 0.5	-70 to 300	1.1			
Fiberglass plain weave, Stevens Style 104 stabilized with approximately 5% of Ultrathene (ethylene vinyl acetate copolymer)	F(1)	F(1)		80w 40f	NT	<16,000w 20,000f	0.5 0.5	-70 to 300				
Dacron batt, National Research Division of Norton, nonwoven, 15 gm/sq yd, 0.0015-inch thick	F	F		7.5w 1.6f	NT	<10,000w NT f	0.5	to 350				
Polyurethane foam, Scott standard pink foam, 100 pores per inch and 0.030-inch thick	F	F		1.5		NT		-30 to 275	2.0			

Code:

F	Flammable
NF	Not Flammable
w	warp direction
f	fill direction
NT	Sample was not testable
E	Excellent
G	Good
P	Poor
al	aluminized side
sp	spacer side

Notes:
(1) Stabilizing polymer is flammable; base material is nonflammable.
(2) Many samples not tested to destruction--tests terminated after 10,000 cycles, sample width 15mm.
(3) Manufacturers specifications
(4) Percent weight change in 10^{-4} torr vacuum after 45 hours at 250°F.

two smooth cylindrical folding surfaces parallel to and symmetrically placed with respect to the axis of rotation. The sample is clamped between the two cylindrical folding surfaces. The position of the axis of rotation is midway between the common tangent planes of the two folding surfaces. The rotary oscillating movement of the head folds the sample to an angle of 135° to the right and to the left of the flat position. In all tests, the specimen was flexed to more than 10,000 cycles or until failure occurred. The results (Table 8) indicate the number of cycles and the loading on the sample.

(4) Stability in Vacuum. Candidate materials were evaluated for stability in a vacuum at room temperature, -320°F, and 250°F. In this evaluation, candidate samples of the material were placed in a temperature-controlled vacuum oven where the pressure was maintained at less than 10^{-4} torr. Two sets of samples were used, one for the ambient temperature and one for both the low- and high-temperature weight-loss tests. In each test, the samples were accurately weighed on a laboratory scale and placed in the chamber, which was then evacuated and maintained at the test temperature. After periods ranging from 22 to 64 hours, the samples were removed and carefully weighed to determine their weight loss. The samples were then returned to the vacuum oven and the test was continued. Results of this series of tests are summarized as the percent change in weight of the sample as a function of exposure time. As expected, the samples all showed an initial weight loss after the first exposure to vacuum. In the case of samples exposed at 250°F, the sample weight loss was noticeably higher than the weight loss for the cold- and ambient-temperature tests. The weight loss occurs sooner at the higher temperature. Table 8 lists stability in a vacuum for most of the important materials used in this study as the percent weight change after 45 hours at 240°F in 10^{-4} torr vacuum.

3. Development of Abrasion-Resistant Radiation Shields

a. Baseline

The baseline insulation used in this study included aluminized polyester (Mylar) radiation shields. As a baseline for development of

abrasion-resistant radiation shields, we used NASA-supplied aluminized polyimide (Kapton) film. We believe that for abrasion resistance of low-emittance surfaces, vapor-deposited aluminum on polyimide behaves in the same way as does vapor-deposited aluminum on polyester.

In the preliminary evaluation of aluminized polyester radiation shields, several samples of NASA-supplied 0.5-mil Kapton with vapor-deposited aluminum on both sides were subjected to wear tests. Visual examination of samples after 100, 500 and 1,000 cycles indicated that noticeable wear begins after approximately 100 cycles and that considerable degradation of the aluminum surface occurs before 1,000 cycles. The emittance of these samples which had been subjected to increasing numbers of cycles in the test machine were measured. Two different compressive loads were used: 0.102 and 0.204 psi. The results of these tests are tabulated for sample numbers 756 through 759 and 761 through 765 in Table 7.

A plot of the results of these emittance degradation tests (Figure 1) indicates that the sample emittance degrades with increasing wear cycles. Under a constant load of one pound (0.204 psi), the sample degrades more rapidly than under a constant load of one-half pound (0.102 psi).

Each of the NASA-supplied samples of double-aluminized Kapton was checked for coating thickness by measuring the resistance per square of both sides. The results indicated that one side had a coating thickness of about 240 Å and the other about 310 Å. The average thickness of 300 Å is less than we have found optimum for radiation shields. In a study for NASA-Lewis Research Laboratories (Reference 4), we found that minimum emittance is obtained when the vapor-deposited aluminum is thicker than 500 Å.

b. Preliminary Surface Coating Investigations

Early in our development of abrasion-resistant surfaces for radiation shields, we tested four techniques, none of which proved feasible. The results of these preliminary tests are listed following Sample 765 in Table 7.

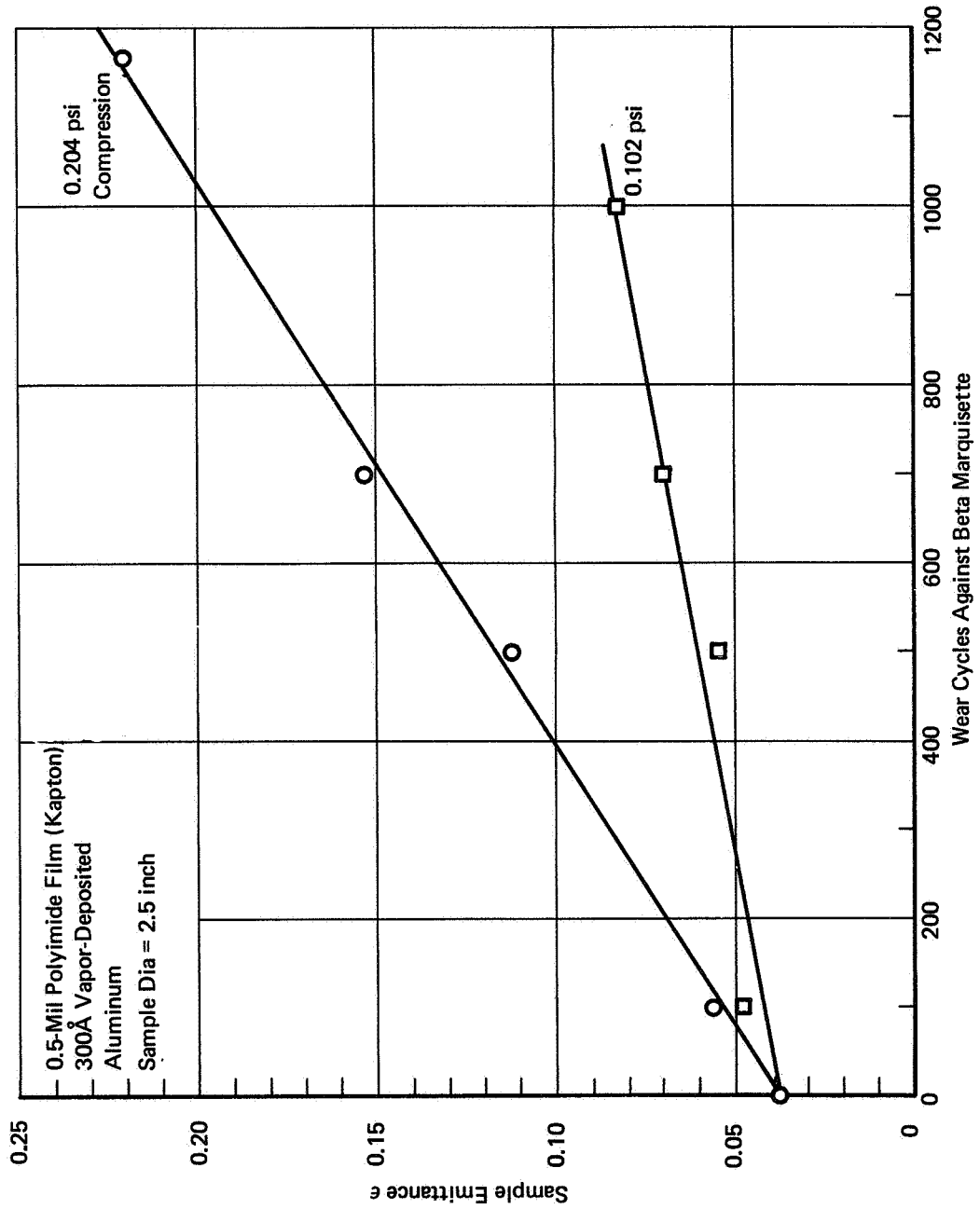

FIGURE 1 SAMPLE EMITTANCE DEGRADATION AS A FUNCTION OF ABRASIVE WEAR

In the first test involving double-coated surfaces, we applied an extremely thick layer (1800 Å) of aluminum on a 1-mil Kapton substrate and anodized this aluminum to a depth of approximately 1000 Å. An overcoating of aluminum was then vapor-deposited on the anodized aluminum undercoating, since, if the top layer of low-emittance aluminum were subjected to wear, the anodized aluminum layer might be exposed. The anodized aluminum transmits infrared energy and the base aluminum still functions as a good radiation shield. This sample was tested at 500 cycles wear at 0.204 psi. Results indicate that the top coat of aluminum did wear through in places, exposing the anodized aluminum layer, and that the adhesion of the base aluminum was poor in spots. We believe that poor control of the anodizing procedure may have caused the poor adhesion of the base aluminum.

In the second test, we vapor-deposited 200-500 Å of chromium on a 1-mil Kapton substrate. We then applied 1800 Å of aluminum on top of the chromium, so that if the aluminum on top was worn away, the hard chromium sublayer (being a fairly good low-emittance surface) would provide a better emitting surface than just the Kapton. This sample was subjected to 500 cycles wear at 0.204 psi. Again, the aluminum wore through over a large area of the sample, exposing the hard chromium sublayer. The concept of a double-coated surface, although considered promising as a result of these tests, was abandoned in favor of other techniques.

In a third test, we coated the Beta marquisette spacer with a heavy layer of indium metal, which, being softer than the aluminum, would act like a lubricant between the fiberglass and the shield. NASA-supplied double-aluminized (300 Å) Kapton was used as the base sample for testing. The aluminum surface was badly worn away after 100 cycles at 0.204 psi. This technique was abandoned.

In the fourth test, we lightly coated a surface of NASA-supplied double-aluminized (300 Å) Kapton with dimethyl polysiloxane. Subjected to 500 cycles wear at 0.204 psi, this sample showed only slight signs of wear. We concluded that small amounts of silicone lubricant might be beneficial.

c. Germanium Overcoating

A 5000 Å layer of germanium was vapor-deposited on a sample of NASA-supplied double-aluminized Kapton. After a 500-cycle wear test at 0.204 psi, there was no visual sign of surface deterioration. Then, 500 additional cycles of wear were made at 0.306 psi and only slight signs of wear appeared. From this initial screening test (listing preceding Sample No. 777 in Table 7), we concluded that a very hard and wear-resistant surface could be achieved on aluminized Kapton by vapor-deposition of germanium.

We continued the study of germanium as an overcoating for aluminized surfaces. Samples of NASA-supplied double-aluminized Kapton were coated with 500, 1100 and 2000 Å of germanium and the emittances were measured both before and after wear (see Tests 777, 781, 782, 786, 783, and 787 in Table 7). The sample with approximately 500 Å of germanium had an emittance of 0.026 before wear (test 782) and the same emittance after wear (test 786). The sample with 1100 Å of germanium had an emittance of 0.025 before wear (test 777) and 0.026 after wear (test 781), and the sample with 2000 Å of germanium had an emittance of 0.065 before wear (test 783) and 0.066 after wear (test 787). From these measurements, we concluded that approximately 500 Å of germanium is sufficient for protecting an aluminized surface on Kapton against rather severe abrasion and that thicknesses of germanium less than 1000 Å do not significantly degrade the emittance of the aluminized surface.

Samples of germanium-overcoated aluminized Kapton were subjected to 500 cycles of wear against Beta marquisette at successively increasing loads from 0.204 psi up to 1.83 psi. (See tests 803, 812, and 813, Table 7.) The measured emittance of the surface of each sample was in the range from 0.027 to 0.029, which indicates very little degradation. We then concluded that a 500 Å germanium coating contributes greatly to the mechanical protection of low-emittance surfaces and does not significantly degrade its low emittance properties.

d. Gold Coatings

Gold coatings for half-mil polyimide (Kapton) films appear to be good alternatives to germanium-overcoated vapor-deposited aluminum on this same substrate. A liquid bright gold process appears to offer a tougher gold surface than does vapor deposition.

(1) Vapor-Deposited Gold. Samples of vapor-deposited gold were applied to one-mil polyimide films. As found in previous programs,[3] gold provides a very low-emittance surface; in this instance the emittance was 0.016. (See test 816, Table 7.) Germanium overcoating was also applied and samples were subjected to the standard wear test. The addition of 500 Å of germanium does not significantly degrade the low-emittance gold surface (see test 817) and with the germanium overcoating, the overall emittance of the sample is less than the overall emittance of the aluminized sample without germanium overcoating.

Samples of both overcoated and unprotected gold on Kapton were subjected to abrasion-wear tests. We found that the unprotected gold did not wear as fast as we had thought it might and that after a severe series of tests, the emittance had not degraded substantially. (See test 820.) The sample of germanium-overcoated gold showed negligible degradation in emittance after the sample had been subjected to wear tests (see test 822).

(2) Liquid Bright Gold Surfaces. We investigated low-emittance gold finishes applied by a commercial low-temperature firing-on procedure. In this technique, we used Hanovia 8342 Liquid Bright Gold* finish which, when applied in solution form and fired at 600°F, produced a brilliant gold finish. When tested for emittance, this surface had an emittance only slightly higher than that of vapor-deposited gold (see tests 823 and 827). Samples prepared by this technique were subjected to wear and then retested for emittance. They exhibited only slight

*Solutions were obtained from Hanovia Division of Engelhard Industries, Newark, N.J.

degradation after a standard series of wear tests. (See test 824.) Samples were also prepared with 500 Å of germanium overcoating and subjected to the same wear tests. The usual degradation in emittance when overcoated with germanium was observed. It thus appears that a commercially available liquid bright gold coating on Kapton film is feasible for achieving low-emittance surfaces for space suit insulation radiation shields. The advantages of this method of surface application are that it does not require a vacuum-deposition procedure and that standard machine-coating techniques are capable of achieving the desired finish at costs which are comparable to or less than those of present vapor-deposition techniques because there is less loss of basic gold raw material than is the case with vapor deposition.

e. Other Coatings

(1) Silicone Lubricants. We quantitatively determined that coating an aluminized surface with silicone oil lubricant does not increase the wear resistance. Several NASA-supplied double-aluminized Kapton samples were coated with Dow Corning 704 silicone oil lubricants suspended in acetone. A few drops of the dilute silicone lubricant were placed on the sample surface and the sample then spun on a rotating table to evenly distribute the lubricant. Several samples with amounts of silicone oil ranging from 0.0001% to 1.0% by weight were subjected to 500 cycles of wear at 0.204 psi and 500 cycles at 0.306 psi. In all instances microscopic examination of the samples showed signs of considerable wear, so they were not tested for emittance. Thus it appears that concentrations of oil in excess of 1% are required to provide minimum protection for the sample.

Several different silicone oils were then tested at the 1% level. Samples of NASA-supplied double-aluminized Kapton were prepared by the spinning method. For each silicone oil tested, two samples were prepared: one was tested as coated and the other was tested after being subjected to 500 cycles at 0.204 psi and 500 cycles at 0.306 psi. The test results (tests 802, 804, and 805 through 809 in Table 7) indicate that the presence of silicone oil in 1% solution does not significantly affect

the emittance of the surface; neither does it provide very much wear protection. For instance, comparing sample 807 with sample 802, we see that the emittance nearly doubles after wear testing.

A test was performed to determine if it would be better to place the lubricating silicone oil on the radiation shield surface or on the spacer material. Comparing tests 778 and 809, we see that by dipping the spacer test cloth in the 1% solution of lubricating oil and then subjecting the standard NASA-supplied double-aluminized Kapton surface to 500 cycles wear at 0.204 psi and 500 cycles at 0.306 psi, the aluminized surface was noticeably degraded and the emittance was increased from 0.025 to 0.034.

(2) Silicon Monozide and Aluminum Oxide Overcoatings. We tried overcoating the NASA-supplied double-aluminized Kapton by vapor-depositing silicon monoxide in thicknesses of approximately 200 Å. When subjected to wear, the silicon monoxide proved to be a very fine surface protector. (See tests 818 and 819.) However, although transparent in the visible spectrum, silicon monoxide is not transparent in the far infrared; consequently, the room-temperature emittance of a silicon monoxide overcoated sample is almost double that of the uncoated samples.

A sample of material was prepared by vapor-depositing a heavy layer of aluminum on a 2.5-inch-diameter sample of Kapton and then anodizing half of the sample until an aluminum oxide layer approximately 200 Å thick was achieved. The sample was then placed in the wear tester and subjected to 500 cycles at a loading of 1.83 psi. During this wear test, the non-anodized surface was rapidly degraded, whereas the anodized surface did not degrade noticeably. Some difficulty was experienced in achieving uniform anodizing on the surface. In some areas, all of the aluminum coating was removed during the anodizing process. Attempts to anodize full samples were not successful.

f. Summary

We found that it is possible to produce on Kapton substrates low-emittance coatings which adhered well and which will withstand the severe abrasion-testing procedures established for this program. The most vulnerable surface is vapor-deposited aluminum. We found that gold surfaces, either vapor-deposited or fired-on by a commercially available

liquid bright gold process, are remarkably tough (particularly the fired-on process).

The use of an overcoating material, such as germanium over aluminum or gold, is very successful in providing the desired wear characteristics for the radiation shields. Of the three materials tested (germanium, silicon monoxide, and anodized aluminum), we found that 500 Å of germanium provides the best protection with the least degradation of emittance. Silicon monoxide, although transparent in the visible spectrum, is not transparent in the infrared. Thus, the emittance degrades quite rapidly when small amounts of silicon monoxide are added to the low-emittance surface. In order to anodize vapor-deposited aluminum surfaces, it will be necessary to develop a special technique for passing the required high currents through the thin surface coating without degrading the aluminum in random spots. Our attempts to achieve uniformly anodized surfaces were not successful.

4. Development of Composite Radiation Shields and Spacers

Early in the program, NASA-MSC provided us with a sample of space suit insulation made with composite radiation shields (Schjeldahl Style X-993) consisting of half-mil, double-aluminized Kapton which had been bonded to a Beta marquisette fiberglass spacer (similar to Stevens Style 2530) with a self-extinguishing adhesive (Schjeldahl No. A-61). The outstanding characteristic of this material is that it is highly flexible, which is desirable in a space suit application. However, by applying the adhesive to one side of the radiation shield, one low-emittance surface of the radiation shield is badly degraded. To overcome this problem, we developed a lamination technique whereby small amounts of silicone adhesive were transferred only to those portions of the Beta marquisette spacer which come in contact with the radiation shield. Thus, we obtained a good bonding contact between the spacer and the radiation shield without excessive adhesive being left on the low-emittance surface.

Early in the development program, we came up with an idea for a composite thermal radiation shield and spacer (Figure 2) which might

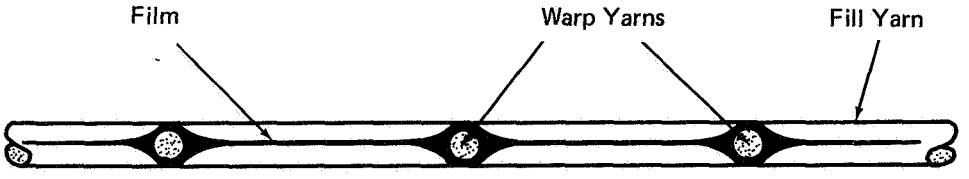

FIGURE 2 COMPOSITE THERMAL RADIATION SHIELD AND SPACER

have good load-bearing capability when compressed, yet at the same time have low thermal conductance. It combines the function of a radiation shield with a spacer in one structure and can be made by dipping an open-mesh Beta fiberglass fabric in a polymeric film solution. Through suitable control, a high-strength film with a smooth, continuous finish will form in the open spaces between the warp and fill yarns of the fabric. After the film is cured, both surfaces of the composite spacer can be coated with a low-emittance material such as vapor-deposited aluminum.

We experimented with various polymeric solutions to achieve bubble-bridging between the yarns of several open-mesh fabrics, including neoprene rubber, acrylic, polyvinyl acetate, polyvinyl alcohol, and polyimide (Kapton). The best results were obtained with samples of Stevens Style 1659 stretched on 15-inch-diameter hoops and dipped-coated in a solution of Kapton (DuPont, Pyre ML, RC-5057).

The samples were then oven-dried, vapor-deposited with aluminum on each surface (thickness approximately 500 Å to 600 Å), and a space suit insulation layup made and tested from this material. (The results of these tests are summarized in Section IV.) Unfortunately, the material which we produced was much too stiff for use as a space suit insulation and, after the thermal conductance measurements were completed, the program for a composite radiation shield-spacer insulation was abandoned.

5. Best Radiation Shields and Spacers

At the conclusion of the materials development phase of the program, we selected four radiation shields, three spacers, and two composite radiation shields and spacers for further study in combination with each other as space suit insulations. The general specifications for these materials are listed in Table 9.

TABLE 9. SELECTED RADIATION SHIELDS, SPACERS AND COMPOSITES

Radiation Shields

Polyimide film with 500 Å vapor-deposited aluminum on both sides.

Polyimide film with 500 Å vapor-deposited aluminum and 500 Å germanium overcoating on both sides.

Polyimide film with 1000 Å liquid bright gold coating on both sides.

Polyimide film with gold coating and germanium overcoating on both sides.

Composite Shield-and-Spacer

Integrated spacer and radiation shield with low-emittance coating on both sides.

Spacer laminated to the radiation shield.

Spacers

Fiberglass fabrics--leno-weave Stevens Style 2530, both unstabilized and stabilized.

Fiberglass fabrics--plain-weave Style 104, both unstabilized and stabilized.

Thin sheets of open-cell flexible polyurethane foam.

IV. EVALUATION OF RADIATION SHIELD AND SPACER COMBINATIONS

Many space suit insulations can be formed from combinations of the four radiation shields, three spacers, and two composite radiation shield and spacer materials specified in Table 9. From the list of shields and spacers, we selected the following four combinations for evaluation of thermal conductance and obtained sufficient materials for the evaluation program:

- Radiation shields of 1.0-mil Kapton with 1700 Å liquid bright gold both sides and 0.030-inch flexible open-cell polyurethane foam spacers.
- Radiation shields of 0.5-mil Kapton with 800 Å aluminum and 500 Å germanium both sides, and 0.030-inch flexible open-cell polyurethane foam spacers.
- Radiation shields of 0.5-mil Kapton with 800 Å aluminum and 500 Å germanium both sides, and Stevens Style 2530 Beta marquisette.
- Radiation shields of 0.5-mil Kapton with 800 Å aluminum and 500 Å germanium both sides, and Style 104 fiberglass scrim stabilized with 5% Ultrathene epoxy.

These samples were subjected to nondestructive simulated wear tests prior to being tested for thermal conductance under compressive loads ranging from zero to 15 psi, temperatures ranging from -250° to 300°F, and at a vacuum of 10^{-5} torr. The two most desirable material combinations (based upon the initial thermal conductance tests) were chosen for further testing in the unworn condition. We also measured the thermal conductance of an insulation which was similar to the layup used in the Gemini space suits and two additional samples: one a laminate and another a composite shield-and-spacer lay-up. In addition to the samples tested under our portion of the program, NASA-MSC provided eight

supplemental samples.

A. SAMPLES EVALUATED

1. Samples for Basic Program

Table 10 summarizes the data on the space suit insulation samples tested under the basic program. The Gemini insulation layup is sample ADL-01. Samples ADL-04 through ADL-07 are the four samples which were subjected to simulated wear prior to being tested.

Germanium-overcoated aluminized radiation shields were chosen on the basis of their demonstrated ability to resist abrasion. The liquid-bright-gold-coated radiation shields were chosen on the basis of their low emittance and surprisingly good resistance to abrasion. The Beta marquisette spacer was chosen because it closely resembles the bridal veil spacer we use successfully in many cryogenic insulation applications, is non-flammable in 100% oxygen, and the basic glass material has low thermal conductance. The open-cell flexible polyurethane foam spacer was chosen because such foams have demonstrated low thermal conductance under compressive loads.

2. NASA-MSC Samples

Table 10 also lists the eight samples provided by NASA-MSC as supplements to the basic program: three experimental NASA layups (MSC-01 through MSC-03) and five supplemental samples which augmented the basic program (MSC-04 through MSC-08).

3. Miscellaneous Samples

In addition, two ADL samples were tested which were not within the direct scope of the contract, but which we believed might improve space suit insulations: one sample (ADL-02) was a laminate of a standard double-aluminized Kapton radiation shield and a Beta marquisette spacer; the other sample was a composite radiation shield and spacer (ADL-03).

B. THERMAL CONDUCTANCE TESTS

When evaluating the effectiveness of multilayer insulations either on a cryogenic tank for space applications or in an astronaut's space

TABLE 10. DESCRIPTION OF EXPERIMENTAL SPACE SUIT INSULATION

Sample Number	Outer Layers	Number and Description of Radiation Shields	Number and Description of Spacers	Sample Weight (oz/sq yd)	Remarks (All samples made up with double bladder David Clark Style 1807 inside layers)
Samples Used in the Basic Program					
ADL-01	(1) 6-oz. HT-1 Nomex	(7) 0.25-mil Mylar with 300 Å aluminum, one side	(7) NRC non-woven Dacron batt	21.7	Gemini space suit insulation; baseline for comparing all insulations in this program
ADL-04	(2) Stevens Style 15035	(7) 1.0-mil Kapton with 1700 Å liquid bright gold both sides	(8) 0.030 in. flexible open-cell polyurethane foam	38.5	Sample subjected to 10,000 cycles of simulated wear before testing
ADL-05	(2) Stevens Style 15035	(7) 0.5-mil Kapton with 800 Å aluminum and 500 Å germanium both sides	(8) 0.030 in. flexible open-cell polyurethane foam	31.8	Sample subjected to 10,000 cycles of simulated wear before testing
ADL-06	(2) Stevens Style 15035	(7) 0.5-mil Kapton with 800 Å aluminum and 500 Å germanium both sides	(8) Stevens Style 2530 Beta marquisette	42.5	Sample subjected to 10,000 cycles of simulated wear before testing
ADL-07	(2) Stevens Style 15035	(7) 0.5-mil Kapton with 800 Å aluminum and 500 Å aluminum both sides	(8) Stevens Style 104 with 5% Ultrathene stabilization	32.6	Sample subjected to 10,000 cycles of simulated wear before testing; shields and spacers adhered during conductance tests
ADL-08	(2) Stevens Style 15035	(7) 0.5-mil Kapton with 800 Å aluminum and 500 Å germanium both sides	(8) Stevens Style 2530 Beta marquisette	39.9	
ADL-09	(2) Stevens Style 15035	(7) 0.5-mil Kapton with 800 Å aluminum and 500 Å germanium both sides	(8) 0.030 in. flexible open-cell polyurethane foam	32.1	
NASA/MSC Samples					
MSC-01	(2) NASA Style 4190B	(7) 0.5-mil Kapton 300 Å aluminized one side	(7) NASA Style 4897 Beta Marquisette	43.0	
MSC-02	(1) NASA Style 4190B with carboxy nitroso coat both sides	(7) laminated composite shield and spacer Schjeldahl Style X993		37.4	
MSC-03	(1) NASA Style 4190B with carboxy nitroso coat both sides	(7) laminated composite shield and spacer Schjeldahl Style X993	(7) NASA Style 4897 Beta Marquisette	47.1	
MSC-04	(2) Stevens Style 15035	(7) 0.5-mil Kapton with 1200 Å liquid bright gold both sides	(24) Burlington Style 104 with 5% fluorel stabilization		
MSC-05	(2) Stevens Style 15035	(7) 0.5-mil Kapton with 800 Å aluminum both sides	(8) Stevens Style 2530 Beta Marquisette	42.3	
MSC-06	(2) Stevens Style 15035	(7) 0.25-mil Mylar with 360 Å aluminum both sides	(8) Stevens Style 2530 Beta Marquisette	39.8	
MSC-07	(2) Stevens Style 15035	(7) 0.25-mil Mylar with 900 Å aluminum both sides	(8) NRC non-woven Dacron batt	27.2	
MSC-08	(2) Stevens Style 15035	(7) 0.5-mil Kapton with 800 Å aluminum both sides	(24) Burlington Style 104 with 5% fluorel stabilization	41.2	
Miscellaneous Samples					
ADL-02	(2) Stevens Style 15035	(7) laminate of NASA 0.5-mil Kapton with 300 Å aluminum both sides; adhered to Stevens Style 2530 Beta Marquisette		41.8	
ADL-03		(7) composite shield and spacer of Stevens Style 1659 dipped in Kapton solution; 500 Å aluminum both sides		47.0	

suit, the important criterion is the amount of heat which will flow through the insulation under any given boundary conditions. Thus, the parameter of importance when comparing various space suit insulations is the heat flux per unit area for a given temperature driving force. This parameter is often called the conductance and is given by the equation:

$$C = \frac{Q}{A(t_{warm} - t_{cold})}$$

Thermal conductivity--defined as the heat flux per unit area per unit of thickness and temperature driving force--is not applicable for space suit insulations because the insulation thickness at all locations on the space suit is unknown (varies unpredictably). Thus, although the measurements include the sample thickness, we have refrained from presenting our results in the standard thermal conductivity form; instead, we use the thermal conductance as defined above.

1. Thermal Conductance Measuring Apparatus

The thermal conductance of space suit insulation layups was measured in the double-guarded cold plate calorimeter described in References 3 and 4. Light compressive loads on the insulation sample are achieved with the low-load floating plate apparatus described in Reference 4.

2. Special Test Techniques

In our measurements of the thermal conductance of candidate space suit insulation systems in the dual temperature ranges of +70° to +300°F and -250 to +70°F, two identical samples of each space suit layup were prepared and mounted in the sample chamber, as shown in Figure 3. The samples were separated by a midplane temperature measurement disc consisting of 0.002-inch-thick aluminum foil sandwiched between two 0.002-inch-thick Mylar films. Three 0.001-0.002-inch-diameter chromel-constantan thermocouples were attached to the aluminum foil and the leads drawn out in such a manner as to minimize conduction to the edge of the foil. The center section of the aluminum foil was 6 inches in diameter and

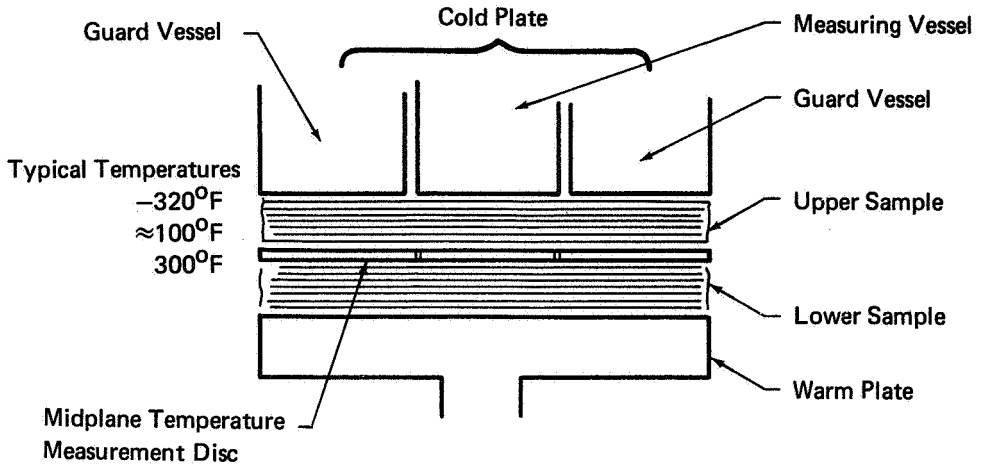

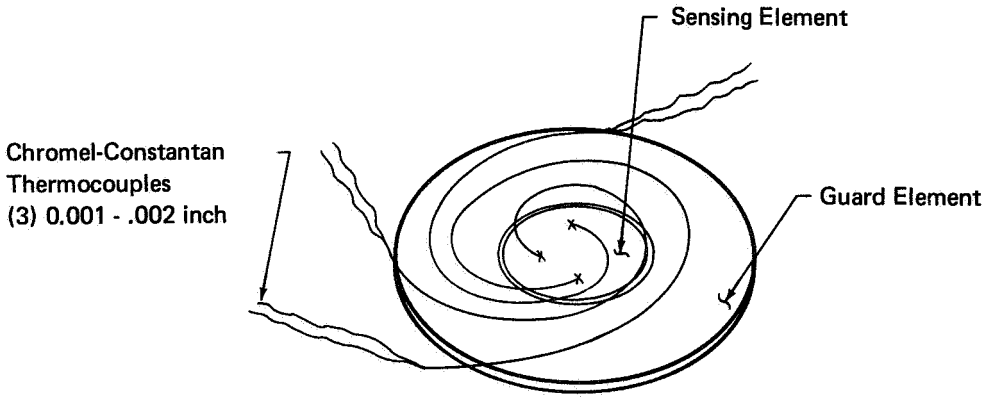

Detail of the Midplane Temperature Measurement Disc

FIGURE 3 MEASUREMENT TECHNIQUE FOR IDENTICAL SAMPLES

separated from the outer section by a 1/16-inch gap to reduce edge losses.

The warm-plate temperature of the apparatus was maintained at either 300°F or 200°F, and the cold-boundary temperature at -320°F, the temperature of liquid nitrogen. Under steady-state conditions, the midplane temperature remained at an intermediate level between the warm and cold plates of the appratus. Because the conductance of multilayer insulation is temperature-dependent and increases with increasing temperature, the midplane temperature between the two insulation samples was always above the midpoint temperature of the given range. The heat flux through both insulation samples, of course, was the same. The important measured quantities were heat flux, compressive load on the sample, and the midplane temperature.

Once the sample was installed and the chamber evacuated to the desired pressure, the guard, measuring, and shield vessels were filled with liquid nitrogen and the warm plate temperature of 200°F was established. The test procedure then consisted of measuring the no-load heat flux by reducing the gap between the sample and the cold plate (located above the sample) in successive stages and measuring the heat flux. As the sample gap was reduced, the heat flux decreased to a minimum value and then increased when the sample contacted the cold plate. The no-load thermal conductance condition was achieved at the point of minimum heat flux just before the sample contacted the cold plate.

Measuring the minimum conductance was often a lengthy procedure. During each measurement, the equilibrium temperature of the temperature measurement disc between the two samples was measured and the thermal heat flux determined by measuring the boil-off rate of the liquid nitrogen from the measuring vessels. When equilibrium conditions were reached and measurements taken at the original temperature, the temperature of the warm plate was then increased to 300°F and another set of equilibrium conditions reached. When both the 200° and 300°F warm plate conditions had been achieved, the compressive load was then increased to 0.01 psi by using the low-load device. Equilibrium was again achieved for warm

plate temperatures of 300°F and 200°F. After the second set of conditions had been achieved, the load was increased again to approximately 0.1 psi and equilibrium heat flux and midplane temperatures again achieved at 300° and 200°F. This procedure was altered for compressive loads of 2.0 psi and 15.0 psi; these loads were applied by the hydraulic ram.

The sample thermal conductance was calculated from the heat flux per unit area and the sample boundary temperature. The test data (summarized in tabular form in the Appendix) include a description of the sample, the individual sample weights, the midplane weight, the compressive load, the outside temperature, the inside temperature, the temperature difference across the sample, the heat flux per unit area, the sample thickness, and the conductance.

3. Simulated Wear of Space Suit Insulation

Part of the program for evaluating combinations of radiation shields and spacers was to determine how the materials interact under laboratory-controlled wear situations. The ideal way for determining how space suit insulation materials behave with each other would have been to build a space suit, exercise it, disassemble it, and see what happened to the insulation; however, this would have been a lengthy process and subject to uncontrollable wear. The object of this portion of the program, therefore, was to develop laboratory-controlled techniques for simulating the wear which the space suit insulations might encounter during normal activity. To achieve this objective, a pilot-model and a full-scale wear tester were developed, samples were worn, tested for emittance and conductance and the results reported.

a. Description of Wear Technique

For the accelerated wear tests, we applied a compressive load and at the same time moved the radiation shields and spacers with respect to each other in an abrading motion. The technique (shown schematically in Figure 4) consists of passing the space suit layup around two rollers in an "S" configuration. Careful examination of the outer and inner layers

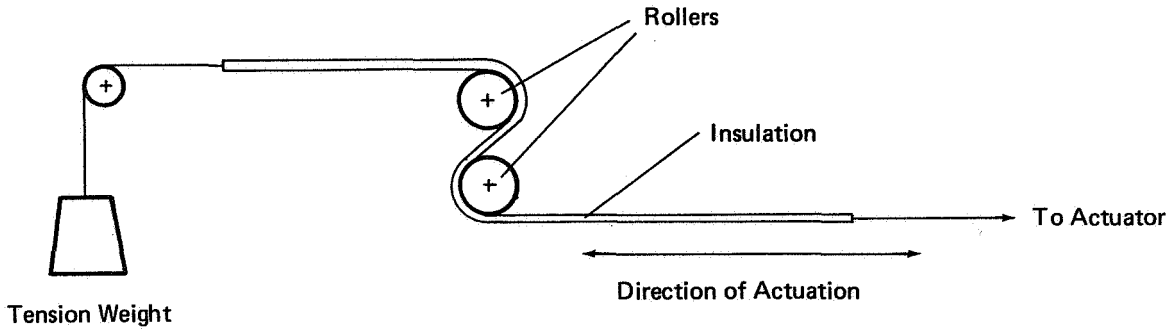

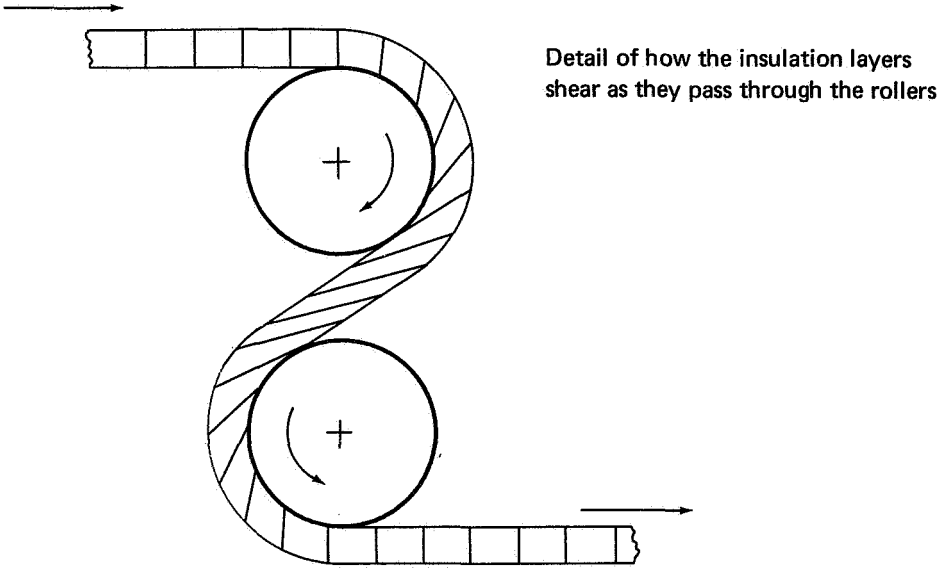

FIGURE 4 SCHEMATIC OF INSULATION WEAR TESTER

of the layup as it passes over one roller through the pinch and out over the other roller indicates that there is relative motion between each layer in the layup. Figure 4 shows how this action distorts the lines drawn normal to the edge of the space suit insulation. Compression of the space suit insulation as it passes over the roller is achieved by tensioning with a weight on a cord attached to the end of the layup.

b. Pilot Model Tester

To check out the principle of the wear tester, we built a unit with two rollers 1.5 inches in diameter and six inches long. An insulation sample consisting of seven layers of NASA-supplied double-aluminized Kapton (300 Å aluminum) and eight layers of Stevens Style 2530 Beta marquisette spacers was installed in this tester and a tension of 3.03 pounds was applied. The sample width was five inches and the compressive load in the sample was approximately 0.81 psi. In this pilot model tester, the action stroke was 4.5 inches. The layup was run for a total of 10,000 wear cycles. After 1000, 1500, 2000, and 10,000 cycles respectively, radiation shields were removed from the layup and their emittance measured. The results of these emittance measurements (summarized in Table 7) are plotted in Figure 5. As indicated in Figure 5, very little surface degradation occurs below 2000 cycles, whereas for 10,000 cycles there is a noticeable increase in surface emittance. This surface degradation was observable by inspection of the radiation shields; there was visual evidence that much of the aluminum was worn away in a regular pattern like the pattern of the spacer material. From these preliminary tests, we determined that with a loading of 0.81 psi, noticeable wear will be produced when the sample has been cycled approixmately 10,000 times.

A second sample was prepared in our laboratory for simulated wear tests. This sample consisted of seven layers of NASA-supplied double-aluminized Kapton (300 Å aluminum) which we overcoated with 500 Å of vapor-deposited germanium. For spacers, we again used eight layers of Stevens Style 2530 Beta marquisette. The sample width was 5 inches, the tension was 3.03 pounds, and the compressive load on the sample was

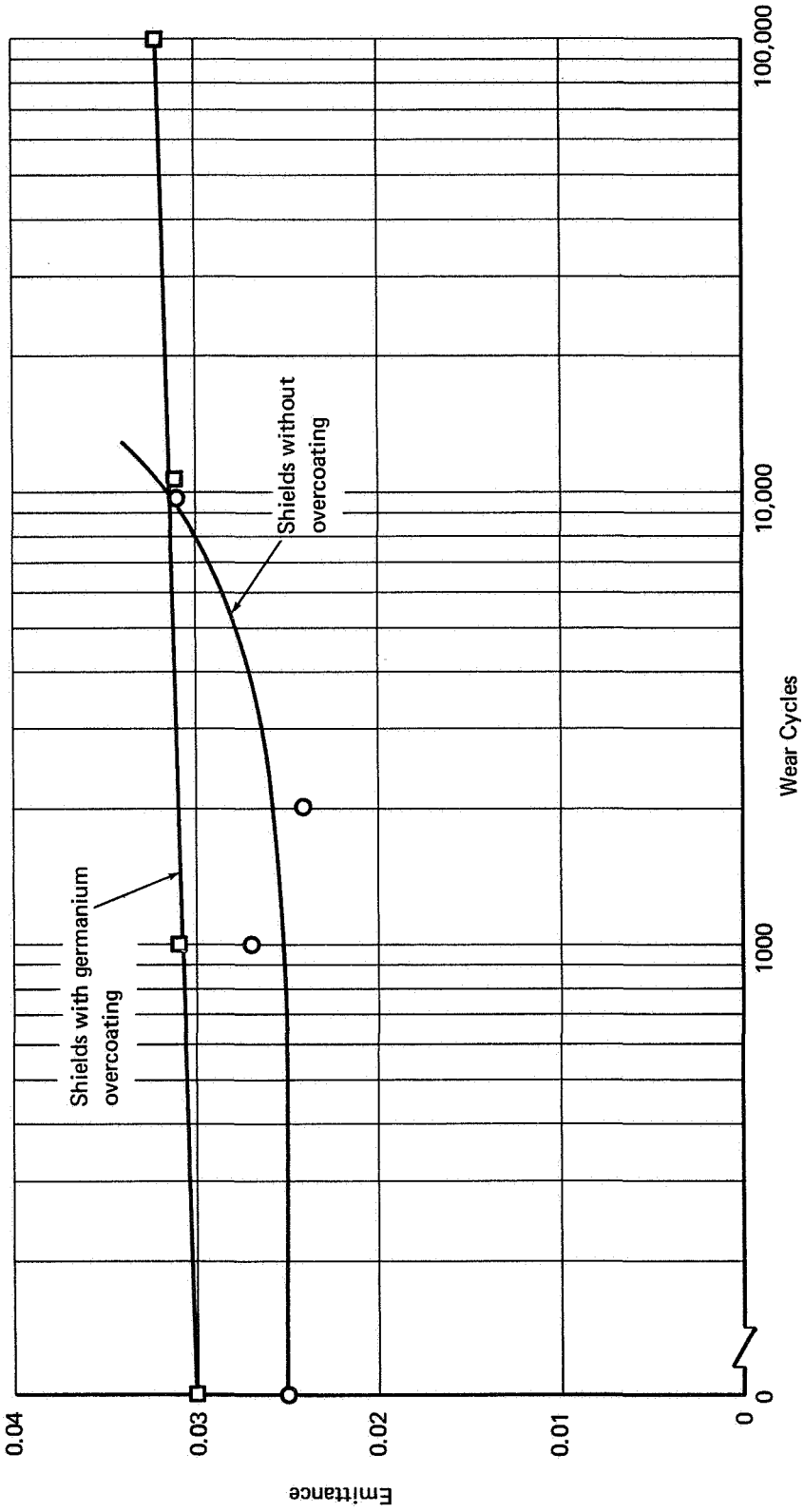

FIGURE 5 EMITTANCE DEGRADATION OF RADIATION SHIELDS SUBJECTED TO WEAR

0.81 psi. This time, the layup was run for a total of 100,000 cycles. After 1000, 10,000, and 100,000 cycles respectively, radiation shields were removed from the layup and their emittances measured. The results of these emittance measurements (summarized in Table 7) are also plotted in Figure 5. From these results, we see that very little degradation of the surface occurred in 10,000 cycles on the germanium protected material (none was visible to the unaided eye), whereas considerable wear had occurred in the nonprotected radiation shields. However, noticeable wear did occur in the germanium-protected sample but only after 100,000 cycles.

From these two tests, we concluded that the application of germanium as an overcoating on the radiation shield is very effective in reducing the surface wear. Quantitatively, the germanium overcoating provides protection which allows the sample to undergo wear approximately one order of magnitude longer before the same amount of shield degradation occurs. In addition, the pilot-scale simulated wear test apparatus proved that systematic wear could be achieved in space suit insulation layups in the laboratory.

c. Full-Scale Wear Tests

A full-scale insulation wear simulator capable of cycling a 16-inch-wide sample of space suit insulation through a maximum stroke of 18 inches was built according to the principles suggested in Figure 4. The test program called for subjecting the individual space suit layups to 10,000 cycles and then cutting 11.5-inch-diameter samples from the center of the worn layups for measurement of thermal conductance. In each of the layups for the wear tester, one extra radiation shield and one extra spacer were included in order to have a sample available for measurement of emittance after wear tests. Usually, a radiation shield from near the middle of the layup was selected for these tests. Descriptions of the space suit insulation layups as they were used in the wear tester are summarized in Table 11.

The first layup test represented a complete space suit extravehicular garment and had two layers of bladder cloth on the inside and two layers

of Beta fiberglass cloth on the outside. In the remaining three samples which were tested, the insulation layup was placed between two bladder layers. The Beta fiberglass outer layers and the two bladder layers in the first sample tested resulted in some undesirable bunching and wrinkling of the insulation sample. This was eliminated in succeeding tests by discarding the excess layers.

After each 2000 cycles of wear, the space suit insulation assembly was removed from the wear tester and inspected. The important results for each sample are noted in Table 11.

In summary, the full-scale wear tests revealed weaknesses in the insulations, particularly cracking of the polyimide substrate. This failure was also observed in both the systems tests. Sample ADL-06 with Beta marquisette spacers and a germanium-overcoated aluminized-Kapton radiation shield survived the wear test better than any of the other three samples tested. A close second was ADL-05 with 0.030-inch-thick polyurethane foam spacers and the germanium-overcoated aluminized-Kapton radiation shields, primarily because the pinch, sheer, and rolling action of the wear tester made the spacer and the radiation shield migrate more and thus caused slightly more wrinkling in the radiation shield than in the sample which utilized the Beta marquisette spacers. However, the differences between the two are not significant and either type of spacer would be a candidate for further exploratory development. Further, inasmuch as the wear test to which all samples were subjected is rather arbitrary, we have no indication that either sample would behave better in a space suit under normal wear conditions.

C. RESULTS OF CONDUCTANCE TESTS

The heat flux through the sample and the boundary temperatures were measured for each sample at zero-load conditions and for successively larger compressive loadings up to 15 psi. The sample conductance was calculated from the heat flux and the sample boundary temperatures. The conductance was not measured at the exact boundary conditions required in the program--lunar daytime conditions (the outside temperature of the space suit at 300°F and the inside at 70°F) and lunar nighttime conditions (the outside of the space suit at -250°F and the inside is at 70°F)--

TABLE 11. INSULATIONS TESTED IN THE WEAR SIMULATOR

Insulation No.	Outside Layers	Radiation Shields	Spacers	Inside Layers	Results after 10,000 Cycles of Testing
ADL-04	(2) Stevens Style 15035 Beta fiberglass cloth	(7) 1-mil Kapton film with 1700 Å of 8432 liquid bright gold	(8) polyurethane foam 0.030-inch thick	(2) bladders	Migration of the spacers caused them to bunch-up; wrinkles appeared in the radiation shields and several cracks, approximately 0.5-inch long, occurred at 90° to the creases; in the vicinity of wrinkles and high sheer, the gold coating was noticeably was worn away on both sides of the shield; remaining gold was poorly adhered and could be lifted easily by the scotch tape test.
ADL-05	(1) bladder	(8) 0.5-mil Kapton film with 500 Å vapor-deposited germanium overcoat on 800 Å vapor-deposited aluminum	(9) polyurethane foam 0.030-inch thick	(1) bladder	Aluminum and germanium were poorly adhered in several small, widely-scattered local areas; otherwise the shields showed very little signs of wear; adhesion was good by the scotch tape test.
ADL-06	(1) bladder	(8) 0.5-mil Kapton film with 500 Å vapor-deposited germanium overcoat on 800 Å vapor-deposited aluminum	(9) Stevens Style 2530 Beta marquisette	(1) bladder	At no time was there any noticeable wear of the radiation shield or the spacer; this sample survived wear tests better than any other sample tested.
ADL-07	(1) bladder	(8) 0.5-mil Kapton film with 500 Å vapor-deposited germanium overcoat on 800 Å vapor-deposited aluminum	(9) Stevens Style 104 plain-weave fiberglass cloth stabilized with 5% Ultrathene epoxy	(1) bladder	Slight pitting and chafing of the shields occurred; spacer yarns showed considerably migration where the stabilization was not sufficient.

instead, all conductance measurements for the cold plate temperature were made at the boiling point of liquid nitrogen (-320°F) and for the warm plate temperature at 200° and 300°F.

The use of a mid-plane temperature measurement between two identical samples of the space suit insulation allowed us to simultaneously measure the conductance of two samples of space suit insulation for each heat flux measurement. In most instances, the midplane temperature was higher than the 70°F required for the inside boundary condition of the space suit; therefore, extrapolations of the basic data were required to determine the insulation conductance for the two conditions. The measured conductance at each sample pressure loading was plotted as a function of the parameter

$$\frac{T_1^4 - T_2^4}{T_1 - T_2}$$

and values of the conductance at the desired temperature differences (300 to 70°F and 70 to -250°F) were obtained by straight line interpolation. (A description of this extrapolation procedure is given in the Appendix.)

The data for all thermal conductance tests performed during this program (summarized in tabular form in the Appendix) include the compressive load, the outside temperatures of the insulation, the inside temperature of the insulation, the temperature difference across each insulation, the heat flux, the conductance of the sample, and the sample thickness.

The insulation samples were in three major groupings: (1) the samples developed during the program, (2) NASA-MSC-supplied samples, and (3) composite samples provided by both NASA-MSC and ADL. For each group of samples, the conductances of the insulation for simulated lunar nighttime conditions (sometimes called the cold conditions), 70° to -250°F, is summarized on one figure; the conductances of the insulation for the lunar daytime conditions (sometimes called the hot conditions), 70° to

300°F, on a second figure.

The conductances for all samples tested under this program are presented in Figures 6-11 as a function of the sample loading. Figures 6 and 7 summarize the conductance as a function of sample loading for the samples developed during the program. Figures 8 and 9 summarize the performance of the NASA-MSC-provided samples, and Figures 10 and 11 summarize the performance of composite samples provided by NASA-MSC and ADL.

At the "no load" condition, the sample rests under its own weight in the thermal conductance apparatus. We accounted for the compressive loads within the sample which result from the sample's own weight. In the case of the samples under lunar nighttime conditions (Figures 6, 8, and 10), the range of the self-compression load in the sample is determined from the weight of the sample divided by its area, the maximum, and one-half of the weight of the sample divided by its area, the minimum. For the samples at lunar daytime conditions (Figures 7, 9, and 11), the range of self-compression load is determined from the sum of the weights of the two samples and the midplane measuring disc divided by the sample area, the maximum, and the sum of one sample weight and the midplane temperature measuring disc divided by the sample area, the minimum.

Of particular interest to this program are the thermal conductances of samples at the no-load condition and at a compressive load of 1.0 psi. In normal operation, the insulation in an astronaut's space suit will be under minimum compression, particularly in orbit, where there is no gravity. For lunar operations, the weight-induced compressive load will be only one-sixth that on earth. It is hard to visualize how compressive loads in excess of 1.0 psi can be sustained in a space suit layup. In isolated circumstances it may be possible to achieve high compressive loads (up to 15 psi) when the astronaut is leaning on his elbow or is down on his knees, but these are considered transient conditions.

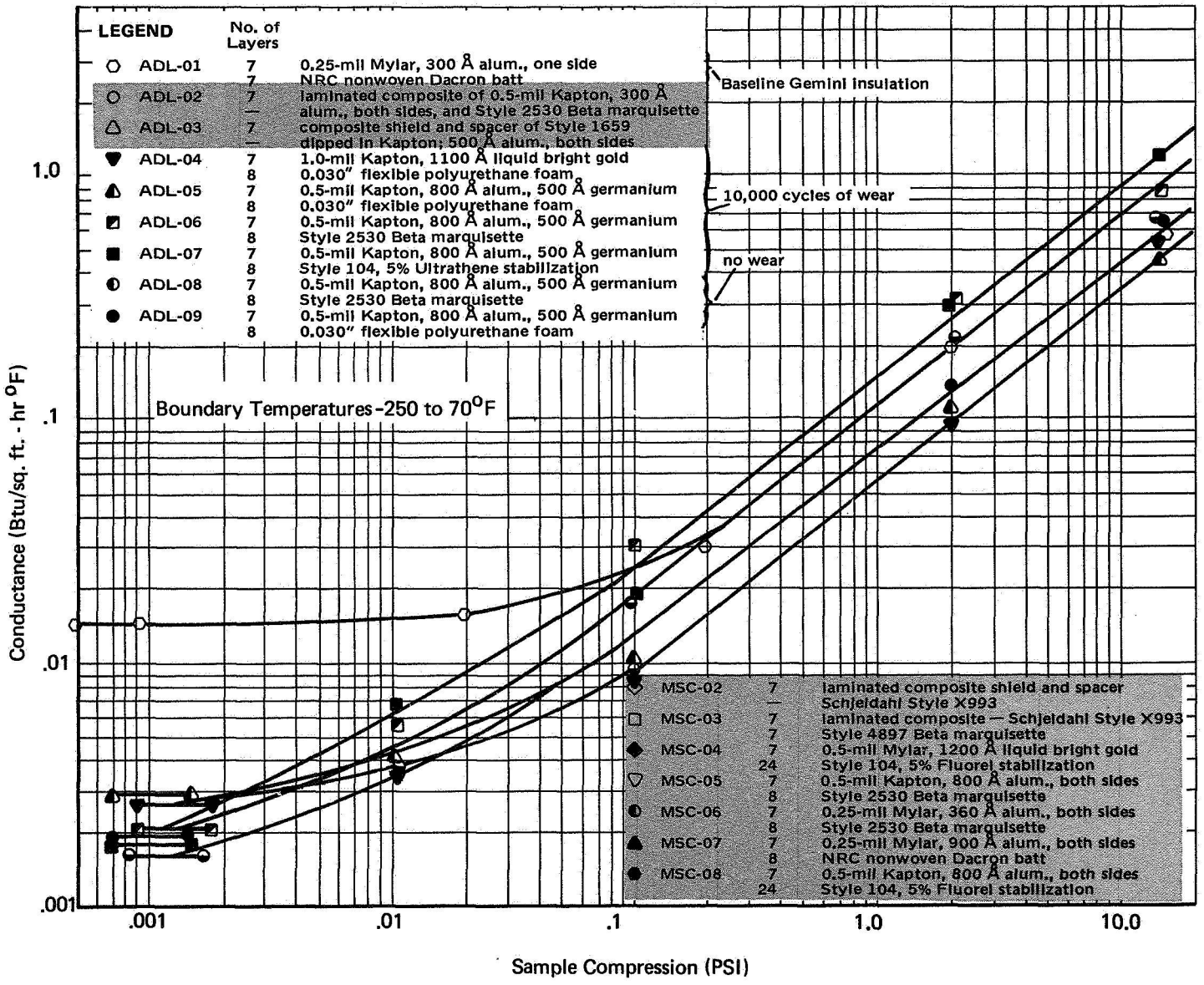

FIGURE 6 SUMMARY OF INSULATION CONDUCTANCE – SAMPLES DEVELOPED IN THE PROGRAM

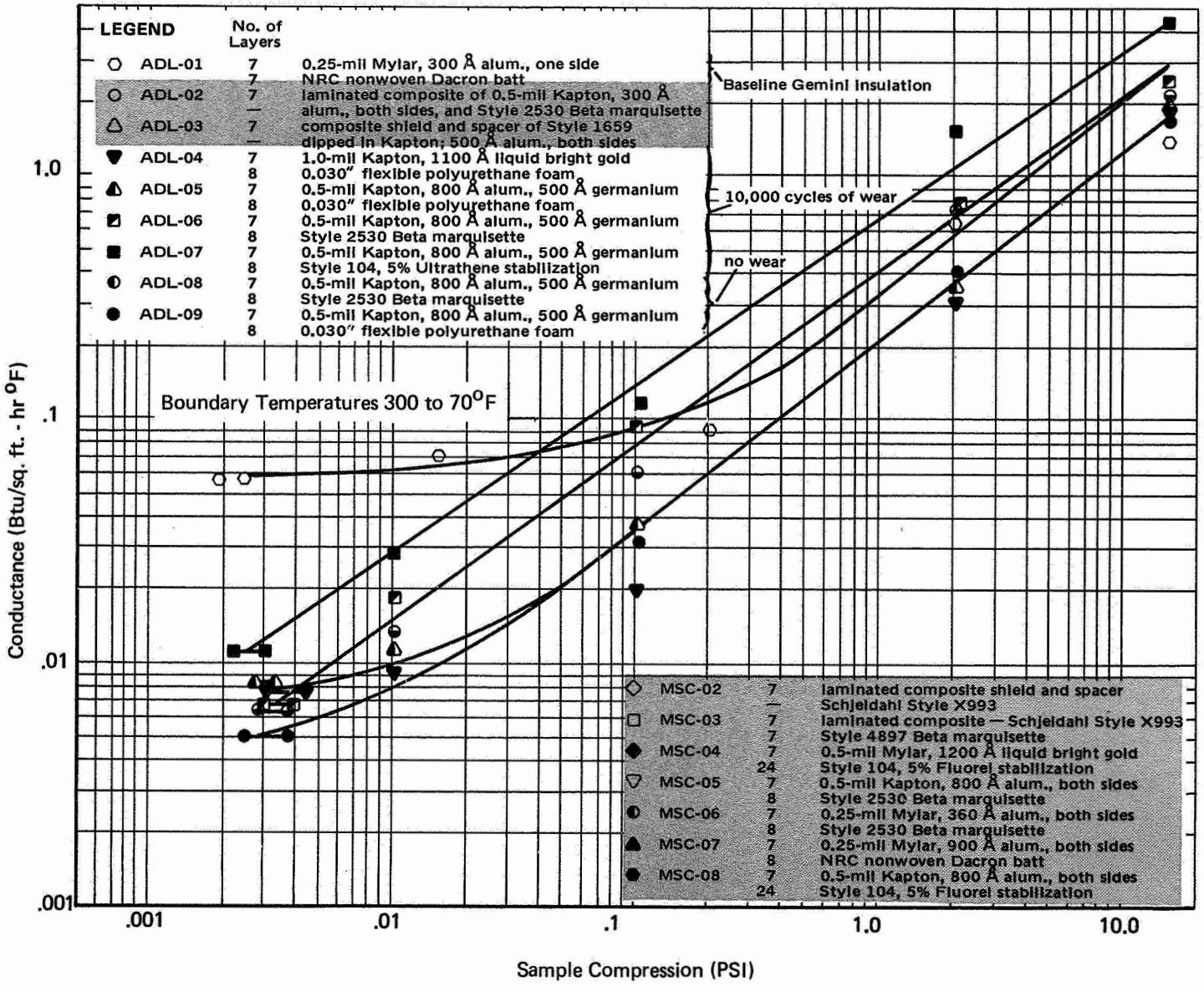

FIGURE 7 SUMMARY OF INSULATION CONDUCTANCE — SAMPLES DEVELOPED IN THE PROGRAM

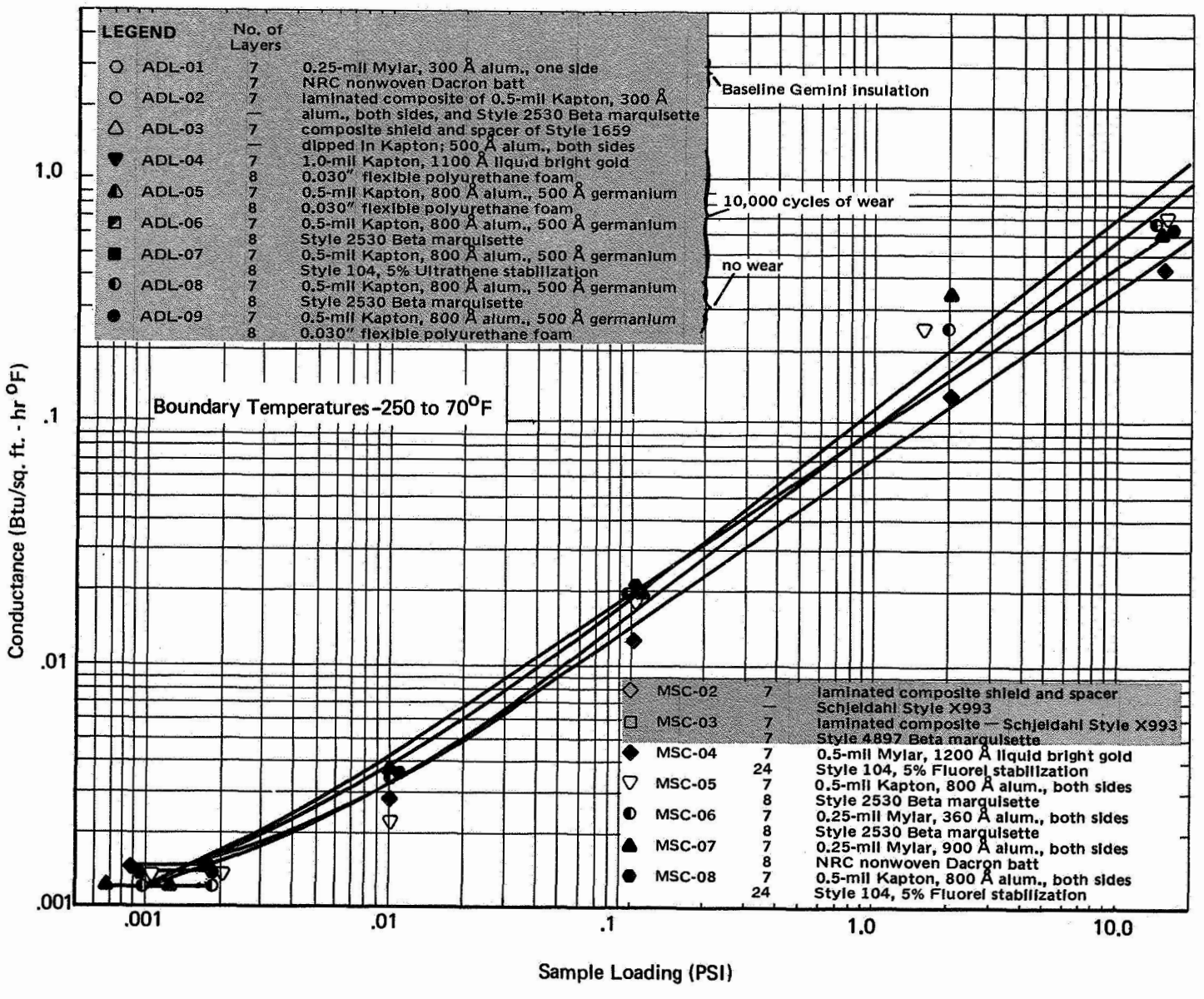

FIGURE 8 SUMMARY OF INSULATION CONDUCTANCE — NASA/MSC SAMPLES

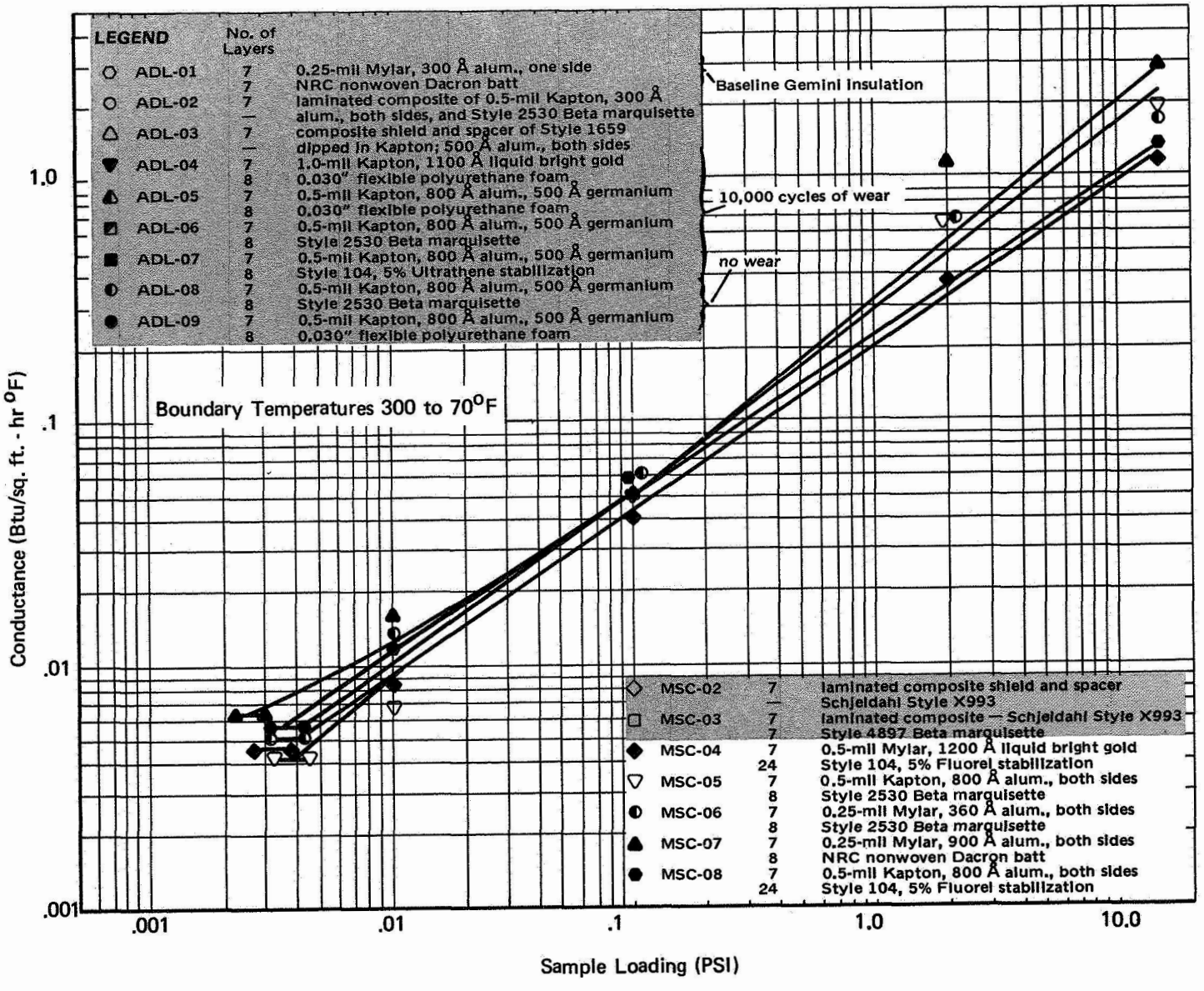

FIGURE 9 SUMMARY OF INSULATION CONDUCTANCE – NASA/MSC SAMPLES

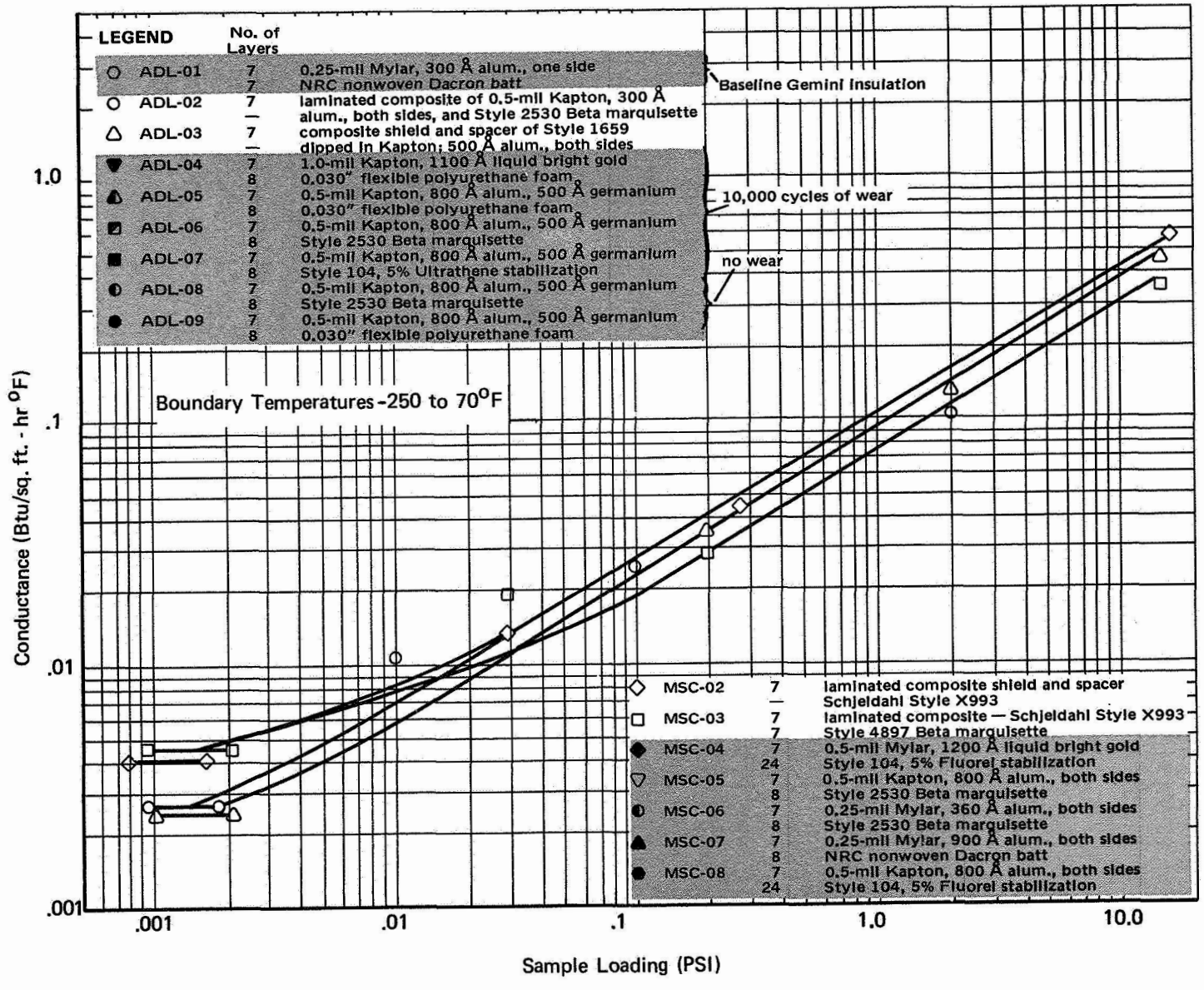

FIGURE 10 SUMMARY OF INSULATION CONDUCTANCE — LAMINATE AND COMPOSITE SAMPLES

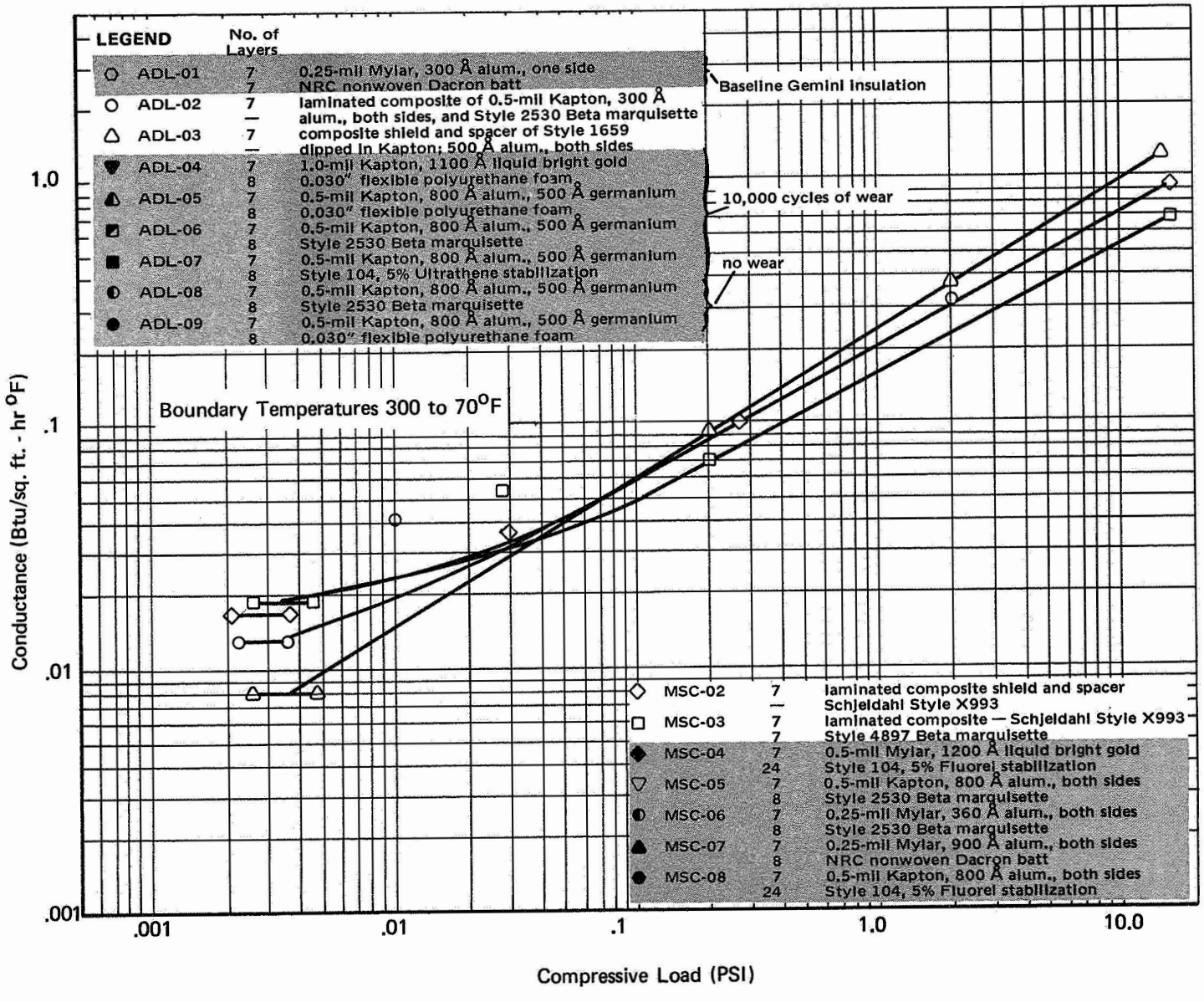

FIGURE 11 SUMMARY OF INSULATION CONDUCTANCE — LAMINATE AND COMPOSITE SAMPLES

Although the data were obtained at compressive loads from no-load to 15 psi, our discussion is focused on the performance at no-load and at 1.0 psi compression.

1. Observations Concerning All Samples Tested

In reviewing all of the data (Figures 7-11), we find that the measured conductance of sample MSC-01 (Figures 8 and 9) is probably in error for all compressive loads. Sample MSC-01 was the first sample tested in this program, and we found during the evaluation of the second sample that there was a part missing from the hydraulic ram used for applying compressive loads above 0.1 psi. This part was replaced when the second sample was tested. It is believed that at compressive loads above 0.1 psi, sample MSC-01 should have conductance similar to sample MSC-05.

The no-load conductance for sample ADL-01 is higher by a factor of 4 to 5 than would be expected on the basis of the radiation shield emittance. ADL-01 had radiation shields with vapor-deposited aluminum on one side only. The theoretical conductance based on radiation heat transfer through shields which have vapor-deposited aluminum on one side should be twice the conductance for shields which have vapor-deposited aluminum on both sides. By comparing ADL-01 (single-aluminized) with MSC-07 (double-aluminized), we observe a tenfold increase in the conductance when single-aluminized sides are substituted for double-aluminized sides. We are unable to explain why the no-load conductance is so high for sample ADL-01 with single-aluminized radiation shields and therefore must discredit the measurements at no-load for ADL-01.

a. Conductance at No-Load--Cold Conditions

The no-load conductances for the cold conditions (70° to -250°F) are shown on Figures 6 and 8. All of the samples with double-aluminized or double-gold-coated radiation shields (exclusive of composite or laminated radiation shields and spacers) have thermal conductances ranging from 0.0012 to 0.003 Btu/sq ft hr°F irrespective of the type of spacer material used between radiation shields.

The samples with composite or laminated radiation shields and spacers (Figure 10) have conductances ranging from 0.0024 to 0.0045 Btu/sq ft hr°F, which are higher than those for separate shield and spacer insulations. Of the laminated insulations, samples MSC-02 and MSC-03 had adhesive spread on one side of the radiation shield (thereby increasing its emittance) prior to being laminated to the spacer. They exhibit slightly higher no-load conductances than laminated sample ADL-02, where care was taken to apply the adhesive only at the points where the spacer contacted the radiation shield.

b. Conductance at No-Load--Warm Conditions

The no-load conductances for the warm condition (70 to 300°F) are summarized in Figures 7, 9, and 11. With the exception of sample ADL-07, in which the radiation shields and spacers adhered during the test, the conductance of the insulations with double-aluminized, double-aluminized with germanium overcoating, or double-gold-coated radiation shields ranges from 0.0044 to 0.0082 Btu/sq ft hr°F. The conductances of the composite sample (ADL-03) and the three laminate radiation shield and spacer samples (MSC-02, MSC-03 and ADL-02 on Figure 11) range from 0.008 to 0.018 Btu/sq ft hr°F. Consequently, space suit insulations made from composite or laminates will have no-load conductances that are almost twice those of space suit insulations which use double-aluminized or double-gold-coated radiation shields and loose spacer materials.

c. Conductance at 1.0 psi--Cold Conditions

For the cold conditions (Figures 6, 8 and 10), the insulations which used 0.030-inch-thick open-cell polyurethane foam spacers have conductances ranging from 0.06 to 0.08 (see samples ADL-04, ADL-05, and ADL-09 on Figure 6). Sample MSC-03 (Figure 10) with one Beta marquisette spacer adhered to each radiation shield and an additional loose Beta marquisette spacer between has about the same conductance (0.074 Btu/sq ft hr°F) for the same conditions.

Sample MSC-08 with multiple spacers of Stevens Style 104 material has about the same conductance as the insulations which have single

spacers of Beta marquisette, as can be seen by comparing sample MSC-08 (Figure 8) with samples MSC-06 and MSC-05 (Figure 8) and samples ADL-08 and ADL-06 (Figure 6), and samples ADL-02 and MSC-02 (Figure 10). The conductance of all of these samples are approximately 0.1 Btu/sq ft hr°F. From these data, the multiple-spacer concept was developed.

d. Conductance at 1.0 psi--Warm Conditions

For the warm conditions (Figures 7, 9, and 11), sample MSC-03 (Figure 11) has a conductance of 0.15 Btu/sq ft hr°F. We believe this low conductance results from the added thermal resistance of two spacers between each radiation shield (one spacer was laminated to the shield and the second was loose). This sample had more spacer material between each radiation shield than any other sample tested and it was the heaviest. The extra layers provide more contact resistance and more conduction resistance to heat flow than in a similar sample with only one spacer. Samples ADL-04, ADL-05, and ADL-09 with foam spacers all have a conductance of 0.2 Btu/sq ft hr°F.

Samples with single loose Beta marquisette spacers have conductances in the range of 0.3 to 0.4 Btu/sq ft hr°F (samples ADL-06 and ADL-08 on Figure 7; and MSC-05 and MSC-06 on Figure 9). Samples MSC-02 and ADL-02 (Figure 11) with single Beta marquisette spacers bonded to the radiation shield have a conductance of 0.2 Btu/sq ft hr°F. This result is anomalous; one would expect that by bonding the spacer to the radiation shield, the point contact resistance would decrease, thereby increasing the conductance compared to samples where the shield and spacer are not bonded. Instead, we found a decrease in conductance when the spacer was bonded to the shield.

2. Observations Concerning Samples Developed During the Program

The thermal performance of samples developed during the program are presented in Figures 6 and 7. In this group of samples, four (ADL-04, ADL-05, ADL-06, and ADL-07) were subjected first to 10,000 cycles of wear before the conductance was measured. Of these four samples tested, unworn materials from two were selected for testing after wear (ADL-08 and ADL-09). These samples had radiation shields of 0.5-mil Kapton

with 800 Å of aluminum and 500 Å of germanium on both sides and either flexible polyurethane foam spacers or Style 2530 Beta marquisette spacers. By comparing the performance of sample ADL-05 and ADL-09 on both Figures 6 and 7, we can see the effect of wear when flexible polyurethane foam spacers are used. Although we can detect a small difference in conductance at the no-load condition, we can see little or no difference between the two samples (worn and unworn) at compressive loadings greater at 0.1 psi.

By comparing samples ADL-06 and ADL-08, we can see the effect of wear on samples which use germanium-overcoated double-aluminized 0.5-mil Kapton radiation shields and Style 2530 Beta marquisette spacers. In this instance, we can see slight degradation of the insulation for both lunar nighttime and daytime conditions at all compressive loads.

Sample ADL-07 performed poorly. Although the no-load conductance for lunar nighttime conditions was low (Figure 6), at the higher compression for both the cold and the warm conditions, its conductance was extremely high. Examination of the sample after tests revealed that the insulation failed because the Ultrathene epoxy used to stabilize the spacer material adhered tightly to the radiation shields and formed a solid mass.

3. Supplemental Samples Provided by NASA-MSC

The thermal conductance of samples supplied by NASA-MSC are summarized in Figures 8 and 9. The performance for the insulation under lunar nighttime conditions is presented in Figure 8 and for lunar daytime conditions in Figure 9. The purpose of these supplemental samples was to evaluate insulations which were outside of the scope of the basic contract.

In this group of samples, all of the radiation shields had good low-emittance coatings on both surfaces of the radiation shields and the insulations had the lowest no-load conductances of all samples tested in the program.

Samples MSC-04 and MSC-08 were fabricated and tested to develop the multiple space concept. Both samples used three spacers of Style 104

scrim between each radiation shield. MSC-04 used liquid-bright-gold-coated 0.5-mil polyimide radiation shields and MSC-08 used vapor-deposited aluminum coatings on the same substrate.

For the boundary temperatures 300° to 70°F and no compressive load, MSC-08 had a conductance of 0.006 Btu/sq ft hr°F and MSC-04 had a conductance of 0.0046 Btu/sq ft hr°F, which was almost the lowest conductance of all samples tested in the program. At a compressive load of 1.0 psi for the same boundary temperatures, both MSC-04 and MSC-08 had a conductance in the range between 0.2 and 0.25 Btu/sq ft hr°F. Only sample MSC-03 had a lower conductance (0.16 Btu/sq ft hr°F) for the same boundary temperatures and loading.

For the boundary temperatures 70 to -250°F and no compressive load, MSC-04 and MSC-08 had almost identical conductances of 0.0014 Btu/sq ft hr°F. Only two samples, MSC-06 and MSC-07, had a lower no-load conductance (0.0012 Btu/sq ft hr°F) and the difference we do not consider significant. At a compressive load of 1.0 psi, MSC-04 had a conductance of 0.08 Btu/sq ft hr°F, which was lower than the conductance of 0.10 Btu/sq ft hr°F for MSC-08. Again, only sample MSC-03 had a lower conductance (0.07 Btu/sq ft hr°F) for the same boundary temperatures and loading.

These data indicate that by using multiple spacers, some improvement can be expected over the load-carrying ability of insulations with single spacers.

4. Laminate and Composite Shield and Spacer Samples

The thermal conductance of samples of laminate and composite radiation shield and spacers provided by both NASA-MSC and ADL are summarized in Figures 10 and 11.

In this series of tests, three of the samples, MSC-02, MSC-03, and ADL-02, had a spacer of Beta marquisette bonded to the radiation shield on one side. One of these samples, MSC-03, had one extra Beta marquisette spacer in addition to the laminate. MSC-03 exhibited the lowest conductance at increased compressive loads of all samples tested; however,

it is the heaviest sample tested (47.1 oz/sq yd). It was on the basis of this low conductance at high compressive loads that samples MSC-08 and MSC-04 (see Figures 8 and 9) were prepared with multiple spacers between each radiation shield.

Sample ADL-03 is an experimental composite radiation shield spacer (see Section III and Figure 2). It has the lowest no-load conductance of the four samples tested in this series for both the lunar nighttime and daytime conditions. However, it is not flexible enough for a space suit insulation and we consider it unsuitable for further development.

V. THERMAL MICROMETEOROID GARMENT ANALYSIS

Minor failures have occurred in the insulations of astronaut thermal micrometeoroid garments. Most of the reported failures have been mechanical, induced by the garment fabrication techniques. We analyzed the insulation assembly techniques, garment fabrication techniques, and reported failures to determine the probable causes of failures. On the basis of this analysis we have recommended that the insulation hang loosely on the garment, only the inner layer of the garment be load-bearing, the multilayer insulation have one more spacer than the number of radiation shields, the radiation shields terminate no closer than 0.5 inch to seams, and the spacer layers be firmly anchored in the seams.

A. REPORTED FAILURES IN SPACE SUIT INSULATIONS

During discussions with personnel from NASA-MSC early in the program, we were told of two failures which have occurred in space suit insulation layups. Eugene Cernan, during his two-hour extravehicular mission in the Gemini IX flight,[5] experienced minor thermal discomfort on an area of his back when part of the multilayer insulation separated in the seam where the overgarment attached to pressure layers of his space suit. Postflight photographs of this insulation layup showed that the radiation shields had separated from a length of seam where the overgarment attached to his space suit. From the photographs, it looked as if the external layers of the overgarment stretched slightly and the radiation shields and their spacers did not stretch, but pulled out at the seam.

We subsequently dismembered a similar type of overgarment and found that the radiation shields and spacers were all firmly anchored in all seams of the garment. Since the radiation shields (aluminized Mylar) have very low tear strength (particularly when pierced many times with a sewing machine needle), the failure was judged to be comparable to the action of a paper that is torn along a perforated line.

Although extremely tough, Mylar films are notch-sensitive, so any notches allow tears to propagate very easily. Because dynamic cycling physically disturbs the mechanical integrity of the insulation layer, tearing of the radiation shields naturally occurs at the weakest points--in the vicinity of the seams. The resulting gaps in the radiation shield layers cause some loss of insulation properties of the garment.

A second type of insulation failure, reported to us verbally by NASA-MSC, involved the degradation of the vapor-deposited surfaces of the radiation shields used in the insulation. In tests at NASA-MSC, a complete layup of the Gemini space suit insulation and pressure garment was made in the shape of a circle. The inner bladder layer was inflated so that the unit assumed the shape of a dome. The Nomex layers of two such inflated domes were placed in contact and under slight compression. The dome layers were then rubbed against each other until the outer Nomex layers wore through. Upon disassembly, it was found that the vapor-deposited aluminum on the Mylar film had been badly worn away. In this particular layup, the spacer was NRC nonwoven Dacron batt. Because no flexing was involved in this test, the mechanism of aluminum loss from the surface was clearly by abrasion of the aluminum against the Dacron batt. Dynamic cycling of the aluminized Mylar caused the vapor-deposited aluminum surfaces to wear, thereby making the initially highly reflective surfaces highly absorbing. The heat flow through the insulation would be expected to greatly increase, particularly at the no-load condition.

Our experience with aluminized polyester film (Mylar) indicates that dampness can also seriously degrade the emittance aluminum surfaces. In a study for NASA/Lewis Research Laboratories,[3] we subjected samples of polyester film to 95% relative humidity at 95°F for 100 hours. At 10-hour intervals the samples were removed from this environment and the surface emittance measured. The base material, with approximately 500 Å vapor-deposited aluminum, had an emittance of 0.025. Little degradation of this emittance was noted for samples removed during the first 50 hours. However, after 50 hours the aluminum surface degraded rapidly, reaching

a value of 0.25 at 100 hours.

The aluminized material was glazed over with a cloudy material, which we believe was low-grade aluminum oxide. Although this type of degradation has not been reported in space suit insulations, it is a potential area of difficulty; therefore, the aluminized radiation shield used in space suits should be stored in low-humidity areas prior to construction, and once the space suit is completed, the unit should also be stored in a low-humidity environment to keep the radiation shields from degrading.

B. CONSTRUCTION DETAILS IN GEMINI SPACE SUIT INSULATIONS

In the Gemini-type of overgarment which we dismembered, we found that all of the internal joints in both radiation shields and spacers were made with pressure-sensitive aluminized tape. These taped seams were one on top of the other. The pressure-sensitive adhesive bled through the thin Dacron batt spacer layers and caused the taped seam to adhere to the radiation shield immediately below. The net result of this seaming technique was that all the spacers and shields were stuck together, making a thermal short circuit through the insulation layup.

The overgarment insulation layers were applied one at a time, alternating spacers and radiation shields, a construction technique similar to generally accepted cryogenic multilayer insulating techniques. This technique should yield an effective garment.

The radiation shields and spacers extended into the seams and penetrations of the garment, where they were tightly stitched--an undesirable construction technique because of the resulting thermal short circuits through the insulation when the layers are tightly compressed. In addition, both the outer and inner layers of this overgarment were load-bearing members and, as such, the insulation was subject to compression and tearing-out at the seams.

The largest difficulty with this space suit layup was that the radiation shields and spacers were all firmly anchored in the seams

and penetrations, thus allowing the short circuit of heat through these seams and penetrations. In addition, if the outer layers of the space suit were stressed during normal activity, the radiation shields often would pull out of the seam along the perforations caused by the stitching. In effect, the insulation layers were load-bearing.

C. ASSEMBLY TECHNIQUES

1. Techniques Used in Cryogenic Multilayer Insulation

In the application of multilayer insulation to cryogenic tanks and spacecraft, it is important to keep the insulation as loose as possible, subject it to a minimum of compressive loads during application, and prevent each radiation shield from touching the shield in the layer above or below it.

Each radiation shield as it is applied is held to itself by pressure-sensitive tape capable of withstanding the temperatures to which the insulation is subjected. Seams in each spacer layer (in this case, open-mesh bridal veil material) are loosely stitched with nylon thread. Slight overlapping of the spacers is allowed at each seam to make stitching easier. As the layup of the insulation progresses, it is the practice to apply a temporary spacer (made from blotter paper or flexible cardboard) immediately before applying the radiation shield spacer. When the layup is complete, the temporary spacers are removed, thereby insuring that there is uniform spacing and tension on each spacer layer.

This spacer application technique is necessary for multilayer insulations used on cryogenic tanks because the extremely low temperatures cause spacer materials to shrink, thereby inducing compressive loads in the insulation. This temperature-induced compression in the insulation is not considered a problem in space suit insulations. However, it does point up the need to prevent the application of unnecessary compressive loads during the insulation layup procedure.

All of the conductance data (Section IV) indicate that very low thermal conductance can be achieved in space suit insulations, provided there are minimum compressive loads. Therefore, an important goal of all

garment fabrication techniques should be to minimize the compressive loads on the insulation. The insulation should hang as loosely as possible on the extravehicular garment and allow the internal layer of the garment to be the load-bearing member--this being the design goal we have utilized in selecting preferred techniques for applying multilayer insulations to extravehicular garments.

2. Preferred Assembly Techniques for Space Suits

In selecting preferred techniques for assembling an extravehicular thermal and micrometeoroid protection garment, we assume that the garment will use all of the basic layers which were used in the measurement of conductance of the space suit insulation: i.e., two tightly-woven Beta fiberglass layers on the outside for abrasion and fire protection, an insulation layup of alternating radiation shields and open-mesh fiberglass spacers, and two inner bladder layers which serve as micrometeoroid protection and as a structural basis. The inner bladder layers of the garment will be the load-bearing members of the garment. The external protection layers (tightly woven Beta fiberglass layers) will lightly hold the insulation layers in place.

Figure 12 indicates the recommended edge-seaming technique. The insulation layers shown consist of alternating radiation shields and fiberglass spacers (typically Stevens Style 2530). The radiation shields should stop just short of the edge seam. The shield spacers are carried into the edge seam and are anchored by firm, tight stitches. The external Beta fiberglass layers are carried around the end of the insulation for flame protection in the event of fire. The seam stitches are made with double threads, one of Nomex and one of Beta fiberglass. The Nomex thread provides good strength at normal operating conditions and the Beta fiberglass thread provides protection in the event of fire that might destroy the Nomex thread. If the radiation shields should migrate away from the seam during normal wear, a small amount of adhesive can be applied to the interface between each radiation shield and its next spacer to anchor the spacer. Care should be taken in this procedure not to allow the radiation shield to be adhered to both adjacent spacers; it

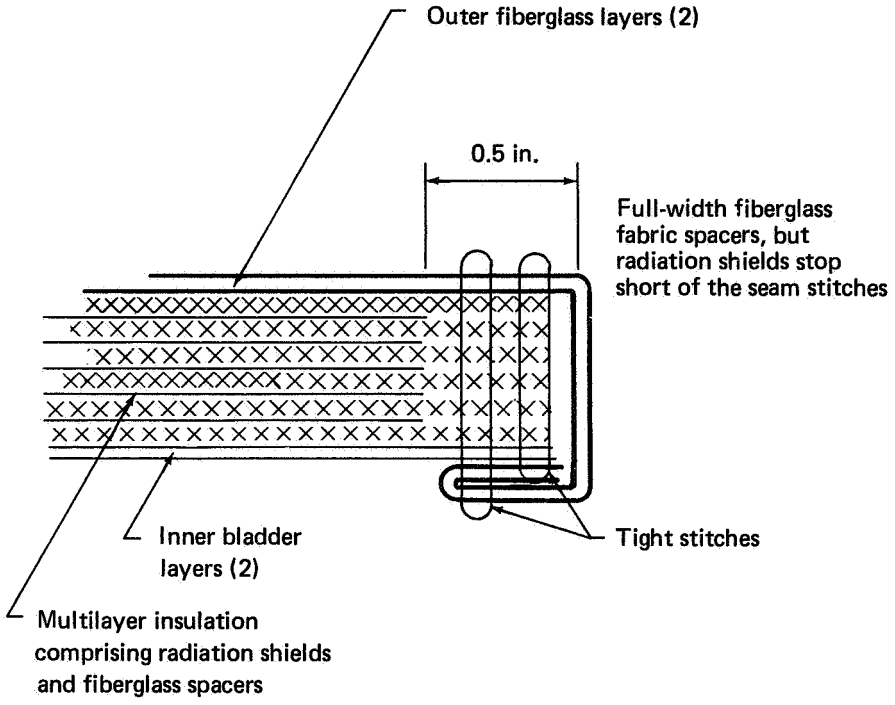

Source: Arthur D. Little, Inc.

FIGURE 12 RECOMMENDED EDGE SEAM

should be adhered to only one spacer.

An alternative edge seam for an insulation which utilizes open-mesh fiberglass spacers is shown schematically in Figure 13. This seam will be useful in areas where considerable stress may be placed upon the insulation layer due to the normal activity. In this seam, the radiation shields again end approximately 0.5 inch from the edge of the seam. The edges of the spacers are attached to thin open-cell polyurethane foam layers which, in turn, adhere to the radiation shields. Again, tight stitches are made through the edge of the seam, thereby firmly anchoring the foam and spacer materials, but not penetrating the radiation shields. Dual-purpose thread is also used in this seam.

A load-bearing edge seam is shown schematically in Figure 14. In this seam, the internal bladder-cloth layers are load-bearing and, as such, are firmly stitched one to another. Through careful seaming techniques, it is possible to anchor the external layers in the bladder cloth layers and then to wrap the seam loosely over the outside of the insulation and anchor it with a single stitch as shown in Figure 14. Again, the radiation shields end approximately 0.5 inch before the edge of the seam.

Edge seams are shown in Figure 15 for insulations which use foam spacers between the radiation shields, which end approximately 0.5 inch short of the edge of the seam. The radiation shield can be cemented to the spacers if the migration of shields is a problem.

For areas in the garment where it will be necessary to anchor the insulation and the inner and outer layers, the tufting technique shown in Figure 16 can be used. In this technique, foam layers (one for each radiation shield) are added to the radiation shield in the area where the tuft is to be placed.

Medium-tight stitches are drawn through this stack of radiation shields, spacers, and thin open-cell foam spacers. A ceramic button on the outside and an epoxy fiberglass button on the inside of the garment are required to distribute the compressive load induced by the stitches. A rule of thumb in making a tuft of this type through multilayer insula-

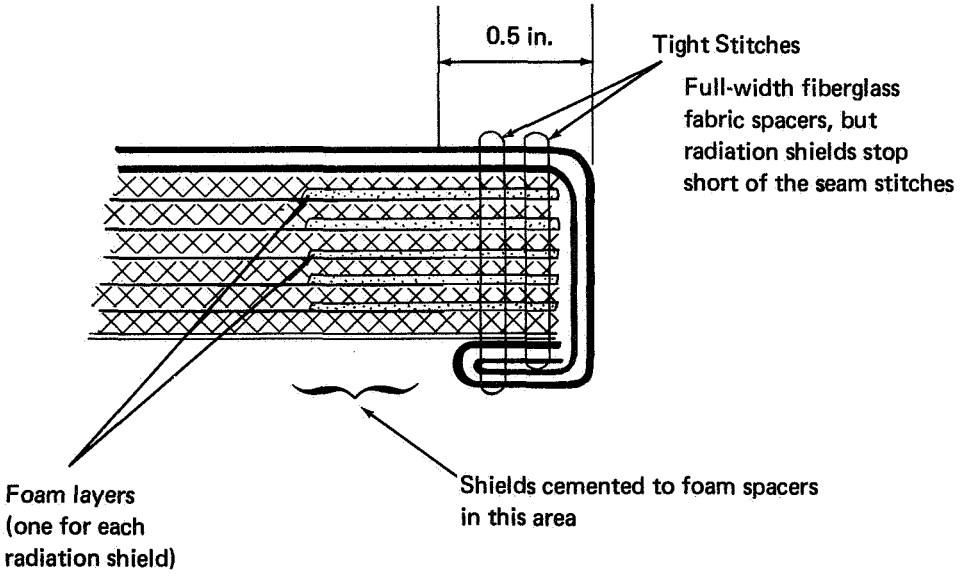

Source: Arthur D. Little, Inc.

FIGURE 13 ALTERNATIVE EDGE SEAM FOR FIBERGLASS SPACERS

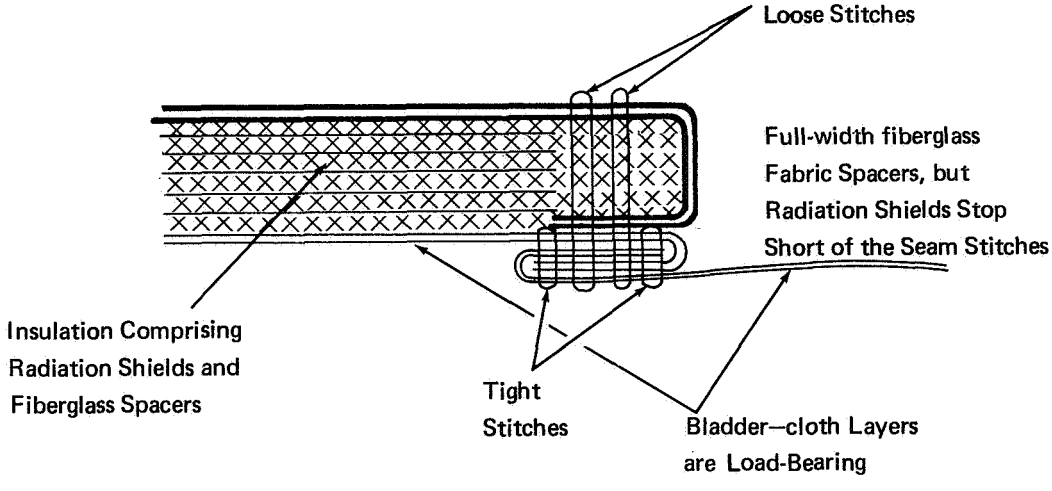

Source: Arthur D. Little, Inc.

FIGURE 14 LOAD-BEARING EDGE SEAM

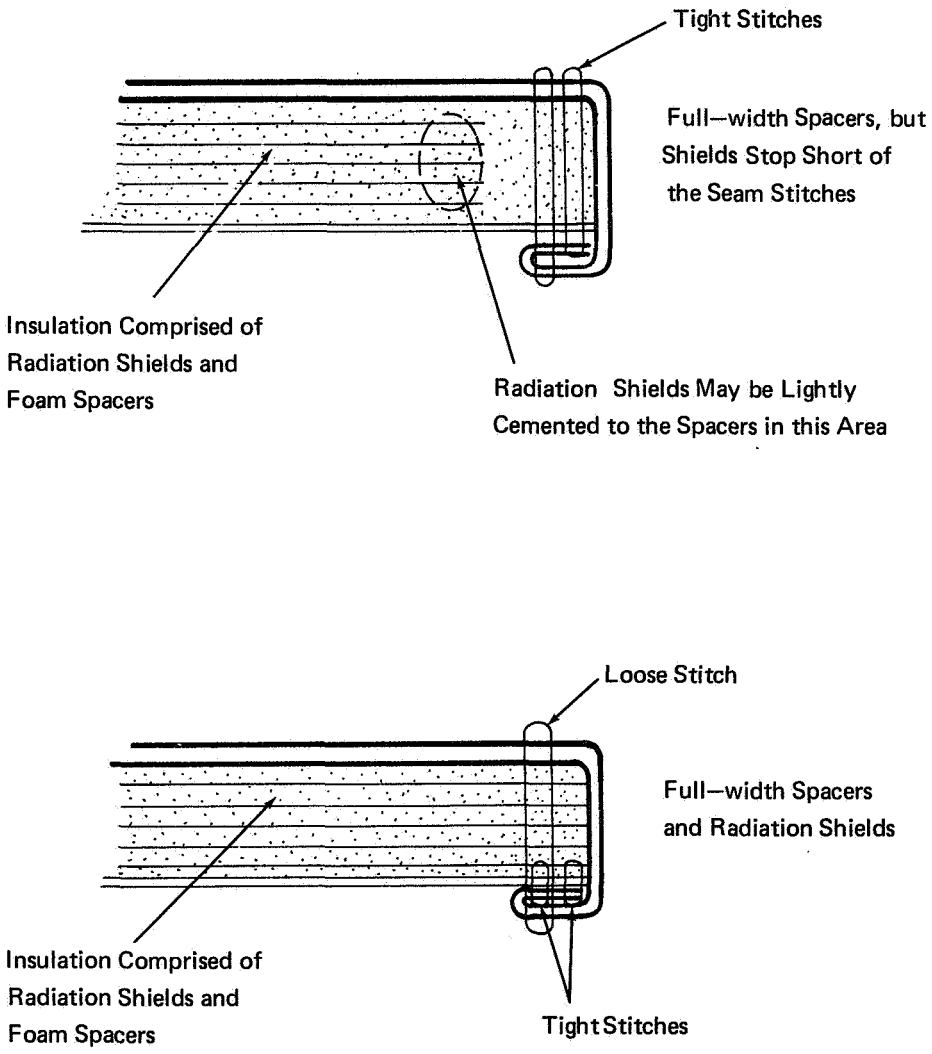

Source: Arthur D. Little, Inc.

FIGURE 15 EDGE SEAMS FOR FOAM SPACERS

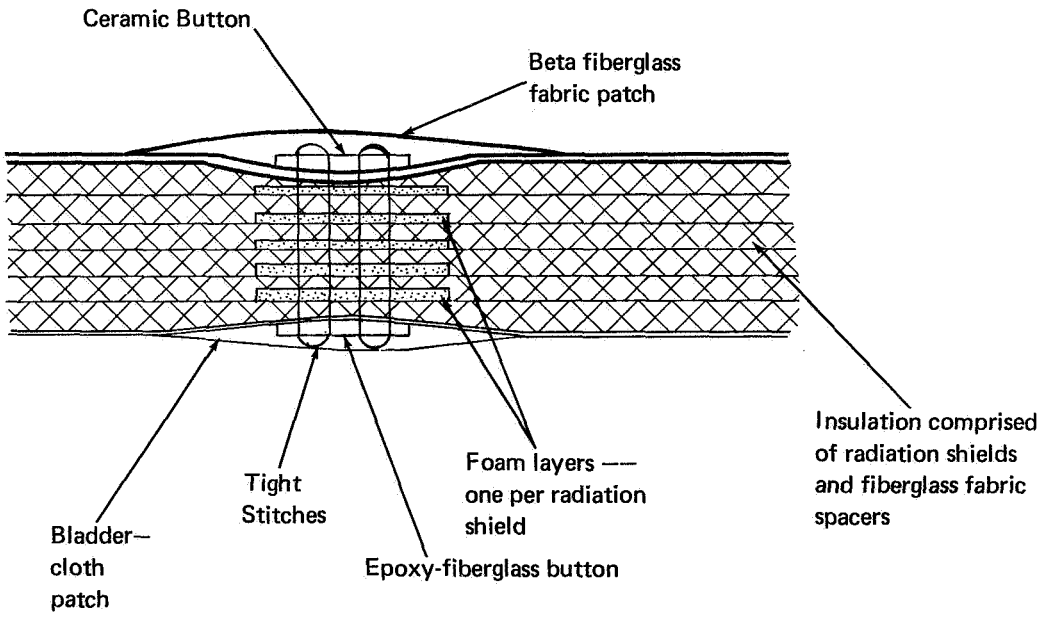

Source: Arthur D. Little, Inc.

FIGURE 16 BUTTON-TUFT FOR INSULATION STABILIZATION

tions is to compress the foam until the overall insulation layer is as thick as it was without the foam. (See Figure 16.) The tuft is completed by adding a Beta fiberglass patch on the outside and a bladder-cloth patch on the inside to prevent snagging and give the garment a smooth surface.

A recommended overlap type of closure, shown schematically in Figure 17, embodies many of the design features already discussed. The inner bladder layers of the garment are load-bearing. The zipper used for structurally closing the garment is firmly anchored in the bladder layers. The outer double layer of Beta fiberglass is used to loosely hold the insulation layers in place on the outside of the garment. An overlap of insulation of at least two inches is necessary to minimize heat migration either in or out through the overlap. A Velcro (or equivalent) type of seal with a suitable edge for grasping during actuation completes the overlap closure.

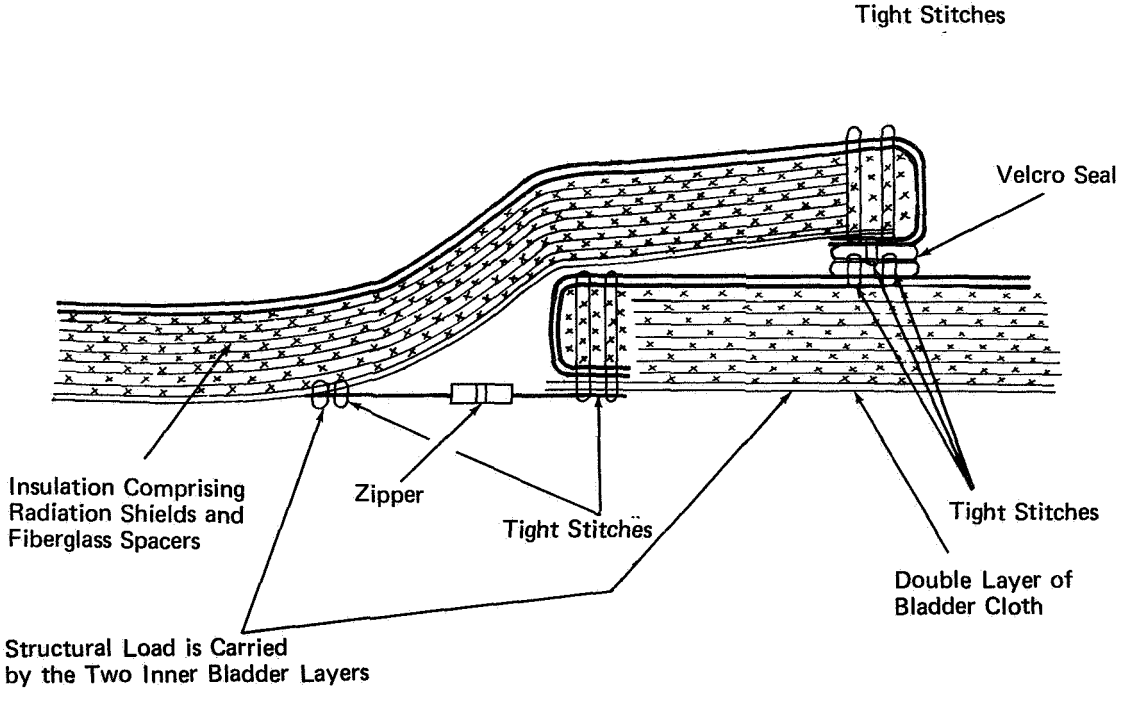

Source: Arthur D. Little, Inc.

FIGURE 17 RECOMMENDED CLOSURE

VI. MEASUREMENTS OF HEAT FLOW IN A TEST SECTION OF AN EXPERIMENTAL THERMAL MICROMETEOROID GARMENT

Thermal and durability evaluations of experimental, development, and flight-quality thermal micrometeoroid garments are expensive and time-consuming when complete garments are used. Since a technique for rapidly evaluating garment subsystems in simulated space and lunar environments was desirable, we developed a flexing elbow calorimeter for evaluating sections of thermal micrometeoroid garments in a laboratory-sized space simulation chamber. Heat flow was measured in an experimental garment section which incorporated the insulation and fabrication techniques developed in this program. Measurements made both before and after the garment section was subjected to 10,000 cycles of flexing confirmed the validity of this method of evaluating thermal micrometeoroid garments and showed that the developed insulation and fabrication techniques were durable.

A. ELBOW CALORIMETER

The elbow calorimeter, shown schematically in Figure 18, consists of a central calorimeter measuring section over which is placed a flexible pressurizable section of a space suit elbow. Guard sections attached at each end of the calorimeter were designed to minimize the heat leak into or out of the calorimeter measuring section. The experimental thermal micrometeoroid garment section covers the calorimeter measuring section and the two guard sections.

Figure 19 shows the assembled calorimeter with the flexible elbow section mounted in the test chamber. The left end of the calorimeter is anchored by low-conductance supports to a support structure in the space simulation chamber. The right end of the calorimeter is attached to a flexing mechanism with a yoke which guides the right end as the elbow section is flexed back and forth. The elbow calorimeter was flexed plus or minus 45 degrees from a normal axis. Ideally, the elbow calorimeter should have been flexed 90° in one direction from the neutral axis, but

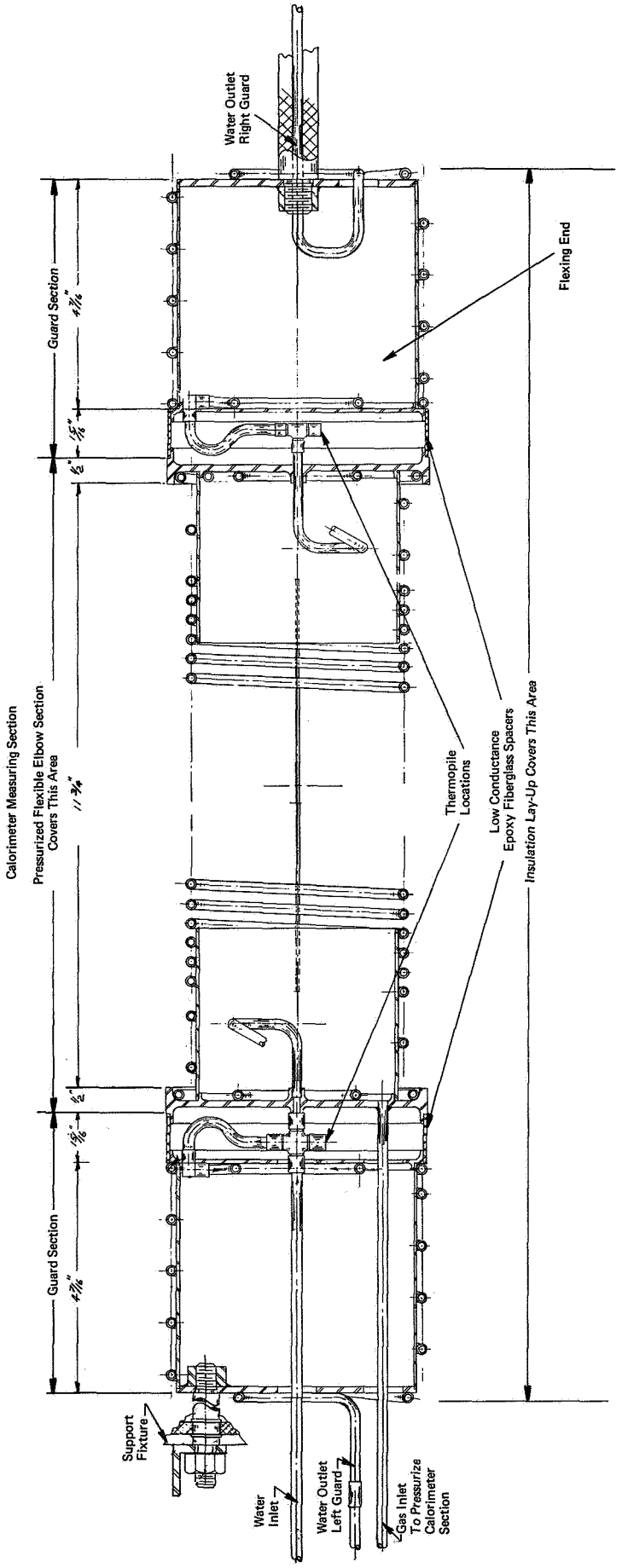

FIGURE 18 ELBOW CALORIMETER ASSEMBLY

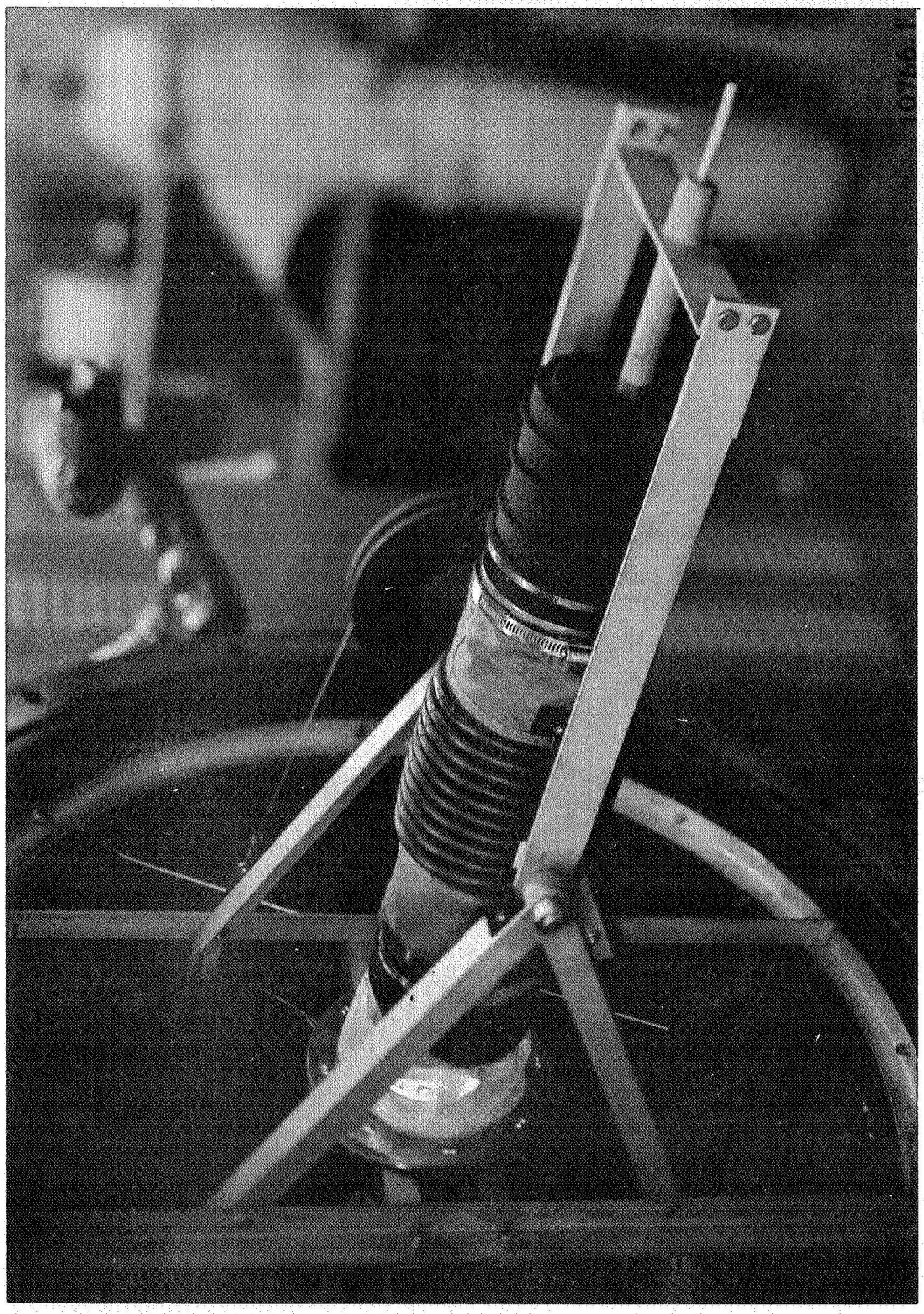

FIGURE 19 GUARDED ELBOW CALORIMETER

space limitations within the test chamber did not allow this range of motion.

1. Calorimeter Design

The requirement that the space suit insulation be tested in both lunar nighttime and lunar daytime conditions made it necessary to have a calorimeter that could measure heat flux outward from the calorimeter during lunar nighttime conditions and inward during lunar daytime conditions. The basic concept--one of many considered--for the calorimeter used in this test program is shown schematically in Figure 20. Water at ambient laboratory temperature is stored in a large insulated tank, pressurized to aid in controlling the water flow through the calorimeter and guard sections. Water flowing from the tank enters the left guard section, where it separates. The main flow passes through the calorimeter section, where the temperature rise is measured with a multijunction thermopile. Inlet temperature to the calorimeter is also measured. The water flowing through the calorimeter continues outward through the right guard section. The flow through the calorimeter and the right guard section is measured downstream of the control needle-valve. At the point where the water flow divides, a portion of the water is diverted back through the left calorimeter guard. Water flow in the left guard is controlled with a needle-valve. Temperatures are measured at the exits of both the right and left guards. Figure 20 also shows the temperature distributions which might be expected in the calorimeter and the two guards for lunar daytime conditions.

Figure 21 shows a flow diagram for the calorimeter. Water at near room temperature (70°F) is brought from the insulated tank into the test chamber through a transfer line which has multilayer insulation to minimize heat losses to the cold walls of the chamber. The transfer tank is located immediately outside of the space simulation chamber to minimize the heat loss or gain between the tank and chamber. The flow through the calorimeter is controlled by valve "A" and the flow through the left guard is controlled by valve "B".

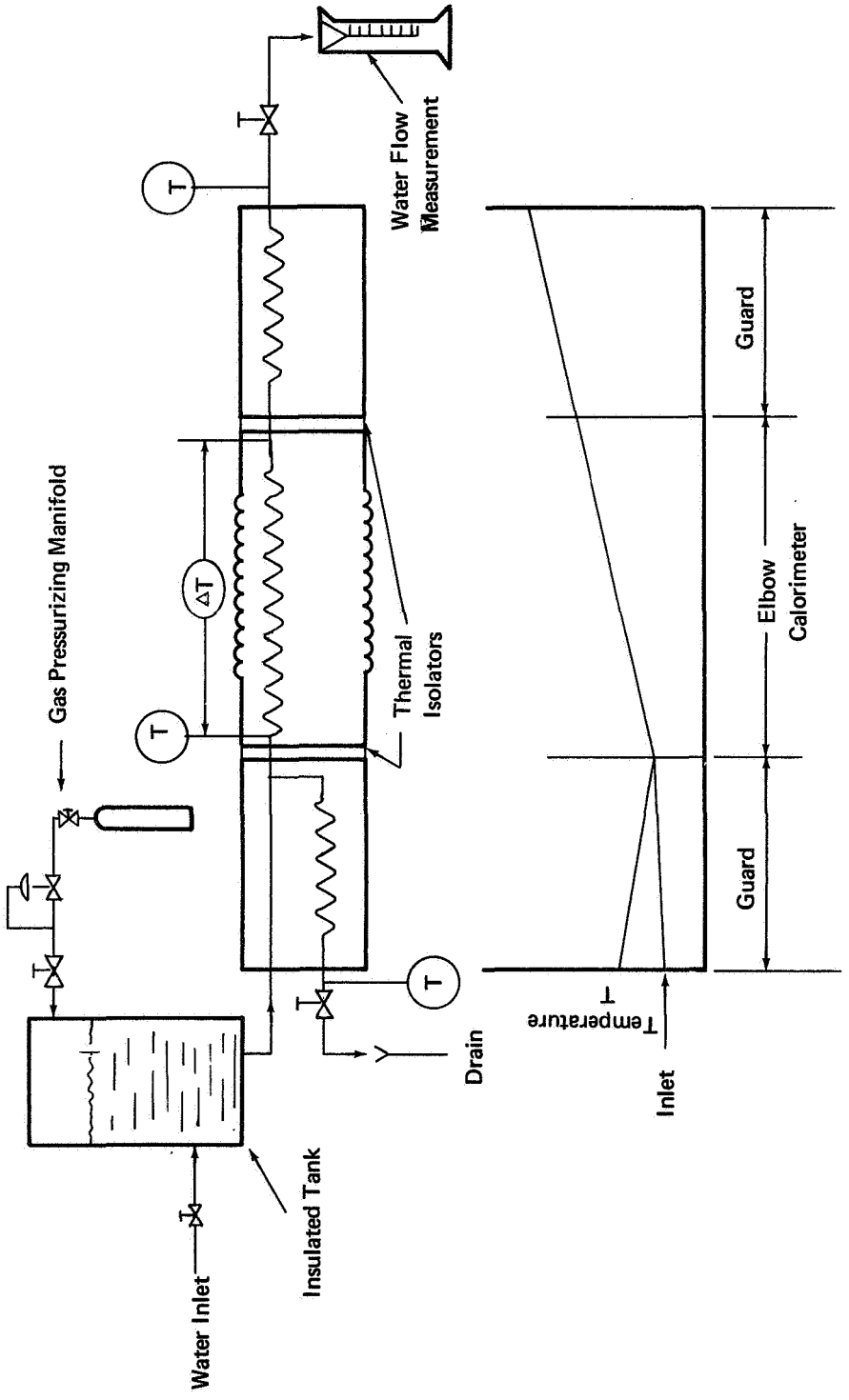

FIGURE 20 SCHEMATIC OF GUARDED ELBOW CALORIMETER

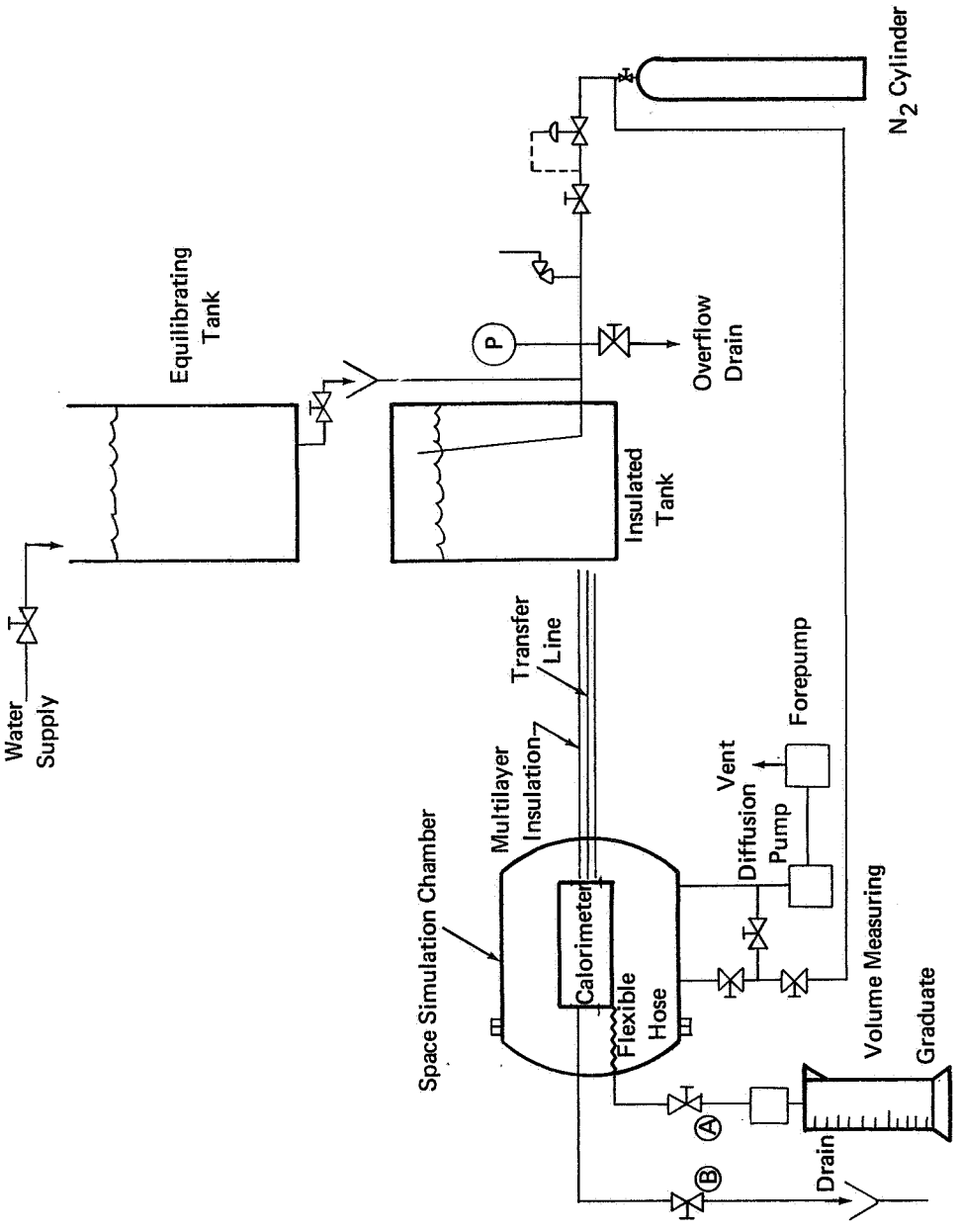

FIGURE 21 FLOW DIAGRAM FOR THE CALORIMETER

Provision is made for equalizing the pressure within the test chamber and the elbow calorimeter during the initial pumpdown. When the chamber pressure is below 32" of mercury, the elbow section can be isolated from the test chamber and back-filled with a small amount of dry nitrogen until the pressure differential between the elbow calorimeter section and the test chamber is approximately 3.0 psia (typical extravehicular space suit pressure). Filling the elbow calorimeter causes it to assume the shape it normally would have during space operations. In addition, the presence of dry nitrogen within the elbow calorimeter thermally couples the calorimeter with the inside wall of the garment and insures good heat transfer from the calorimeter to the wall.

Care was exercised in the design of the elbow calorimeter to insure that the expected heat flow through the test insulation could be accurately determined. In the design, we assumed that the insulation had an average thermal conductance like sample ADL-08 as measured in the guarded cold-plate calorimeter. Although the elbow calorimeter was designed for the average conductance (given in Table 12), we also checked the performance for conditions where the garment conductance was half a magnitude higher and half a magnitude lower.

For both the average and the extreme conductances, we calculated the expected heat flows through the insulation and, for various water flow rates through the calorimeter, we calculated the water temperature rise in the calorimeter. The lowest heat flow into the calorimeter was of the order of 1 Btu/hr. Under these conditions, at low water flow rates (less than 5 pounds of water per hour) the temperature rise across the calorimeter would be of the order of 0.2°F. For this low temperature rise, the accuracy of measurement of the temperature rise across the calorimeter should be 0.01°F in order to keep the error in the heat flux measurement to less than $\pm$ 5%. We used a 10-junction copper-constantan thermopile to achieve this accuracy.

In addition, we determined the error which would result from small temperature rises in the calorimeter due to temperature rise in the inlet water. We determined that to keep the error in the heat flux less

TABLE 12. THERMAL PROPERTIES OF THE GARMENT TEST SECTION

Layer Sequence

Outside:	2 layers Stevens Style 15035 tightly woven Beta fiberglass cloth.
Insulation:	7 radiation shields of 0.5-mil polyester film with 800 Å vapor-deposited aluminum and 500 Å vapor-deposited germanium on both sides.
Inside:	8 spacers of Stevens Style 2530 Beta marquisette with 9362 finish.
	2 bladder layers--David Clark Style 1807 with neoprene-coated surfaces together.

Garment Conductance

No-load conductance for sample ADL-08 from Figures 6 and 7.

	Boundary Temperatures	
	-250 to 70°F	300 to 70°F
Conductance (Btu/sq ft hr°F)	0.0017	0.0066

than ± 2%, we would have to limit the temperature rise in the calorimeter to less than 0.1°F per hour.

B. THERMAL MICROMETEOROID GARMENT SECTION

A section of a thermal micrometeoroid garment was made from the improved materials and the improved garment fabrication technique developed in the program. The section was 24 inches long and was fabricated on a mandrel which was 5.75 inches in diameter. The layers in this garment section are described in Table 12. The spacers and radiation shields were applied to the insulation layup one layer at a time in accordance with the construction procedures described in Section V. Care was taken to insure adequate spacing between each radiation shield and spacer by inserting a layer of blotter paper between the radiation shield and the next spacer. When the layup was complete, these blotter layers were removed by pulling them out axially. Seams in the radiation shields and the bladder layers were cemented with Dow-Corning type 503 silicone adhesive. The edges of spacers were stabilized with Fluorel cement type R/M-L-3203-6 (supplied by NASA-MSC) prior to cutting to exact dimensions. Shield spacers were attached to the layup with loose cross-stitches of nylon thread. In fabrication of a flight-qualifiable space suit insulation, a Beta fiberglass yarn would be used for stitching the shield spacers.

Care was exercised while making the garment section to insure that the radiation shields terminated at least 0.5 inch before the edge of the spacers so that, when the final seam was made, the radiation shields were not anchored in the seam. The outer layers of the garment section were made from Stevens Style 15035. These layers were made separately and stitched along the longitudinal axis with nylon thread. (In the actual space garment layup, double-stitching with Nomex and Beta fiberglass threads would be used.) The sequence of the layup before the end seam was made (Figure 22) shows that the radiation shield ends approximately 0.5 inch short of the end of the spacers. In addition, some of the tac stitches used to anchor the shield spacers are shown. The completed end seam is shown in Figure 23.

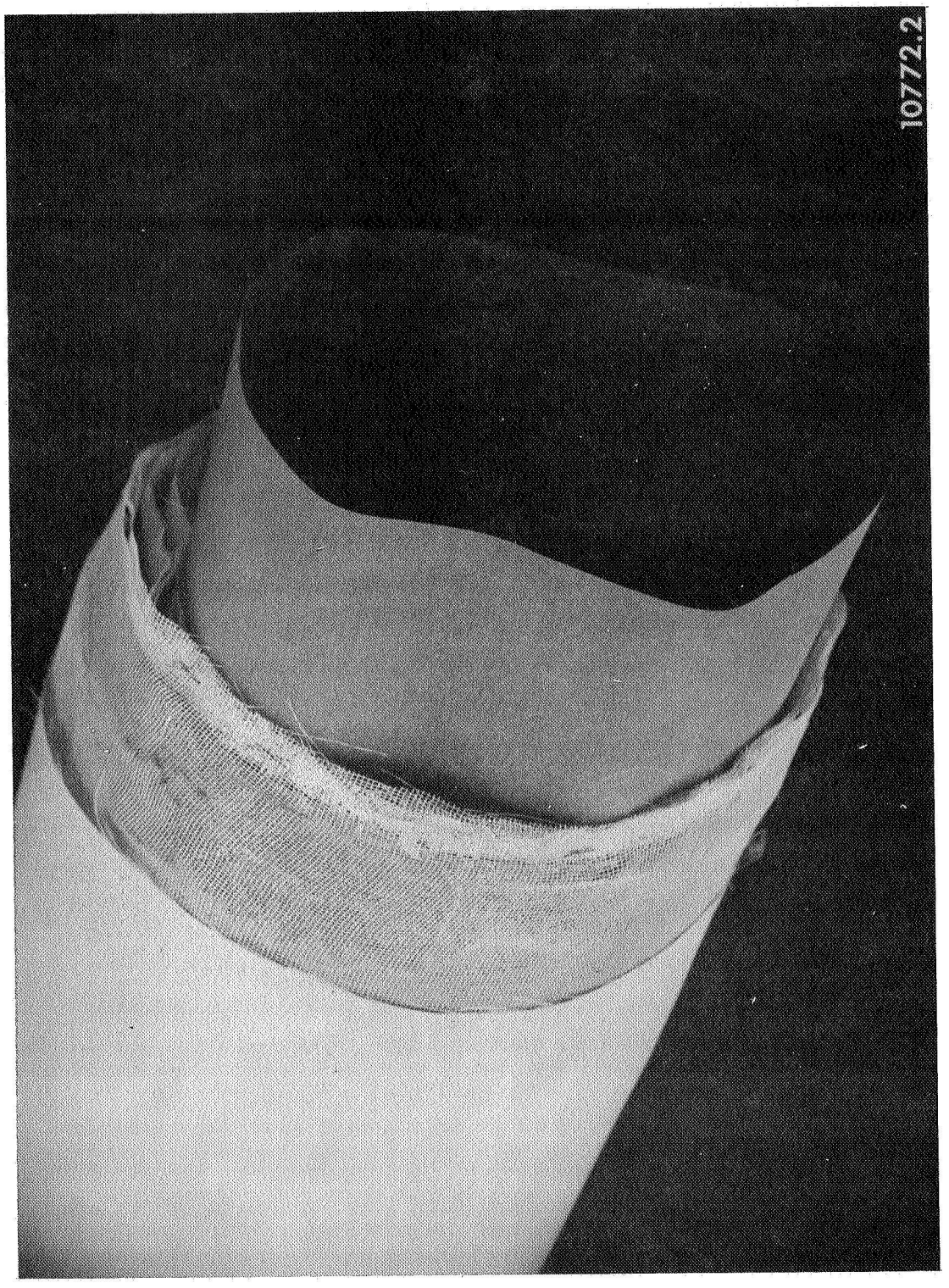

FIGURE 22 LAY-UP OF GARMENT TEST SECTION

FIGURE 23 COMPLETED GARMENT TEST SECTION

The thermal micrometeoroid garment section was installed on the elbow calorimeter for testing. To insure that the heat loss from the ends of the insulation and the calorimeter section are minimized, cap insulations consisting of single radiation shields of double-aluminized Mylar and double spacers of silk bridal veil were attached over the end seams. The complete layup with the end radiation shield guard is shown in Figure 24. The elbow calorimeter is bent slightly to show how the space garment was flexed during the 10,000-cycle wear portion of the test program.

C. SPACE SIMULATION CHAMBER

The garment section was tested on the elbow calorimeter in the ADL three-foot diameter space simulation chamber. This chamber is equipped with blackened shrouds through which liquid nitrogen circulates to simulate lunar nighttime conditions. The use of liquid-nitrogen-cooled shrouds is considered adequate for simulation of lunar nighttime conditions in this test program. For the lunar daytime conditions, we simulated the high temperature on the outside surface of the space suit insulation by enclosing the garment and calorimeter in a heated baffle as shown in Figure 25. Under these conditions, the elbow calorimeter is held in the axially elongated position. The heated baffle has three layers of double-aluminized Mylar radiation shields to minimize the heat loss from its outside wall. During the test, a heater attached to the inside of the heated baffle was used to raise the temperature to +300°F. During the test at lunar daytime conditions, liquid nitrogen was circulated in the test chamber shrouds to cryopump the chamber and achieve pressures below 10^{-4} torr.

The temperature of the calorimeter was measured with copper constantan thermocouples located at the positions shown in Figure 26. Thermocouple millivolt outputs were measured with a digital voltmeter. The output of the 10-junction thermopile was continuously recorded on a Honeywell Electronic 19 recorder so that trends in the temperature could be determined. Accurate measurements of the thermopile output were made with a Leeds and Northrup K-3 potentiometer. In addition, the inlet temperature

FIGURE 24 GARMENT TEST SECTION ON THE ELBOW CALORIMETER

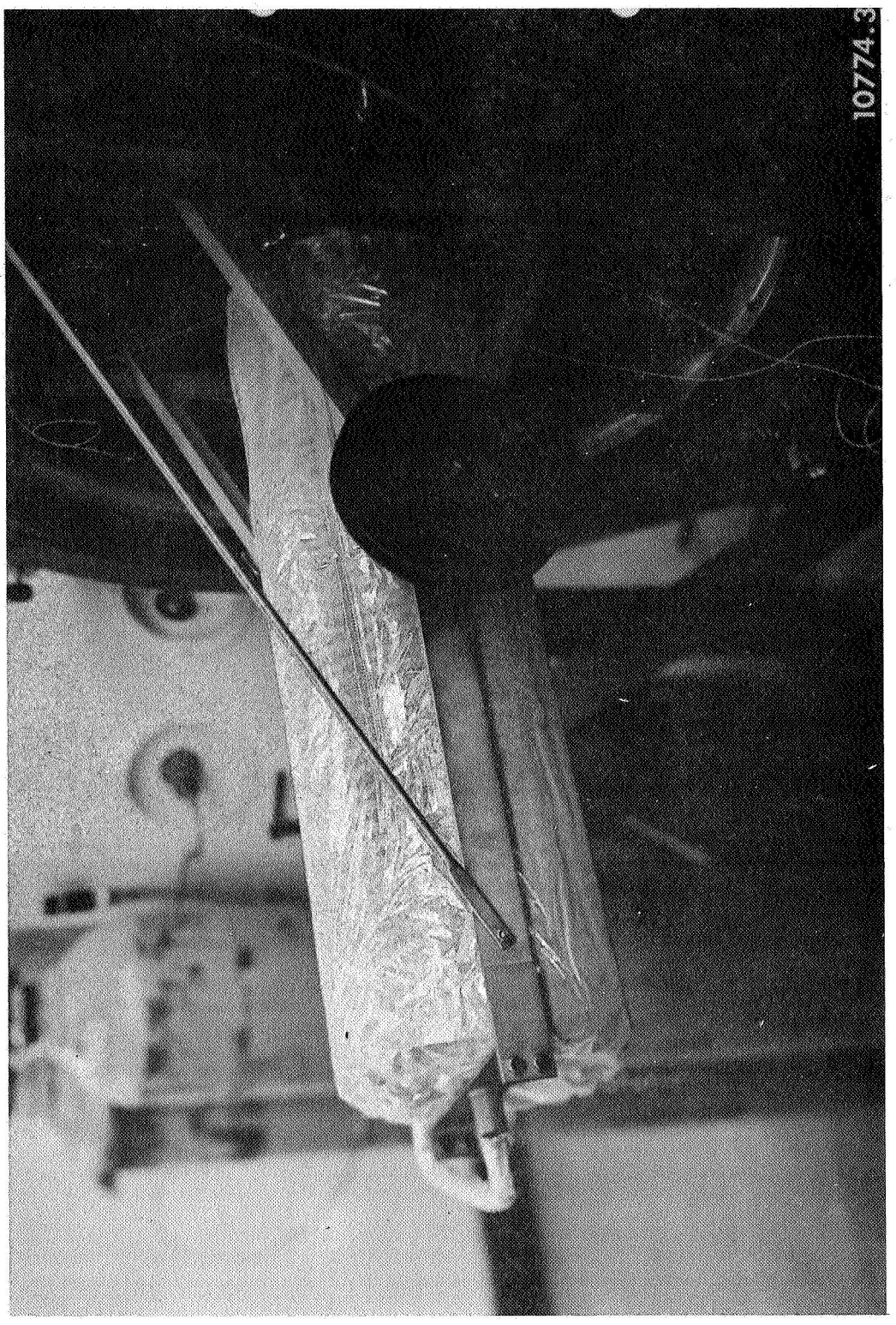

FIGURE 25 HEATED BAFFLE LOCATED OVER THE ELBOW CALORIMETER

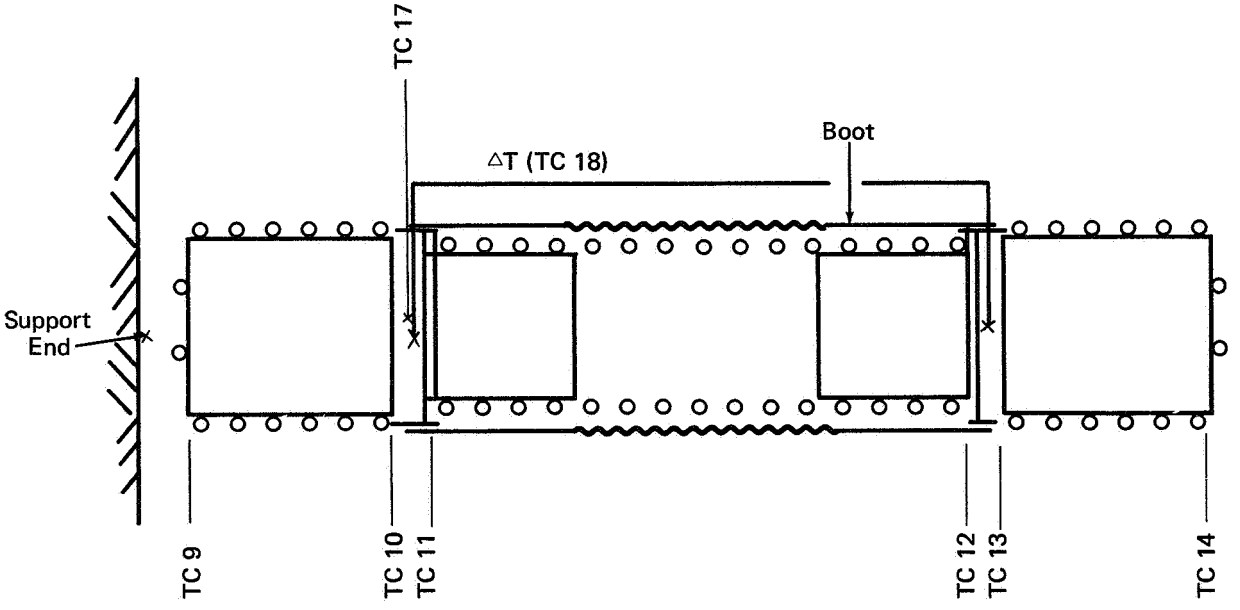

FIGURE 26 THERMOCOUPLE LOCATIONS IN THE ELBOW CALORIMETER

to the calorimeter was accurately measured with the K-3 potentiometer.

The calorimeter water flow rate was determined by collecting the water and carefully weighing the amount accumulated at the end of each hour. In addition, one-minute measurements of flow rate were taken occasionally during the test period.

Temperature and flow measurements were made every hour after equilibrium was reached. For all tests, the equilibrium heat flux either into or out of the calorimeter varied less than $\pm$ 5% from the average. Equilibrium measurements were made for a period of 6 to 9 hours.

D. TEST PROGRAM FOR ELBOW CALORIMETER

In determining the thermal performance of the developmental thermal micrometeoroid garment with the elbow calorimeter, the first step in the test sequence was to measure the heat flow into the garment section during simulated lunar daytime conditions, requiring the use of the hot baffle (Figure 25). The test chamber was evacuated, checked for leaks, and then the hot baffle was adjusted until an equilibrium temperature of approximately 300°F was achieved. Liquid nitrogen was used in the chamber baffles to insure that the pressure remained below 10^{-4} torr during these lunar daytime conditions. At the conclusion of the lunar daytime test prior to wear, the test chamber was opened, the hot baffle was removed and the chamber was then closed again.

Lunar nighttime conditions were then simulated by cooling the shrouds in the chamber to liquid nitrogen temperatures. When equilibirum was reached for lunar nighttime conditions, the flexure mechanism was started and attempts were made to flex the elbow section 10,000 times. Failure of the flexible return line from the elbow calorimeter due to freezing forced the termination of the flexure after 7,000 cycles of wear. We were unable to achieve an equilibrium thermal condition during the flexure, and with failure of the return line, we abandoned the efforts to measure heat flux during flexure. The remaining 3000 cycles of wear were achieved in vacuum at lunar nighttime conditions but without calorimeter water flow.

At the conclusion of the 10,000 cycles of wear, the performance of the garment section was measured under cold conditions with the elbow section in its axial position. At the conclusion of the cold tests, the chamber was again opened and the hot baffle placed over the garment and elbow calorimeter. Then the performance for the warm condition was measured again.

Thus, the performance of the thermal micrometeoroid garment was measured for lunar daytime and nighttime conditions prior to wear and for lunar nighttime and daytime conditions after wear.

E. MEASURED PERFORMANCE OF THERMAL MICROMETEOROID GARMENT SECTION

Table 13 lists the thermal performance for the four test conditions described above. The measured heat loss from the garment during simulated lunar nighttime conditons was 0.54 Btu/sq ft hr before wear and 0.76 Btu/sq ft hr after 10,000 cycles of flexing. The heat flow into the garment during simulated lunar daytime conditions was 1.47 Btu/sq ft hr before wear and 1.92 Btu/sq ft hr after 10,000 cycles of wear. Thus the insulation was degraded by 10,000 cycles of flexure wear.

At the conclusion of all tests, the third radiation shield in the insulation layup was removed and the emittance of both sides was measured in the emissometer. (See Tables 9 and 13.) From the emittances after tests, and the measured emittances of the unworn radiation shield, we calculated the heat flow to the insulation based on radiation heat transfer alone. As noted on Table 13, the heat flux per unit area based on radiative heat transfer alone accounts for between one-third and one-half of the measured heat flux per unit area. This leads us to believe that the remainder of the heat flux is accounted for by solid conduction through the spacers.

We next calculated the heat flow through the insulation based on data for the measured conductance of samples from the guarded cold-plate calorimeter for both the unworn and the worn conditions (see samples ADL-08 and ADL-06, Figures 6 and 7). The measured heat flux per unit area in the garment section before wear was 23% higher than was predicted

TABLE 13. THERMAL PERFORMANCE OF A SECTION OF A THERMAL-MICROMETEOROID GARMENT

	Unworn	After 10,000 Cycles of Flexure
SUMULATED LUNAR DAY		
Measured temperatures (inside/outside)	72/254	75/262
Measured heat flux per unit area Btu/sq ft hr)	1.47	1.92
Measured shield emittance (Table 7)	0.022	0.041
Heat flux per unit area based on the radiative heat transfer (Btu/sq ft hr)	0.484	0.95
Measured conductance--guarded cold-plate calorimeter data (Figure 7) (Btu/sq ft hr°F)	0.0066	0.0068
Heat flux per unit area based on measured conductance (Btu/sq ft hr)	1.201	1.27
SIMULATED LUNAR NIGHT		
Measured temperatures (inside/outside)	78/-310	70/-310
Measured heat flux per unit area (Btu/sq ft hr)	0.54	0.76
Measured shield emittance (Table 7)	0.022	0.041
Heat flux per unit area based on the radiative heat transfer (Btu/sq ft hr)	0.23	0.39
Measured conductance--guarded cold-plate calorimeter data (Figure 6) (Btu/sq ft hr°F)	0.0017	0.0019
Heat flux per unit area based on measured conductance (Btu sq ft hr)	0.66	0.72

from conductance measurements for lunar daytime conditions and 18% lower than predicted for lunar nighttime conditions.

The measured heat flux per unit area in the garment section after 10,000 cycles of wear was 50% higher than was predicted from conductance measurements in the calorimeter for lunar daytime conditions, and equal to the performance predicted for the lunar nighttime conditions.

F. POST-EXAMINATION OF THE THERMAL MICROMETEOROID GARMENT SECTION

The thermal micrometeoroid garment section was removed from the elbow calorimeter and partially disassembled so we could examine the condition of the insulation and other components. The third radiation shield from the outside was removed for careful examination. This radiation shield showed signs of wear on the lateral side of the elbow section. From this area, we removed two pieces of the radiation shield for emittance measurements, both sides. Where the emittances of the unworn germanium-overcoated radiation shields ranged from 0.021 to 0.023, in the worn condition after 10,000 cycles of wear, the emittances ranged from 0.038 to 0.045 (see Tables 7 and 13). This degradation in the emittance of the radiation shield is not unexpected, considering the condition of the radiation shield after flexure wear. Examination of this third radiation shield showed that although the germanium adhered well to the aluminum, and the aluminum adhered well to the shield substrate, the substrate itself failed, as evidenced by several small cracks in the radiation shield. In addition, in a pattern covering less than 1% of the radiation shield area repeated flexure-crinkling of the shield had caused the germanium to separate from the aluminum surface. Most of these areas had short (approximately 0.5 inch maximum) marks in an irregular pattern uniformly distributed over the surface, with a higher concentration located on the lateral sides. Abrasion of these areas with a pencil eraser easily removed the remaining aluminum and germanium, revealing the Kapton substrate. Adjacent areas which did not exhibit these marks resisted the abrasion of the eraser very well. The most serious failure observed in this third radiation shield was the cracking of the substrate. Several holes large enough to pass a pencil

lead were observed in the vicinity of the lateral side of the elbow. In addition, several cracks approximately 1/2" long were observed in this area.

Examining the remaining shields in the insulation layup in situ, we found that the same type of substrate failure had occurred. Pencil-lead-sized holes and occasional tears were noticed in the area on the lateral side of the insulation. There was no evidence on the germanium-overcoated radiation shields of abrasive wear against the Beta fiberglass spacers. Examination of the insulation indicated no failure of the spacers or of the bladder layers. The external layer of the space suit--two layers of Stevens Style 15035 material--showed evidence on the top and bottom surfaces of failure by mutual abrasion in an area where a wrinkle was induced during each cycle.

In summary, the post-test examination indicated that the germanium-overcoated radiation shield stands up well against any abrasion which might be induced due to normal flexure of the space suit and that significant improvement was achieved in the insulation abrasion-resistance. There is some evidence that sharp flexing of the radiation shield will cause a small amount of the germanium overcoating to detach from the aluminum substrate. However, the loss of coating amounts to less than 1% of the total surface area, even in areas where there is a large amount of flexure-crinkling activity. There was evidence that the 0.5-mil polyimide substrate failed as a result of repeated flexures. The failures appeared to have been induced by the combined flexure bending and sheer which occurs locally within the radiation shields as the garment is flexed. This failure of the polyimide substrate indicates the necessity, for lengthy space missions, of developing substrates which are less prone to cracking and tearing. There was no observable degradation in the garment layup technique and no evidence of radiation shield migration during this test. The abrasion failure of the external surface layer of the space suit is considered to be characteristic of the material--this type of failure has been observed in other garments made from Style 15035 Beta fiberglass cloth.

VII. PRELIMINARY SPECIFICATIONS FOR THERMAL INSULATION AND GARMENT FABRICATION

These preliminary specifications are valid only for experimental and development purposes. The capability of thermal insulations made according to these specifications has been demonstrated in laboratory simulated lunar nighttime and lunar daytime conditions. Garments made according to these specifications have not been space-flight qualified.

A. INSULATION

The multilayer insulation used in extravehicular space garments should consist of alternate layers of radiation shields and spacers. The radiation shields should have low-emittance surfaces (both sides) which minimize radiant heat transfer; the spacers should keep the individual radiation shields from touching each other, thereby minimizing thermal conduction through the layup, particularly when the insulation is compressed. An insulation layup should begin with a spacer and end with a spacer; therefore, the layup should always have one more spacer than radiation shields. The end spacer between the outermost shield and the garment outer layer keeps the shield from touching and assuming the temperature of the outer layer.

1. Radiation Shields

a. Film Substrate

The film substrate for the radiation shields should be 0.5-mil (0.0005 inch) polyimide film (duPont Kapton or equivalent) because it is less flammable than polyester film in air.

b. Vapor-Deposited Aluminum Surface with Germanium Overcoating

Aluminum with a minimum purity of 99.99% should be vapor-deposited on each side of the substrate film. Each aluminum coating should have a thickness of no less than 600 Å and no greater than 800 Å, applied in a single pass at the most rapid rate possible to provide a coating of uni-

form thickness and a bright luster.

An overcoating of germanium, also with a minimum purity of 99.99%, should be vapor-deposited on each side of the aluminized film. Each germanium coating should be between 450 Å and 550 Å thick and be applied in a single pass at the most rapid rate possible to produce the greatest uniformity.

The coatings should be free of windows (unaluminized areas), except for openings such as pin holes in the polyimide film. The film should be free of creases and the wrinkling of the film should be no greater in kind and degree than that found in the original mill-wound roll. Until both aluminum coatings are complete, all wind-rewind operations should be performed in the coating chamber at vacuum to prevent incomplete coating that can occur if dust accumulates on the film.

Prior to applying the germanium overcoating, the aluminum coating thickness should be determined by the electrical-resistance method, using an impedance bridge and a resistance head consisting of a 2" x 3" Micarta block with copper knife edges attached to the long side of the block. The measurement should be made on a 2" x 3" sample with the measuring head set across sample to measure a 2" x 2" square. The thickness in Angstroms can be computed from the relation, $t = \frac{285}{R}$, where R is the measured electrical resistance of the coating in ohms.

The germanium coating thickness should be determined by a suitable thin-film thickness monitor (such as the Speedyvac Model FTH-1 made by Edwards High Vacuum Corporation) within the chamber and at the velocity of travel of the film.

c. Gold-Coated Surface (Alternative)

An alternative low-emittance surface which does not require germanium overcoating for abrasion protection can be achieved by a single application of a liquid-bright-gold on both sides of the polyimide film with a

solution of liquid bright gold No. 8342* in accordance with AGC Corporation specification 555 or equivalent. The solution, when properly applied, dried, and baked out at 600°F, should have a thickness between 750 Å and 1250 Å. The gold coating thickness should also be determined by the electrical resistance method. The thickness in Angstroms can be computed from the relation, $t = \frac{244}{R}$, where R is the measured electrical resistance of the coating in ohms.

2. Spacers

Radiation shield spacer material should be fireproof in 100% oxygen, thin, lightweight, extremely flexible and have a fine hand and drape. In addition, it should be nonraveling and easy to handle during fabrication.

a. Single Layer Radiation Shield Spacer

The preferred radiation shield spacer for space suit application is a single layer of open-mesh leno weave fiberglass fabric. A good material for this application is Stevens Style 2530 (sometimes called Beta marquisette), whose specifications are given in Table 14.

b. Multiple Radiation Shield Spacers

An alternative radiation shield spacer would be two or three layers of thin open-weave fabric, such as that described in Table 15.

c. Finishes and Stabilization

A lubricating finish is required to improve the abrasion resistance of these spacers. For the single-layer leno weave fabrics, J. P. Stevens Co., Inc., proprietary finish No. 9362 should be used. This finish, equivalent to the NASA finish No. FO-17-A, a dimethylsilicone polymer in an emulsion which is 3% silicone by weight, leaves about 0.3% organic content in the fabric.

*Material is supplied by the Hanovia Division of Engelhard Industries, Newark, N.J.

TABLE 14. SPECIFICATIONS FOR PREFERRED SPACER MATERIAL

J. P. Stevens Style No. 2530 or equivalent (Beta marquisette) with No. 9362 finish. This is an open-mesh leno weave fiberglass fabric made with superfine filament.

Weight (ounces/square yard)	1.80 ± 10%
Thickness (inches)	0.005 ± 10%
Thread count (yarns/inch)	
Warp	42 ± 4
Fill	25 ± 2
Breaking strength (pounds/inch)	
Warp	42 ± 4
Fill	25 ± 2

Finish 9362 substantially improves abrasion resistance and has been tested and found nonflammable in pure oxygen at 16.5 psia.

Style 2530, Finish 9362, is the equivalent of NASA Style No. 48970, Finish No. FO-17-A.

Source: J. P. Stevens and Co., Inc.

TABLE 15. SPECIFICATIONS FOR AN ALTERNATIVE SPACER MATERIAL

J. P. Stevens Style 104 (or equivalent) with 5% finish of Fluorel R/M-L-3203-6[a] for yarn stabilization. This is a plain weave fiberglass made from yarns spun from E glass.

Weight (ounces/square yard)	0.58 ± 6%
Thickness (inches)	0.0013 ± 10%
Thread count (yarns/inch)	
Warp	60 ± 2
Fill	52 ± 2
Breaking strength (pounds/inch)	
Warp	40
Fill	10

[a] Fluorel finish R/M-L-32-3-6 is approximately 80% hexafluoropropene by weight, 20% vinylidinefluoride, and additional filler materials and quenching agents.

Source: J. P. Stevens and Co., Inc.

Thin open weave materials (such as style 104) are particularly susceptible to unraveling. Between 5% and 8% by weight is required for yarn stabilization to ease handling and fabrication. One material which can be used for stabilization is Fluorel cement type R/M-L-3203-6 developed by the 3M Company. Fluorel is approximately 80% hexafluoropropene by weight, 20% vinylidinefluoride, and additional filler materials and quenching agents. This stabilizing finish should be applied by diluting the material with five parts of solvent such as methyl ethyl ketone and spraying it on the fiberglass fabric until the desired weight gain has been achieved. Bake-out at 300°F for one-half hour is required.

B. FABRICATION

1. Insulation Layup

In thermal insulation systems where the primary mode of heat transfer is by radiation, it is desirable to use a series of radiation shields which are as completely isolated from each other as possible. Such radiation shields are called perfect or isolated radiation shields. Since it is impossible to achieve perfect radiation shielding, the best that can be done is to approach perfect radiation shielding through the use of good insulation construction techniques.

In applying multilayer insulation to an extravehicular space suit, use of the following basic construction technique will minimize deviation from the perfect radiation shielding concept:

- Hang the insulation as loosely as possible on the extravehicular garment.
- Minimize compressive loading on the insulation.
- Have each radiation shield form a single monolithic shell and be completely isolated from the next radiation shield.
- Avoid stitching through radiation shields; if such stitching is necessary, make it loose to minimize compressive load and chances of tearing the shields.

- Have spacer layers overlap radiation shield layers by at least one-half inch at all seams.

2. Garment Fabrication

The extravehicular space suit must serve dual purposes of isolating the astronaut from his external environment and shielding him from the infrequent micrometeoroid particles which he may encounter.

a. Layer Sequence

Starting from the outside of the garment, the garment elements (Figure 27) should be:

(1) Two layers of tightly woven fiberglass cloth made from Beta filament fiberglass yarns (J. P. Stevens Co., Inc., Style No. 15035 with No. 9362 finish, 6.2 oz/sq yd, or

Two layers of super Beta fiberglass cloth style NASA-MSC Style 4484. (This material differs from regular Beta fiberglass cloth Style 15035 in that the yarns are coated with Teflon before being woven into cloth.)

(2) An insulation layer consisting of seven alternate layers of double-aluminized polyimide (Kapton) film with overcoating of germanium and light open-mesh fiberglass spacers (see insulation specifications above), 18.7 oz/yd.

(3) Two layers of nylon rip-stop bladder cloth which have been neoprene-coated on one side (David Clark Co., Inc., Style 1807 or equivalent). The weight of the complete layup is estimated to be 47 oz/sq yd.

b. Representative Seams and Penetrations

Figure 12 illustrates a recommended seam or penetration edge termina-

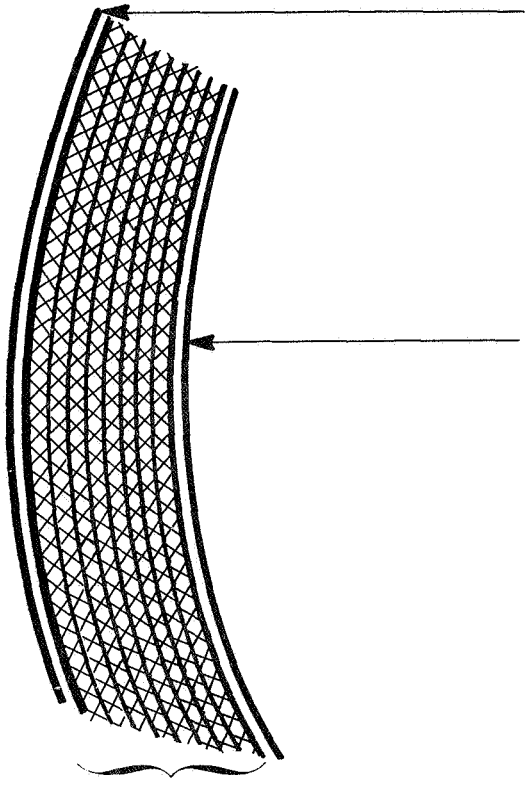

Insulation made from:

- 7 radiation shields – 0.5-mil Kapton film with 500 Å aluminum and 500 Å germanium overcoating, both vapor-deposited on the surfaces.
- 8 shield spacers – one per shield plus an extra, Stevens Style 2530 open mesh fabric (Beta marquisette) with 9362 finish

Weight = 47 oz/sq yd (Estimated from manufacturer's specifications)

FIGURE 27 LAYER SEQUENCE FOR RECOMMENDED THERMAL–MICROMETEOROID PROTECTION GARMENT

tion technique. The two inner bladder layers and the two outer layers surround the seven-radiation-shield multilayer insulation. Note that the radiation shields end about 0.5 inch before the edge of the seam. The outer fiberglass layers wrap around the end of the seam and a double stitch is taken through all layers except the radiation shields. This should be a tight stitch so that all components will be well anchored. If migration of the shields should prove to be a problem, the individual shields should be anchored lightly to the spacers with Fluorel cement.

c. Representative Closure

Figure 17 illustrates a recommended closure for an extravehicular garment. An important construction detail is that the inner layer of the garment (in this case double layers of bladder cloth) should carry the load and that the external layer of the closure should be loosely fitting on the garment.

d. Stitching Material

The stitching in the seams of the thermal-micrometeoroid extravehicular garment should be with double threads: one of Nomex and one of Beta fiberglass. The Nomex thread provides good strength for normal operating conditions and the Beta fiberglass thread insures the integrity of the seam in the event that fire destroys the Nomex thread. The Beta fiberglass thread should be size 0 and conform to Owens Corning Part No. E9 or Belding Corticelli Part No. 747-J1.* The Nomex thread should be made from non-melting aromatic polyamid yarn and meet the following requirements:**

Construction:	3-ply Z twist
Finish:	Unbonded
Breaking strength:	6.0 pounds minimum
Elongation:	20 to 40 percent
Yield:	6,000 yards per pound minimum

*ILC Industries, Inc., Specification Control Drawing ST15G274-02

**ILC Industries, Inc., Specification Control Drawing ST15N055-02

APPENDIX

A. CONDUCTANCE OF SPACE SUIT INSULATION

The data for all thermal conductance tests made during this program are summarized in Tables 16-32. The conductances of samples developed during the program (ADL-01 through ADL-09) are summarized in Tables 16-24 and the conductances of NASA/MSC-supplied samples (MSC-01 through MSC-08) are summarized in Tables 25-32. The data include a description of the insulation; the measured quantities were: compressive load (psi), the outside temperature of the insulation (the cold plate and hot plate temperatures in the conductance apparatus, °F), the inside temperature of the insulation (the midplane temperature, °F), the heat flux through the insulation (Btu/sq ft hr), the sample thickness (inches), and the sample and midplane weights (grams); and the derived quantities were: temperature difference across each of the two samples measured (°F), and the sample conductance (Btu/sq ft hr°F).

B. CONDUCTANCE DATA EXTRAPOLATION

The conductance was not measured at the exact boundary conditions required in the program--lunar daytime conditions (the outside temperature of the space suit at 300°F and the inside at 70°F) and lunar nighttime conditions (the outside of the space suit at -250°F and the inside at 70°F)--instead, all conductance measurements for the cold plate temperature were made at the boiling point of liquid nitrogen (-320°F) and for the warm plate temperature at 200°F and 300°F.

The use of a midplane temperature measurement between two identical samples of the space suit insulation allowed us to simultaneously measure the conductance of two samples of space suit insulation for each heat flux measurement. In most instances, the midplane temperature was higher than the 70°F required for the inside boundary condition of the space suit; therefore, extrapolations of the basic data were required to determine the insulation conductance for the two conditions.

In the extrapolation procedure, we assumed that the heat flux through the insulation was comprised of two components, solid conduction and radiation, as given by Equation 1.

$$Q = \frac{k}{x} A(T_1 - T_2) + \frac{A\sigma}{n(\frac{2}{\varepsilon} - 1)} (T_1^4 - T_2^4) \quad (1)$$

Introducing the definition of conductance

$$C = \frac{Q}{A(T_1 - T_2)} \quad (2)$$

and rearranging Equation 1

$$C = \frac{k}{x} + \frac{\sigma}{n(\frac{2}{\varepsilon} - 1)} \frac{T_1^4 - T_2^4}{T_1 - T_2} \quad (3)$$

We assumed that at a given compressive load on the insulation, the solid conductance ($\frac{k}{x}$) and the shield emittance (ε) are independent of the temperature difference across the insulation. Thus from Equation (3) the insulation conductance is linearly dependent on the parameter

$$\frac{T_1^4 - T_2^4}{T_1 - T_2}$$

The measured conductance at each sample pressure loading was plotted as a function of this parameter and values of the conductance at the desired temperature differences (300 to 70°F and 70 to -250°F) were obtained by straight line interpolation, as shown on Figure 28.

TABLE 16. PERFORMANCE OF SAMPLE ADL-01--
BASELINE INSULATION

Description: (1) 6 oz. HT Nomex
(7) 0.25-mil Mylar with 300 Å aluminum, one side
(7) NRC nonwoven Dacron batt
(2) bladder layers

Sample weights: Top 45.2 gm, midplane 20.2 gm, bottom 44.8 gm

Vacuum: less than 4×10^{-5} torr

Compressive Load (psi)	Outside Temperature (F)	Inside Temperature (F)	ΔT (F)	Heat Flux (Btu/hr ft^2)	Sample Thickness (in)	Conductance (Btu/ft^{2}hr°F)
1.9 to 2.4 x 10^{-3}	184	57.9	126	4.96	0.053	0.0394
4.9 to 9.8 x 10^{-4}	-320	57.9	378	4.96	0.053	0.0131
1.9 to 2.4 x 10^{-3}	291	182	109	7.90	0.058	0.0725
4.9 to 9.8 x 10^{-4}	-320	182	502	7.90	0.058	0.0157
0.02	290	162	128	10.94	0.054	0.0854
0.02	-320	162	482	10.94	0.054	0.0227
0.02	186	57	129	4.95	0.053	0.0384
0.02	-320	57	377	4.95	0.053	0.0131
0.20	203	36	167	8.84	0.049	0.0529
0.20	-320	36	356	8.84	0.049	0.0248
0.20	290	127	163	16.5	0.051	0.101
0.20	-320	127	447	16.5	0.051	0.0369
15.0	264	81.0	183	241.5	0.029	1.32
15.0	-320	81.0	501	241.5	0.029	0.62
15.0	199	34.3	165	196.5	0.029	1.19
15.0	-320	34.3	354	196.5	0.029	0.55
15.0	264	76	188	240.0	0.030	1.28
15.0	-320	76	396	240.0	0.030	0.000
2.0	194	12.5	181.5	45.2	0.036	0.0250
2.0	-320	12.5	332.5	45.2	0.036	0.136
2.0	290	119	171	117.8	0.037	0.689
2.0	-320	119	439	117.8	0.037	0.268
2.0	196	46.7	149.3	72.7	-	0.487
2.0	-320	46.7	366.7	72.7	-	0.198

TABLE 17. PERFORMANCE OF SAMPLE ADL-02--LAMINATED SHIELD AND SPACER INSULATION

Description: (2) Stevens Style 15035 tight-weave Beta fiberglass
(7) laminate of NASA 0.5-mil Kapton with 300 Å aluminum both sides; adhered to Stevens Style 2530 Beta marquisette
(2) bladder layers

Sample weight: top 78.5 gm, midplane 20.3 gm, bottom 77.5 gm

Vacuum: less than 4×10^{-5} torr

Compressive Load (psi)	Outside Temperature (F)	Inside Temperature (F)	ΔT (F)	Heat Flux (Btu/hr ft^2)	Sample Thickness (in)	Conductance (Btu/ft^{2}hr°F)
2.3 to 4.1 x 10^{-3}	296	180	116	2.28	0.128	0.020
0.92 to 1.8 x 10^{-3}	180	-320	500	2.28	0.128	0.0046
2.3 to 4.1 x 10^{-3}	182	87	95	1.12	0.131	0.012
0.92 to 1.8 x 10^{-3}	87	-320	407	1.12	0.131	0.0027
0.01	182	75	107	3.31	0.101	0.031
0.01	75	-320	395	3.31	0.101	0.0084
0.01	295	147	148	6.59	0.100	0.045
0.01	147	-320	467	6.59	0.100	0.014
0.1	197	72	105	8.08	0.142	0.077
0.1	72	-320	392	8.08	0.142	0.021
0.1	289	135	154	12.3	0.143	0.080
0.1	135	-320	455	12.3	0.143	0.027
0.1	289	140	149	14.8	0.092	0.099
0.1	140	-320	460	14.8	0.092	0.032
2.0	291	125	166	49.5	0.086	0.030
2.0	125	-320	445	49.5	0.086	0.11
2.0	191	67	124	34.6	0.084	0.28
2.0	67	-320	387	34.6	0.084	0.090

TABLE 18. PERFORMANCE OF SAMPLE ADL-03--INTEGRATED SHIELD-AND-SPACER INSULATION

Description: (2) Stevens Style 15035 tight-weave Beta fiberglass

(7) composite shield and spacer of Stevens Style 1659 dipped in Kapton solution; 500 Å aluminum both sides

(2) bladder layers

Sample weights: top 98.9 gm, midplane 20.3 gm, bottom 97.1 gm

Vacuum: less than 4×10^{-5} torr

Compressive Load (psi)	Outside Temperature (F)	Inside Temperature (F)	ΔT (F)	Heat Flux (Btu/hr ft^2)	Sample Thickness (in)	Conductance (Btu/ft^{2}hr°F)
2.5 to 4.6 x 10^{-3}	289	142	147	1.34	0.179	0.00910
1.0 to 2.1 x 10^{-3}	142	-320	462	1.34	0.179	0.00290
2.5 to 4.6 x 10^{-3}	198	47	150	8.76	0.090	0.0582
1.0 to 2.1 x 10^{-3}	47.8	-320	368	8.76	0.090	0.0238
0.01	-190	44.8	145	7.75	0.092	0.0533
0.01	44.8	-320	365	7.75	0.092	0.0212
0.01	293	118	175	11.5	0.092	0.0658
0.01	118	-320	438	11.5	0.092	0.0260
0.2	295	120	175	17.7	0.090	0.0893
0.2	120	-320	440	17.7	0.090	0.0403
0.2	195	51.8	143	11.1	0.090	0.0775
0.2	51.8	-320	372	11.1	0.090	0.0298
2.0	189	33.7	155	35.8	0.074	0.231
2.0	33.7	-320	354	35.8	0.074	0.101
2.0	296	113	183	63.3	0.074	0.346
2.0	113	320	433	63.3	0.074	0.146
15	292	113	179	201	0.060	1.12
15	113	-320	433	201	0.060	0.464
15	198	48.8	149	151	0.058	1.01
15	48.8	-320	369	151	0.058	0.409

TABLE 19. PERFORMANCE OF SAMPLE ADL-04

Description: (2) Stevens Style 15035 tight-weave Beta fiberglass
(7) 1.0-mil Kapton with 1700 Å liquid bright gold both sides
(8) 0.030 in. flexible open-cell polyurethane foam
(2) bladder layers

Sample Weights: top 79.3 gm, midplane 12.5 gm, bottom 80.6 gm

Vacuum: less than 4×10^{-5} torr

Sample was subjected to 10,000 cycles of wear

Compressive Load (psi)	Outside Temperature (F)	Inside Temperature (F)	ΔT (F)	Heat Flux (Btu/hr ft^2)	Sample Thickness (in)	Conductance (Btu/ft^{2}hr°F)
2.9 to 3.8 x 10^{-3}	202	72	130	0.91	0.379	0.0070
0.87 to 1.7 x 10^{-3}	-320	72	392	0.91	0.379	0.0023
2.9 to 3.8 x 10^{-3}	292	130	162	1.27	0.378	0.0078
0.87 to 1.7 x 10^{-3}	-320	130	450	1.27	0.378	0.0028
0.01	194	63	131	1.03	0.303	0.0078
0.01	-320	63	383	1.03	0.303	0.0027
0.01	294	127	167	1.64	0.378	0.0098
0.01	-320	127	447	1.64	0.378	0.0037
0.01	193	75	118	2.58	0.271	0.0218
0.01	-320	75	395	2.58	0.271	0.0065
0.01	294	135	159	4.74	0.274	0.0298
0.01	-320	135	455	4.74	0.274	0.0104
2.0	192	87	105	28.3	0.109	0.269
2.0	-320	87	407	28.3	0.109	0.0695
2.0	287	141	146	51.7	0.100	0.351
2.0	-320	141	461	51.7	0.100	0.112
15	288	138	150	283	0.052	1.88
15	-320	138	458	283	0.052	0.618
15	192*	90*	102	187	0.053	1.82
15	-320	90*	410	187	0.053	0.456

*Estimated values, data were lost

TABLE 20. PERFORMANCE OF SAMPLE ADL-05

Description: (2) Stevens Style 15035 tight-weave Beta fiberglass
(7) 0.5-mil Kapton with 800 Å aluminum and 500 Å germanium both sides
(8) 0.030 in. flexible open-cell polyurethane foam
(2) bladder layers

Sample Weights: top 65.5 gm, midplane 12.5 gm, bottom 67.0 gm

Vacuum: less than 4×10^{-5} torr

Sample was subjected to 10,000 cycles of wear

Compressive Load (psi)	Outside Temperature (F)	Inside Temperature (F)	ΔT (F)	Heat Flux (Btu/hr ft^2)	Sample Thickness (in)	Conductance (Btu/ft^{2}hr°F)
2.5 to 3.1 x 10^{-3}	201	70	131	1.04	0.366	0.0080
0.7 to 1.4 x 10^{-3}	-320	70	390	1.04	0.366	0.0027
2.5 to3.1 x 10^{-3}	293	129	164	1.36	0.365	0.0083
0.7 to 1.4 x 10^{-3}	-320	129	449	1.36	0.365	0.0030
0.01	293	125	168	1.86	0.293	0.011
0.01	-320	125	445	1.86	0.293	0.0042
0.01	186	52	134	1.21	0.287	0.0090
0.01	-320	52	372	1.21	0.287	0.0033
0.10	201	65	136	3.47	0.270	0.025
0.10	-320	65	385	3.47	0.270	0.009
0.10	295	127	168	5.68	0.273	0.034
0.10	-320	127	447	5.68	0.273	0.013
2.0	291	141	150	49.4	0.098	0.33
2.0	-320	141	461	49.4	0.098	0.11
2.0	189	67	122	40.7	0.094	0.33
2.0	-320	67	387	40.7	0.094	0.10
15.0	190	82	108	185	0.054	1.7
15.0	-320	82	402	185	0.054	0.46
15.0	294	133	161	314	0.052	1.95
15.0	-320	133	453	314	0.052	0.70

TABLE 21. PERFORMANCE OF SAMPLE ADL-06

Description: (2) Stevens Style 15035 tight-weave Beta fiberglass
(7) 0.5-mil Kapton with 800 Å aluminum and 500 Å germanium both sides
(8) Stevens Style 2530 Beta marquisette
(2) bladder layers

Sample weights: top 88.0 gm, midplane 12.5 gm, bottom 88.7 gm

Vacuum: less than 1.4×10^{-4} torr

Sample was subjected to 10,000 cycles of wear

Compressive Load (psi)	Outside Temperature (F)	Inside Temperature (F)	ΔT (F)	Heat Flux (Btu/hr ft^2)	Sample Thickness (in)	Conductance (Btu/ft^{2}hr°F)
2.8 to 3.7 x 10^{-3}	207	80	127	0.78	0.168	0.0061
0.86 to 1.7 x 10^{-3}	-320	80	400	0.78	0.168	0.0020
2.8 to 3.7 x 10^{-3}	298	148	150	1.06	0.168	0.0071
0.86 to 1.7 x 10^{-3}	-320	148	468	1.06	0.168	0.0023
0.01	297	142	155	3.18	0.111	0.020
0.01	-320	142	462	3.18	0.111	0.0069
0.01	194	72	122	1.81	0.110	0.015
0.01	-320	72	392	1.81	0.110	0.0046
0.1	194	60	134	9.57	0.101	0.071
0.1	-320	60	380	9.57	0.101	0.025
0.1	294	142	152	15.9	0.105	0.105
0.1	-320	142	462	15.9	0.105	0.034
2.0	191	54	147	80.5	0.077	0.55
2.0	-320	54	374	80.5	0.077	0.22
2.0	292	118	174	142	0.076	0.82
2.0	-320	118	438	142	0.076	0.32
15.0	185	52	133	227	0.058	1.7
15.0	-320	52	372	227	0.058	0.61
15.0	294	130	164	425	0.055	2.6
15.0	-320	130	450	425	0.055	0.95

TABLE 22. PERFORMANCE OF SAMPLE ADL-07

Description: (2) Stevens Style 15035 tight-weave Beta fiberglass
(7) 0.5-mil Kapton with 800 Å aluminum and 500 Å aluminum both sides
(8) Stevens Style 104 with 5% Ultrathene stabilization
(2) bladder layers

Sample weights: Top 68.4, midplane 12.5 gm, bottom 67.2 gm

Vacuum: less than 1.2×10^{-5} torr

Sample was subjected to 10,000 cycles of wear

Compressive Load (psi)	Outside Temperature (F)	Inside Temperature (F)	ΔT (F)	Heat Flux (Btu/hr ft^2)	Sample Thickness (in)	Conductance (Btu/ft^{2}hr°F)
2.24 to 2.89 x 10^{-3}	203	111	92	0.88	0.121	0.0096
0.67 to 1.34 x 10^{-3}	-320	111	431	0.88	0.121	0.0020
2.24 to 2.89 x 10^{-3}	299	183	116	1.57	0.120	0.014
0.67 to 1.34 x 10^{-3}	-320	183	503	1.57	0.120	0.0031
0.01	300	164	136	4.06	0.074	0.030
0.01	-320	164	484	4.06	0.074	0.0085
0.01	201	94	107	2.73	0.073	0.025
0.01	-320	94	414	2.73	0.073	0.0066
0.1	202	99	103	7.03	0.061	0.068
0.1	-320	99	419	7.03	0.061	0.017
0.1	296	175	121	16.5	0.050	0.14
0.1	-320	175	495	16.5	0.050	0.035
2.0	196	96	100	116	0.047	1.2
2.0	-320	96	416	116	0.047	0.28
2.0	317	178	139	291	0.047	2.1
2.0	-320	178	498	291	0.047	0.29
15.0	208	99	110	386	0.031	3.5
15.0	-320	99	419	386	0.031	0.92
15.0	305	158	147	768	0.031	5.2
15.0	-320	158	478	768	0.031	1.6

TABLE 23. PERFORMANCE OF SAMPLE ADL-08

Description: (2) Stevens Style 15035 tight-weave Beta fiberglass
(7) 0.5-mil Kapton with 800 Å aluminum and 500 Å germanium both sides
(8) Stevens Style 2530 Beta marquisette
(2) bladder layers

Sample weights: top 83.6 gm, midplane 12.5 gm, bottom 82.5 gm

Vacuum: less than 7×10^{-5} torr.

Compressive Load (psi)	Outside Temperature (F)	Inside Temperature (F)	ΔT (F)	Heat Flux (Btu/hr ft^2)	Sample Thickness (in)	Conductance (Btu/ft^{2}hr°F)
2.68 to 3.48×10^{-3}	201	89	112	0.678	0.169	0.0061
0.82 to 1.63×10^{-3}	-320	89	409	0.678	0.169	0.0017
2.68 to 3.48×10^{-3}	294	158	136	0.918	0.170	0.0068
0.82 to 1.63×10^{-3}	-320	158	478	0.918	0.170	0.0019
0.01	196	85	111	1.053	0.125	0.0095
0.01	-320	85	405	1.053	0.125	0.0026
0.01	291	160	131	2.150	0.124	0.0164
0.01	-320	160	480	2.150	0.124	0.0045
0.1	209	87	122	7.00	0.097	0.057
0.1	-320	87	407	7.00	0.097	0.0172
0.1	294	149	145	10.3	0.099	0.071
0.1	-320	149	469	10.3	0.099	0.022
2.0	209	77	132	75.2	0.075	0.569
2.0	-320	77	397	75.2	0.075	0.189
2.0	291	135	156	139.5	0.068	0.894
2.0	-320	135	455	139.5	0.068	0.307
15.0	192	69	123	211.0	0.055	1.72
15.0	-320	69	389	211.0	0.055	0.542
15.0	295	136	159	347.0	0.054	2.18
15.0	-320	136	456	347.0	0.054	0.761

TABLE 24. PERFORMANCE OF SAMPLE ADL-09

Description: (2) Stevens Style 15035 tight-weave Beta fiberglass
(7) 0.5-mil Kapton with 800 Å aluminum and 500 Å germanium both sides
(8) 0.030 in. flexible open-cell polyurethane foam
(2) bladder layers

Sample weights: top 67.0 gm, midplane 20.3 gm, bottom 66.4 gm

Vacuum: less than 3×10^{-5} torr.

Compressive Load (psi)	Outside Temperature (F)	Inside Temperature (F)	ΔT (F)	Heat Flux (Btu/hr ft^2)	Sample Thickness (in)	Conductance (Btu/ft^{2}hr°F)
2.36 to 3.01 x 10^{-3}	198	60	138	0.567	0.369	0.0041
0.65 to 1.31 x 10^{-3}	-320	60	380	0.567	0.369	0.0015
2.36 to 3.01 x 10^{-3}	295	120	175	0.945	0.392	0.0054
0.65 to 1.31 x 10^{-3}	-320	120	440	0.945	0.392	0.0021
0.01	194	54	140	0.594	0.315	0.0042
0.01	-320	54	374	0.594	0.315	0.0016
0.01	294	119	175	0.903	0.319	0.0052
0.01	-320	119	439	0.903	0.319	0.0021
0.1	192	56	136	2.92	0.274	0.0215
0.1	-320	56	376	2.92	0.274	0.0078
0.1	290	120	170	5.79	0.277	0.0341
0.1	-320	120	440	5.79	0.277	0.0132
2.0	187	65	122	52.3	0.088	0.429
2.0	-320	65	385	52.3	0.088	0.136
2.0	288	136	152	60.3	0.092	0.397
2.0	-320	136	456	60.3	0.092	0.132
15.0	187	72	115	178.6	0.056	1.55
15.0	-320	72	392	178.6	0.056	0.456
15.0	298	126	172	343.0	0.053	1.99
15.0	-320	126	446	343.0	0.053	0.769

TABLE 25. PERFORMANCE OF SAMPLE MSC-01

Description: (2) NASA Style 4190B tight-weave Beta fiberglass
(7) 0.5-mil Kapton 300 Å aluminized one side
(7) NASA Style 4897 Beta marquisette
(2) bladder layers

Sample weights: top 89.5 gm, midplane 20.3 gm, bottom 90.2 gm

Vacuum: less than 1×10^{-4} torr

Compressive Load (psi)	Outside Temperature (F)	Inside Temperature (F)	ΔT (F)	Heat Flux (Btu/hr ft^2)	Sample Thickness (in)	Conductance (Btu/ft^{2}hr°F)
0.01	280	129	151	2.93	0.108	0.0194
0.01	-320	129	449	2.93	0.108	0.00652
1.25	287	97	190	36.7	0.075	0.193
1.25	-320	97	417	36.7	0.075	0.0880
15	283	73	210	159	0.049	0.757
15	-320	73	393	159	0.049	0.404
0.01	298	147	151	5.05	0.105	0.0334
0.01	-320	147	467	5.05	0.105	0.0108
2.3 to 4.2 x 10^{-3}	227	106	121	5.0	0.131	0.0413
0.95 to 1.89 x 10^{-3}	-320	106	426	5.0	0.131	0.0117

TABLE 26. PERFORMANCE OF SAMPLE MSC-02

Description: (1) NASA Style 4190B with carboxy nitroso coating on both sides

(7) laminated composite shield and spacer Schjeldahl Style X993

(2) bladder layers

Sample weight: Top 78.3 gm, midplane 20.3 gm, bottom 75.3 gm

Vacuum: less than 1×10^{-4} torr

Compressive Load (psi)	Outside Temperature (F)	Inside Temperature (F)	ΔT (F)	Heat Flux (Btu/hr ft^2)	Sample Thickness (in)	Conductance (Btu/ft^{2}hr°F)
2.1 to 3.7 x 10^{-3}	310	172	138	3.02	0.127	0.0219
0.83 to 1.66 x 10^{-3}	-320	172	492	3.02	0.127	0.00615
2.1 to 3.7 x 10^{-3}	299	167	132	2.74	0.127	0.0208
0.83 to 1.66 x 10^{-3}	-320	167	487	2.74	0.127	0.00563
0.03	302	137	165	6.63	0.106	0.0402
0.03	-320	137	457	6.63	0.106	0.0145
0.27	302	112	190	19.8	0.085	0.104
0.27	-320	112	432	19.8	0.085	0.0457
16.	295	64	231	209.	0.059	0.905
16.	-320	64	384	209.	0.059	0.545
0.0016-0.003	302	145	157	2.16	0.135	0.0137
0.0016-0.003	-320	145	465	2.16	0.135	0.00465

TABLE 27. PERFORMANCE OF SAMPLE MSC-03

Description: (1) NASA Style 4190B with carboxy nitroso coating on both sides

(7) Laminated composite shield and spacer Schjeldahl Style X993

(7) NASA Style 4897 Beta marquisette

(2) bladder layers

Sample weights: top 99.0 gm, midplane 20.3 gm, bottom 99.0 gm

Vacuum: less than 5×10^{-5} torr

Compressive Load (psi)	Outside Temperature (F)	Inside Temperature (F)	ΔT (F)	Heat Flux (Btu/hr ft^2)	Sample Thick-Ness (in)	Conductance (Btu/ft^{2}hr°F)
2.5 to 4.6 x 10^{-3}	294	163	131	2.56	0.151	1.95 x 10^{-2}
1.05 to 2.1 x 10^{-3}	-320	163	483	2.56	0.151	5.31 x 10^{-3}
2.5 to 4.6 x 10^{-3}	177	73	104	1.62	0.152	1.56 x 10^{-2}
1.05 to 2.1 x 10^{-3}	-320	73	393	1.62	0.152	4.12 x 10^{-3}
0.029	286	122	164	9.20	0.137	5.60 x 10^{-2}
0.029	-320	122	442	9.20	0.137	2.08 x 10^{-2}
0.20	303	123	180	13.3	0.128	7.40 x 10^{-2}
0.20	-320	123	443	13.3	0.128	3.00 x 10^{-2}
16	304	83	221	149	0.076	6.75 x 10^{-1}
16	-320	83	403	149	0.076	3.70 x 10^{-1}

TABLE 28. PERFORMANCE OF SAMPLE MSC-04

Description: (2) Stevens Style 15035 tight-weave Beta fiberglass
(7) 0.5-mil Kapton with 1200 Å liquid bright gold both sides
(24) Burlington Style 104 with 5% fluorel stabilization
(2) bladder layers

Sample weights: top 90 gm, midplane 8.7 gm, bottom 90 gm

Vacuum: less than 1×10^{-6} torr

Compressive Load (psi)	Outside Temperature (F)	Inside Temperature (F)	ΔT (F)	Heat Flux (Btu/hr ft^2)	Sample Thickness (in)	Conductance (Btu/ft^2 hr°F)
2.80 to 3.67 x 10^{-3}	203	84	119	0.534	0.174	0.00449
0.87 to 1.75 x 10^{-3}	-320	84	404	0.534	0.174	0.00132
2.80 to 3.67 x 10^{-3}	301	141	160	0.775	0.174	0.00484
0.87 to 1.75 x 10^{-3}	-320	141	461	0.775	0.174	0.00168
0.01	204	80	124	0.979	0.105	0.00790
0.01	-320	80	400	0.979	0.105	0.00245
0.01	300	149	151	1.615	0.105	0.0107
0.01	-320	149	469	1.615	0.105	0.00344
0.1	205	81	124	4.14	0.086	0.0334
0.1	-320	81	401	4.14	0.086	0.0103
0.1	305	150	155	7.43	0.087	0.0479
0.1	-320	150	470	7.43	0.087	0.0158
2.0	209	64	145	48.2	0.062	0.332
2.0	-320	64	384	48.2	0.062	0.126
2.0	303	134	169	69.3	0.064	0.410
2.0	-320	134	454	69.3	0.064	0.153
15.0	209	68	141	131.4	0.050	0.930
15.0	-320	68	408	131.4	0.050	0.322
15.0	312	137	175	223.6	0.050	1.28
15.0	-320	137	457	223.6	0.050	0.490

TABLE 29. PERFORMANCE OF SAMPLE MSC-05

Description: (2) Stevens Style 15035 tight-weave Beta fiberglass
(7) 0.5-mil Kapton with 800 Å aluminum both sides
(8) Stevens Style 2530 Beta marquisette
(2) bladder layers

Sample weights: Top 88.8 gm, midplane 20.2 gm, bottom 87.1 gm

Vacuum: less than 1×10^{-5} torr

Compressive Load (psi)	Outside Temperature (F)	Inside Temperature (F)	ΔT (F)	Heat Flux (Btu/hr ft^2)	Sample Thickness (in)	Conductance (Btu/ft^2 hr°F)
3.38 to 4.35 x 10^{-3}	198	75.5	122.5	.491	0.1623	.0040
0.98 to 1.97 x 10^{-3}	-320	75.5	395.5	.491	0.1623	.0012
3.38 to 4.35 x 10^{-3}	294	140	154	.710	0.1613	.0046
0.98 to 1.97 x 10^{-3}	-320	140	460	.710	0.1613	.0015
0.01	196	73	123	.624	0.1331	.0051
0.01	-320	73	393	.624	0.1331	.0016
0.01	292.5	138.5	154	1.21	0.1331	.0078
0.01	-320	138.5	458.5	1.21	0.1331	.0026
0.1	197	60	137	5.32	0.1035	.0388
0.1	-320	60	380	5.32	0.1035	.0140
0.1	303	138.6	164.4	10.133	0.1056	.0616
0.1	-320	138.6	458.6	10.133	0.1056	.0221
2.0	197	54.8	142.2	87.2	0.0758	.6132
2.0	-320	54.8	374.8	87.2	0.0758	.2326
2.0	299.5	127.8	171.7	126.0	0.0758	.7338
2.0	-320	127.8	447.8	126.0	0.0758	.2813
15.0	202.5	65.5	137	220.0	0.0570	1.605
15.0	-320	65.5	385.5	220.0	0.0570	.5706
15.0	296.5	128.3	168.2	350.0	0.0570	2.081
15.0	-320	128.3	448.2	350.0	0.0570	.781

TABLE 30. PERFORMANCE OF SAMPLE MSC-06

Description: (2) Stevens Style 15035 tight-weave Beta fiberglass
(7) 0.25-mil Mylar with 360 Å aluminum both sides
(8) Stevens Style 2530 Beta marquisette
(2) bladder layers

Sample weights: Top 83.7 gm, midplane 20.5 gm, bottom 82.0 gm

Vacuum: less than 7×10^{-6} torr

Compressive Load (psi)	Outside Temperature (F)	Inside Temperature (F)	ΔT (F)	Heat Flux (Btu/hr ft^2)	Sample Thickness (in)	Conductance (Btu/ft^{2}hr°F)
3.22 to 4.13 x 10^{-3}	189	82.8	106.2	0.466	0.2085	0.0043
0.93 to 1.85 x 10^{-3}	-320	82.8	402.8	0.466	0.2085	0.0011
3.22 to 4.13 x 10^{-3}	302.2	166.5	135.7	0.94	0.210	0.0069
0.93 to 1.85 x 10^{-3}	-320	166.5	486.5	0.94	0.210	0.0019
3.22 to 4.13 x 10^{-3}	102	20	82	0.278	0.2085	0.0033
0.93 to 1.85 x 10^{-3}	-320	20	342	0.278	0.2085	0.0008
0.01	204.5	98	106.5	1.4	0.1175	0.0131
0.01	-320	98	418	1.4	0.1175	0.0033
0.01	303.5	168	135.5	2.089	0.1181	0.0154
0.01	-320	168	488	2.089	0.1181	0.0042
0.1	197.4	77.4	120	5.54	0.0993	0.0461
0.1	-320	77.4	397.4	5.54	0.0993	0.0139
0.1	295.6	146.3	149.3	10.2	0.1003	0.0683
0.1	-320	146.3	466.3	10.2	0.1003	0.0218
2.0	202.8	59.9	143	82.7	0.07315	0.5783
2.0	-320	59.9	380	82.7	0.07315	0.2176
2.0	301	133.8	167.2	122.9	0.07315	0.7350
2.0	-320	133,8	453.8	122.9	0.07315	0.2708
15.0	200	31.7	168.3	228.9	0.047	1.36
15.0	-320	31.7	351.7	228.9	0.047	0.6508
15.0	298.2	142.2	156	327	0.0528	2.096
15.0	-320	142.2	462.2	327	0.0528	0.7074

TABLE 31. PERFORMANCE OF SAMPLE MSC-07

Description: (2) Stevens Style 15035 tight-weave Beta fiberglass
(7) 0.25-mil Mylar with 900 Å aluminum both sides
(8) NRC nonwoven Dacron batt
(2) bladder layers

Sample weights: Top 56.6 gm, midplane 20.5 gm, bottom 56.6 gm

Vacuum: less than 1×10^{-5} torr

Compressive Load (psi)	Outside Temperature (F)	Inside Temperature (F)	ΔT (F)	Heat Flux (Btu/hr ft^2)	Sample Thickness (in)	Conductance (Btu/ft^{2}hr°F)
2.39 to 3.03 x 10^{-3}	204	89.3	114.7	0.577	0.168	0.00503
0.64 to 1.29 x 10^{-3}	-320	89.3	409.3	0.577	0.168	0.0014
2.39 to 3.03 x 10^{-3}	309	194	115	1.01	0.166	0.0088
0.64 to 1.29 x 10^{-3}	-320	194	514	1.01	0.166	0.0019
.01	206.5	76.3	130.2	1.348	0.107	0.0103
.01	-320	76.3	396.3	1.348	0.107	0.0034
.01	304	181.7	122.7	2.59	0.108	0.0211
.01	-320	181.7	501.7	2.59	0.108	0.0052
.01	206	50.1	155.9	6.83	0.070	0.0438
.01	-320	50.1	370.1	6.83	0.070	0.0185
.01	292.5	145.3	147.2	8.48	0.060	0.0576
.01	-320	145.3	465.3	8.48	0.060	0.0182
2.0	199	59	140	111.9	0.035	0.799
2.0	-320	59	379	111.9	0.035	0.2952
2.0	295.9	156.5	139.4	183.1	0.036	1.313
2.0	-320	156.5	476.5	183.1	0.036	0.3842
15.0	196	50.5	145.5	121.7	0.029	0.8364
15.0	-320	50.5	370.5	121.7	0.029	0.3285
15.0	301.5	121	180.5	536.9	0.030	2.974
15.0	-320	121	441	536.9	0.030	1.217

TABLE 32. PERFORMANCE OF SAMPLE MSC-08

Description: (2) Stevens Style 15035 tight-weave Beta fiberglass
(7) 0.5-mil Kapton with 800 Å aluminum both sides
(24) Burlington Style 104 with 5% fluorel stabilization
(2) bladder layers

Sample weight: Top 84.3 gm, midplane 20.9 gm, bottom 87.0 gm

Vacuum: less than 2×10^{-5} torr

Compressive Load (psi)	Outside Temperature (F)	Inside Temperature (F)	ΔT (F)	Heat Flux (Btu/hr ft^2)	Sample Thickness (in.)	Conductance (Btu/ft^{2}hr°F)
3.30 to 4.26 x 10^{-3}	197	96	101	.556	0.166	.005
0.93 to 1.87 x 10^{-3}	-320	96	416	.556	0.166	.00133
3.30 to 4.26 x 10^{-3}	298.8	166	132.8	.825	0.157	.0062
0.93 to 1.87 x 10^{-3}	-320	166	486	.825	0.157	.0017
.01	202	82	120	1.22	0.107	.0101
.01	-320	82	402	1.22	0.107	.0030
.01	302	145.5	156.5	2.22	0.103	.0142
.01	-320	145.5	465.5	2.22	0.103	.0047
.01	200.5	73.7	126.8	5.06	0.084	.0399
.01	-320	73.7	393.7	5.06	0.084	.0128
.01	302	145.5	156.5	11.22	0.084	.0716
.01	-320	145.5	465.5	11.22	0.084	.0241
2.0	200.6	26.9	173.7		0.052	
2.0	-320	26.9	346.9		0.052	
2.0	300	71.5	228.5	83.2	0.059	.364
2.0	-320	71.5	391.5	83.2	0.059	.213
15.0	200	20.6	179.4	186.7	0.044	1.040
15.0	-320	20.6	340.6	186.7	0.044	.548
15.0	302.5	97	205.4	264.8	0.044	1.289
15.0	-320	97	417	264.8	0.044	.635

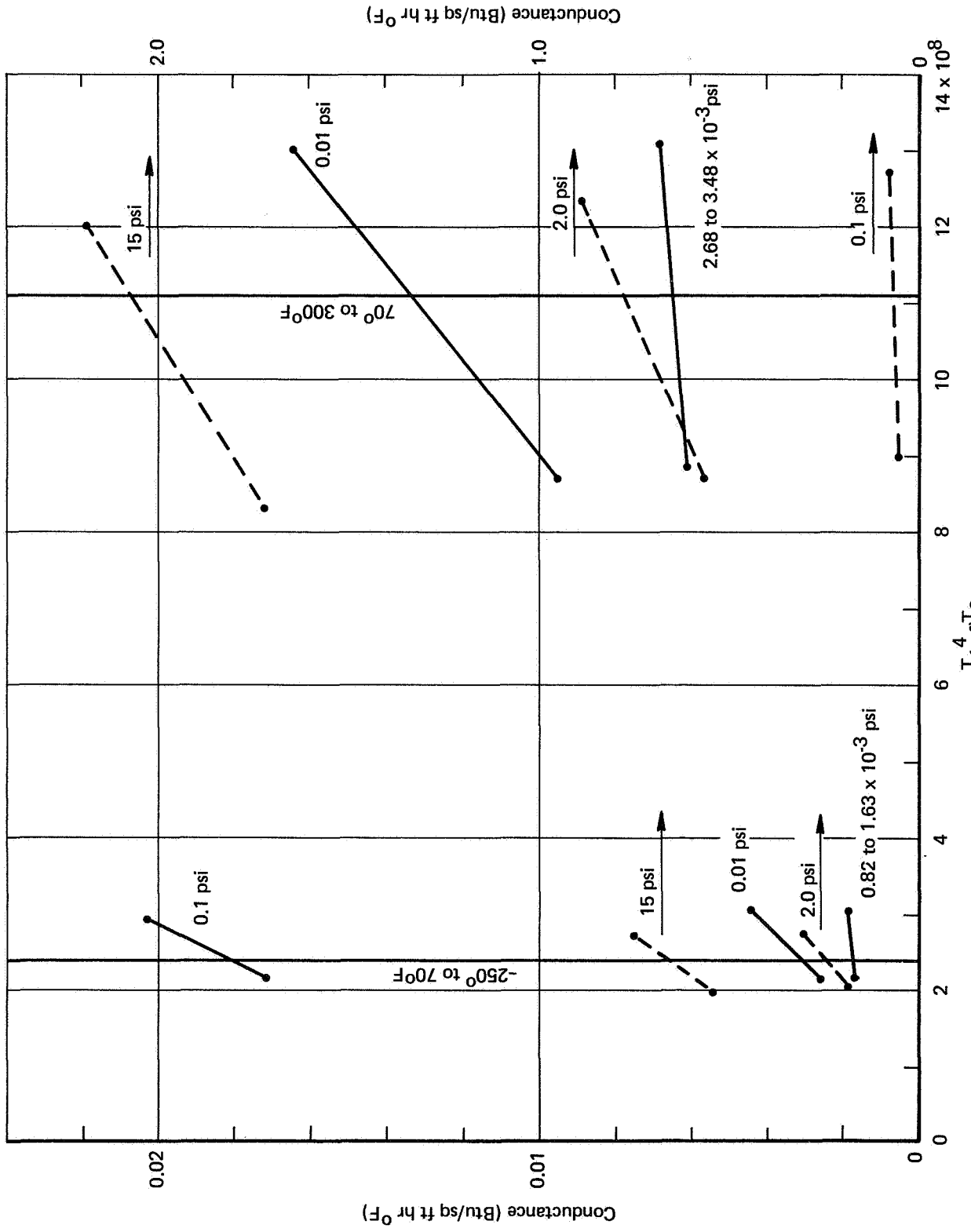

FIGURE 28 CONDUCTANCE DATA EXTRAPOLATION FOR SAMPLE ADL-08

VIII. REFERENCES

1. E. M. Roth, Bio-energetics of Space Suits for Lunar Exploration NASA SP-84, National Aeronautics and Space Administration, 1966.

2. G. S. Karp, and E. Fried, Measurement of Thermal Conductance of Multilayer and Other Insulation Materials, General Electric Co., Document No. 66SD4207, NASA Contract NAS9-3685, January 1966.

3. Arthur D. Little, Inc., Advanced Studies on Multi-layer Insulation Systems, Report No. NAS CR-54929, Contract NASA 3-6283, June 1966.

4. Arthur D. Little, Inc., Basic Investigations of Multi-layer Insulation Systems, Report No. NASA CR-54191, Contract NAS3-4181, October 1964.

5. NASA Manned Spacecraft Center, Gemini IX Pilots Report, 17 June 1966.

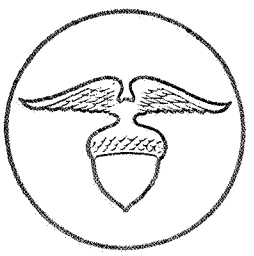

CAMBRIDGE • CHICAGO • ATHENS • BRUSSELS • ZÜRICH
WASHINGTON • PARIS • TORONTO • SANTA MONICA
NEW YORK • MEXICO CITY • LONDON • SAN FRANCISCO